

N72-75433

STARTING THRUST TRANSIENTS OF
SOLID ROCKET ENGINES

by


W. J. Most and M. Summerfield

July, 1969

Aerospace and Mechanical Sciences Report No. 873

This research was sponsored by the Office of Advanced Research and Technology, National Aeronautics and Space Administration, under NASA Grant NGR 31-001-109, supervised by Langley Research Center.

Transmitted by:


Martin Summerfield
Principal Investigator

Guggenheim Laboratories for the Aerospace Propulsion Sciences
Princeton University, Princeton, New Jersey

REPRODUCED BY
NATIONAL TECHNICAL
INFORMATION SERVICE
U. S. DEPARTMENT OF COMMERCE
SPRINGFIELD, VA. 22161

125

NOTICE

THIS DOCUMENT HAS BEEN REPRODUCED FROM THE BEST COPY FURNISHED US BY THE SPONSORING AGENCY. ALTHOUGH IT IS RECOGNIZED THAT CERTAIN PORTIONS ARE ILLEGIBLE, IT IS BEING RELEASED IN THE INTEREST OF MAKING AVAILABLE AS MUCH INFORMATION AS POSSIBLE.

STARTING THRUST TRANSIENTS OF
SOLID ROCKET ENGINES*

by

W. J. Most and M. Summerfield

July, 1969

Guggenheim Laboratories for the Aerospace Propulsion Sciences
Princeton University, Princeton, New Jersey

ABSTRACT

In the past, the design engineer has been forced to rely on empirical and statistical knowledge of previous firings in order to design the ignition system of a solid rocket motor or to predict the starting delay time of a given rocket-igniter system. In order to predict the entire ignition transient analytically, the processes of local ignition, heat transfer and subsequent flame propagation and the gas dynamics of the combustion chamber must all be described quantitatively. Each of these elements has been the focus of extensive research in itself. The purpose of this paper is to present the results of these research efforts, in our laboratory and elsewhere, in relation to the objective of predicting analytically the entire ignition transient.

A particular analytical model, developed for the class of engines with large port-to-throat area ratios and head-end mounted pyrogen igniters, is presented. This model characterizes the local ignition event by ascribing to the propellant a critical surface temperature for ignition and by including a surface heat release term to account for exothermic decomposition while the surface is still below the critical temperature. Flame spreading is described by coupling this ignition model with a general description of the heat transfer from the gas phase to the unignited propellant grain. Any propellant burning rate law, steady or nonsteady, can be used once ignition has been achieved. The model is completed by the dynamic energy and continuity equations for the motor free volume. This particular model is compared to others which have appeared in the literature, with special attention paid to those reports in which comparisons between theoretical predictions and experimental test firings are offered.

The limitations of the various models are examined, especially with regard to those particular assumptions which cannot be justified experimentally. The applicability of the various models for the prediction of marginal (hangfire) situations is examined.

This paper concludes that the analytical models now available can provide useful predictions of the entire ignition transient, at least for the class of motors for which they have been developed, and this has been verified experimentally.

*

This research was sponsored by the Office of Advanced Research and Technology, National Aeronautics and Space Administration, under NASA Grant NGR 31-001-109, supervised by Langley Research Center.

ACKNOWLEDGEMENTS

This research was sponsored by the Office of Advanced Research and Technology, National Aeronautics & Space Administration under Research Grant NGR 31-001-109. The Program Manager for this program was Mr. Robert W. Ziem, Chief, Solid Propellant Technology, Office of Advanced Research and Technology. The Technical Manager for this program was Mr. Earl E. Van Landingham, Head, Applied Rocket Research Section, Propulsion Branch, NASA, Langley Research Center. The Contracting Officer for the program was Mr. John McDonald, Code DHC-5, Office of Grants and Research Contracts.

A number of workers in the Guggenheim Laboratories at Princeton University contributed to this research. Mr. C. R. Felsheim assisted with propellant formulation and processing. Mr. J. H. Semler was instrumental in the fabrication of the experimental equipment. Advice on matters of instrumentation and assistance with the experimental firing program was given by Mr. S. O. Morris.

Conditions of Reproduction

Reproduction, translation, publication, use and disposal in whole or in part by or for the United States Government is permitted.

TABLE OF CONTENTS

	Page
Title Page	i
Abstract	ii
Acknowledgements	iii
Table of Contents	iv
Nomenclature	v
Chapter	
I. PHENOMENOLOGICAL INTRODUCTION TO THE IGNITION TRANSIENT	1
II. PHYSICAL MODEL OF THE IGNITION TRANSIENT	2
A. Local Ignition and Solid Phase Heat-up	3
B. Propagation of Ignitedness	6
C. Gas Dynamic Model	9
1. Momentum Equation	9
2. Mass Continuity Equation	10
3. Energy Equation	11
D. Burning Rate Behavior	15
E. Sample Theoretical Predictions	15
III. REVIEW OF PREVIOUS LITERATURE ON THE IGNITION TRANSIENT	16
A. Correlation Studies	17
B. Analytical Models	19
C. Convective Heat Transfer	25
D. Hypergolic Ignition	32
E. Aft-End Ignition	33
IV. EXPERIMENTAL INVESTIGATION OF THE IGNITION TRANSIENT	36
A. Photographic Observations	38
B. Gas Temperature and Heat Loss Experiments	39
C. Pressure Measurements	40
1. Series A - Exhaust Nozzle Varied	40
2. Series B - Igniter Duration Varied	41
3. Series C - Igniter Flow Rate Varied	41
4. Series D - Marginal Igniter Durations	43
5. Series E - Effect of Aluminum Addition	44
6. Series F - Practical Motor Configurations	45
7. Series G - Pyrotechnic Igniter	46
V. CONCLUSIONS AND PROBLEMS FOR FUTURE WORK	47
A. Conclusions	47
B. Problems for Future Work	49
Acknowledgements	49
References	50
Tables	62
Figures	76
Distribution List	117

NOMENCLATURE

- A total area exposed to igniter action
- a leading edge parameter (a length)
- A total propellant grain area
- A port area
- A_s Arrhenius pre-exponential for surface heat release
- A_t rocket exhaust nozzle throat area
- $A_{t,ign}$ igniter nozzle throat area
- C hypergol concentration at surface
- C_m hypergol concentration in main stream
- C_m^o hypergol concentration leaving ignited region
- C_p specific heat
- C^* characteristic velocity = $\sqrt{RT_c}/\Gamma$
- D_p diameter of port
- D_{ign} diameter of igniter nozzle
- d_t diameter of exhaust nozzle throat
- E_{100} threshold ignition energy at 100 psig
- e internal energy of gas
- ΔH_{tot} total enthalpy difference across boundary layer, per unit mass
- ΔH_r heat of reaction per unit mass
- h enthalpy per unit mass
- h_{conv} heat transfer coefficient
- h_{ign} heat transfer coefficient due to igniter alone
- $K_n A_p/A_t$
- k constant in burning rate law, $r_{ss} = kP_c^n$
- k_m mass transfer coefficient
- L length of propellant grain
- L^* characteristic length of rocket chamber = V_c/A_t
- \dot{m}_B mass burning rate
- m_c instantaneous mass of gas in combustion chamber
- m_{eq} mass of gas in combustion chamber at equilibrium
- \dot{m}_{ign} igniter mass flow rate
- m_{ign} total mass of igniter gas
- \dot{m}_N mass flow rate through exhaust nozzle
- n power in burning rate law
- n' reaction order
- Nu_D Nusselt Number based on diameter
- Nu_{DB} Dittus-Boelter Nusselt Number = $0.023 Re_D^{0.8} Pr^{0.4}$
- Nu_x Nusselt Number based on x
- P perimeter of port
- P dimensionless chamber pressure = P_c/P_{eq}
- P_c chamber pressure
- P_{eq} chamber pressure at equilibrium
- P_i pressure achieved by firing igniter in inert motor
- Pr Prandtl Number
- Q heat release parameter
- Q_t total igniter heat release
- q_r required ignition energy per unit surface area
- \dot{q}_{conv} convective heat flux
- \dot{q}_{self} self heating energy flux
- r dimensionless burning rate = r_{ss}/r_{eq}
- r_b dynamic burning rate
- r_{eq} burning rate at equilibrium chamber pressure

\dot{r}_p rate of flame propagation
 \dot{r}_{ss} quasi-steady burning rate
 R specific gas constant
 Re_D Reynolds Number based on diameter
 Re_x Reynolds Number based on x
 S dimensionless burning area = S_B/A_B
 S_B instantaneous burning area
 St Stanton Number
 t time
 t^* characteristic time of chamber = $L^*/\Gamma^2 c^*$
 T dimensionless chamber temperature = T_c/T_f
 T_c chamber temperature
 $T_{c,ign}$ temperature of igniter gas
 T_f flame temperature
 T_g gas temperature
 T_{ig} ignition temperature of propellant
 T_i initial temperature of propellant
 T_s surface temperature of propellant
 u gas velocity
 u_m main stream gas velocity
 V_c chamber volume
 x axial distance
 y distance normal to propellant surface
 ΔY species change due to chemical reaction

Greek

α_p thermal diffusivity of propellant
 ϵ^* ratio of annular area between igniter nozzle and motor nozzle to motor throat area
 γ ratio of specific heats
 Γ a function of γ , $= \sqrt{\gamma \left(\frac{\gamma}{\gamma-1} \right)^{\frac{\gamma}{\gamma-1}}}$
 λ_g thermal conductivity of chamber gases
 λ_p thermal conductivity of propellant
 μ_g viscosity of chamber gases
 ρ_g density of chamber gases
 ρ_p density of propellant
 τ dimensionless time = t/t^*
 τ_{on} time for first element of surface to ignite (induction time of rocket motor)
 σ area normal to flux

I-INTRODUCTION. The continuing trend toward larger, more sophisticated, and more expensive solid propellant rocket motors requires greater accuracy in the prediction and control of the thrust transient during ignition. This is the interval between the beginning of the igniter action and the attainment of full thrust at the design operating conditions. In the past, the design engineer has been forced to rely only on empirical and statistical knowledge of previous rocket firings. This approach is costly, time consuming and unending. It requires test firings under all possible conditions of altitude and ambient temperature under which the rocket motor may be required to function, since there is no reliable means of predicting the effects of such variables. This is an unending process because no knowledge is gained about the basic mechanisms involved. The experience gained in an extensive test firing program with one rocket motor can be extrapolated to the next motor only with great caution, and only if the two motors are of similar design. The purpose of this paper is to review in a critical manner the attempts to achieve rational quantitative answers to these design problems on the basis of a theoretical treatment of the underlying physical processes involved in the ignition transient, at least for those classes of rocket motors which have been treated analytically to date.

The increasingly rigid specification of rocket motor performance characteristics forces the designer to concern himself with various aspects of the ignition transient. The overall time of the transient and the shape of the pressure rise curve are of primary importance. The time from initiation of the ignition signal to the onset of full thrust must be kept within specified limits and must be reproducible. The igniter must be perfectly tailored to the motor to avoid pressure overshoots above the design conditions in order to avoid exceeding the stress limits of the motor casing. Since the propellant grain and the motor casing have a viscoelastic nature, the rate of pressurization as well as the maximum pressure are critical parameters in the structural design. An excessive pressurization rate (ignition shock) can cause a failure even when the pressure is below the design limit. This is particularly critical at low ambient temperatures. Often even more stringent requirements are placed on the pressurization rate by the need to protect delicate payloads and guidance systems. Detailed knowledge of the thrust variation during the ignition transient may be required when solid propellant rocket motors are used for critical trajectory and attitude control.

The sequence of events and physical processes which take place during the ignition transient of any solid propellant rocket motor are exceedingly complex and difficult to model analytically. Many of the physico-chemical processes which are only a part of the overall ignition transient have been the subject of active research for many years. Before any theoretical modelling is attempted, a description of the overlapping chain of steps in the ignition transient is in order. At zero time the igniter is ignited by an initiator. This initiator is commonly an electric match, a bridge wire or some such device. This begins a "sub-sequence of events" in the igniter chamber which is similar to the sequence of the motor itself. However, due to the small scale of the igniter compared to the main motor, quasi-steady igniter operation for pyrogen igniters is usually achieved on a time scale small compared to events in the main motor. Some types of pyrotechnic igniters never reach quasi-steady operation, but their action times are short. In either case, we take the igniter output as a pre-calibrated input for the motor. As the igniter begins to operate, the propellant grain begins to receive an ignition stimulus. A flow pattern and a pressure are established within the motor free volume. The establishment of

this flow pattern may be accompanied by traveling shock waves. The ignition stimulus may take many forms: convection from hot igniter gases, impingement by hot condensed phase particles directly on the propellant grain, radiation from hot gases and particles and/or chemical attack by hypergolic materials. The areas of the propellant grain receiving the highest ignition stimulus are brought to ignition first. The chamber pressure begins to rise due to the mass addition. The region(s) of first ignition begin to spread. The mass flux from the burning surface augments the igniter stimulus and interacts with the flow field. Due to the rising chamber pressure, the behavior of the igniter may be affected, for example, by unchoking of the igniter nozzle or by significantly altering the penetration into the motor free volume of an aft end igniter jet. At some time full ignitedness of the exposed propellant grain is achieved. This generally occurs when the pressure is approximately half of the design operating pressure^(5,6,7,8). The chamber pressure continues to rise until the equilibrium operating conditions are established. Throughout this sequence of events the mass addition from the propellant grain may be a function of the instantaneous pressure, the rate of change of pressure and gas velocity in the motor port.

Out of this description emerge the elements essential to any overall theoretical model of the ignition transient. First, the igniter and its output must be described in terms of placement (head-end, aft-end or distributed), type of igniter, principal products, dominant mode(s) of energy transfer, time history, and flow pattern established by the igniter. Second, the local ignition event must be defined and the response of the propellant to the various possible stimuli must be characterized. Third, the mechanism for the propagation of ignition (flame spreading) must be described. This must involve a description of the energy flux (heat transfer) from the hot gas to the solid, and into the subsurface regions, until the moment of ignition. Fourth, the burning rate behavior of the solid propellant must be described, once ignition has been achieved. In particular, the coupling of the burning rate to the rapidly changing pressure (dynamic burning response) and velocity (erosive burning) must be considered. Fifth, the proper gas dynamic equations must be written for the gas flow in the chamber. All of these elements are, of course, coupled one to the other, resulting in a complex assembly of simultaneous equations to describe the ignition transient. The first element, characterization of the igniter and its output, is not amenable to general analysis. However, given a theoretical model for elements two through five, the igniter designer will at least have a rational means of optimizing the igniter output, time history and placement.

A particular model and analysis of the entire ignition transient will now be presented. It is not surprising that this particular analysis is the evolved result of work of the authors of this paper and previous co-authors. This model is presented at this juncture of the paper in order that the reader can connect the confusing coupling of the many complex processes described above with more concrete and tangible concepts. Having given substance to the essential elements which any analysis must encompass, the literature can then be efficiently explored for alternate approaches and possible improvements and modifications.

II. PHYSICAL MODEL OF THE IGNITION TRANSIENT. The analytical model of the ignition transient developed here is most directly (but not exclusively) applicable to the class of rocket motors with large port-to-throat area ratios, which are ignited by gas-producing (pyrogen) igniters located in the forward end of the

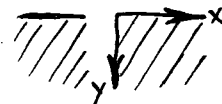
engine. Igniters of this class are actually small, easily ignited rocket motors which exhaust their combustion products into the port of the main motor. Among the basic characteristics of motor-igniter combinations in this class are that the gas flow is directed primarily toward the motor exhaust nozzle and that the ignition of the main propellant grain depends on convective and radiative heat transfer from the flowing gases. Usually, there is a stationary shock pattern within the igniter exhaust jet. Downstream of this shock pattern the flow is a highly turbulent subsonic flow. This igniter jet shock pattern will move in response to the rising pressure within the motor port. For the purposes of this work the boundary condition is considered just downstream of the shock pattern. Thus, this study does not consider the nonsteady interaction of the flow or pressure fields with the shock pattern.

As will be seen in the analysis, certain elements of the model are closely coupled to this particular class of solid propellant rocket motor and igniter combination. However, other aspects of the model do not depend in any way on the simplifying assumptions permitted by this particular class of motors. Both the restrictions and general applications of the analysis should be borne in mind.

II-A. LOCAL IGNITION AND SOLID PHASE HEAT-UP. The basic ignition mechanism of solid propellants is the subject of continuing intensive investigation. Various models of the elementary ignition events discussed in the research literature have been reviewed extensively elsewhere (Price, et. al. (115)). At this point, however, the only "model" which can be easily applied to the propagation of ignition over a propellant grain is the simple thermal theory: the attainment of some critical ignition temperature at the surface of the propellant. This, of course, is an extremely simplified view of the complex events leading to ignition. This is justified on the theoretical grounds for relatively slow ignitions (ten milliseconds or more) in which the heating up of the surface represents the largest part of the overall ignition time. In rapid ignitions, the physico-chemical rate processes become prominent, and then the simple concept of a critical ignition temperature must give way to a more elaborate description of the ignition event. See Reference 116 by Ohlemiller and Summerfield for a discussion of the point. The surface temperature criterion has been adopted in the present treatment of the pressure transient because the rate of ignition and flame spreading is relatively slow in the class of engines described above.

The adoption of the simple critical ignition temperature criterion requires a description of the solid phase heat-up process. The complete heat equation for an element of the solid Δx in length is written as

$$\rho_p C_p \frac{\partial T}{\partial t} = \lambda_p \nabla^2 T + \rho_p C_p F \cdot \nabla T + \rho_p \dot{Q}$$



The following simplifying approximations are made: It is assumed that $\frac{\partial T}{\partial y^2} \gg \frac{\partial T}{\partial x^2}$, so that the latter can be neglected. The convective term is considered to be negligible during the ignition interval. (This assumption is examined below.) The propellant is assumed to be completely inert internally until the critical ignition temperature is reached, and above this temperature the burning rate is assumed to be governed by a given burning rate equation. (The propriety of the many possible burning rate expressions, both

steady and nonsteady, is discussed in Section II-D below.) These approximations reduce the equation to the form

$$\frac{\partial T}{\partial t} = \alpha_p \frac{\partial^2 T}{\partial y^2}$$

with the accompanying boundary conditions,

$$\begin{aligned} T(x, y, 0) &= T_0 \\ T(x, \infty, t) &= T_0 \\ \lambda_p \frac{\partial T}{\partial y} \Big|_{y=0} &= -\dot{q}_{gas}(x, t) \end{aligned}$$

The heat diffusion equation and the boundary conditions are solved by the Laplace transform (see, for example, Ref. 129) for the propellant surface temperature.

$$T_s = T_0 + \frac{1}{\lambda_p} \sqrt{\frac{\alpha_p}{\pi}} \int_0^t \frac{\dot{q}_{gas}}{\sqrt{t-\tau}} d\tau$$

Given this relationship between surface temperature and time, the assumption made above, that the convective term is negligible during the ignition interval can be examined. This assumption has been justified by the numerical calculations of Hermance⁽¹³¹⁾. However, it can be reasoned in a less laborious way: The rate of change of surface temperature is obtained by considering a constant heat flux and differentiating the expression for T_s .

$$\frac{\partial T_s}{\partial t} = \frac{1}{2\lambda_p} \sqrt{\frac{\alpha_p}{\pi}} \frac{\dot{q}}{\sqrt{t}}$$

If an Arrhenius type pyrolysis law is assumed for \bar{r} , the convective term can be evaluated at the surface by using the boundary condition on the heat flux.

$$\bar{r} \cdot \nabla T = r \frac{\partial T}{\partial y} \Big|_{y=0} = \left(-A e^{-E_s/RT_s} \frac{\dot{q}}{\lambda_p} \right) \Big|_{y=0}$$

By evaluating these expressions for $\partial T_s / \partial t$ and $r \partial T / \partial y$, it can be shown that the two terms are the same order of magnitude near the ignition temperature. However, the absolute value of the convective term is increasing exponentially, with the power of the exponential proportional to $1/t^{1/2}$. $\partial T_s / \partial t$ is decreasing proportional to $1/t^{1/2}$. From this it can be reasoned that, despite the fact that the two terms become the same order of magnitude near the ignition temperature, the integrated effect of the convection term is negligible.

The simple critical ignition temperature criterion and solid phase heat-up description can be used successfully by the igniter designer only if it is approached with caution. It must be insured independently, for example, that the pressure environment is above the minimum ignition pressure. The simple criterion in itself would predict ignition even in a hard space vacuum! The simple criterion must also be viewed with caution when considering the mode of energy transfer and the rates of transfer which can be reasonably expected from a given igniter. The criterion may become a bad approximation at lower flux levels for radiation input than for convection or conduction input. Bastress⁽⁷⁹⁾ has successfully correlated convective ignition times with the simple thermal theory in the range of 150-200 cal/cm², but Ohlemiller⁽¹¹⁷⁾ and Baer and Ryan⁽⁹⁸⁾ have reported radiative ignition data which shows divergence from the simple theory for considerably lower flux levels. This earlier breakdown of the simple ignition

criterion for radiative situations has been reasoned^(116,117) to be due to the fact that the incipient gas phase reactions are more temperature sensitive in the cold atmosphere-radiation case than in the hot atmosphere-convection case.

Another point which must be considered in regard to the mode of energy transfer has to do more with the solid phase heat-up than with the ignition criterion itself. The energy input to the solid, due to convection or conduction heat transfer or hypergolic heat generation at or near the surface, can, in general be considered to be deposited right at the surface. However, radiative transfer may be received by the propellant in quite a different way. In this case reflection and scattering at the propellant surface and energy penetration in-depth must be considered.

With these danger areas in mind various degrees of sophistication can be added to the simple ignition temperature criterion. For example, the ignition temperature as a function of pressure level can be determined empirically from properly conducted ignitability experiments using a variety of energy sources: convection or radiation (arc image or laser).

As was pointed out above, one generally becomes suspicious of the critical surface temperature criterion when the ignition times become short. However, this work presents another improvement in the criterion at the other end of the ignition time spectrum, i.e., for very long ignition times. It was observed that the quality of the comparison between computer predictions of the ignition transient and experimental test firings degenerated for increasingly marginal situations. (The complete basis for these theoretical predictions and the details of the experimental work has not yet been presented. The reader is asked to bear with this obvious disordering so that the analytical model can be presented in its entirety. The experimental work related to this aspect of the model is presented in Chapter IV, Section C-3.) It is hypothesized that the discrepancy between theory and experiment is caused by the simple ignition temperature criterion. This criterion states that the propellant is completely inert thermochemically until a critical ignition temperature is reached. However, it is known that exothermic preignition reactions in the gas phase and/or on the surface contribute to the heating up process (Refs. 119, 120 and 121). This heat is released close to the surface by decomposing ammonium perchlorate and perhaps by interface reactions between the AP and the fuel binder⁽¹³²⁾. This contribution seems to be negligible in vigorous heating, rapid flame spreading situations, but its character seems to be of critical importance in marginal (hangfire) cases. This energy release rate at the propellant surface (or near it), while the surface temperature is still below the ignition temperature, is described in this work in a very approximate way by:

$$\dot{q}_{\text{SURFACE}} = p_p r Q = p_p Q A e^{-E_s/RT_s}$$

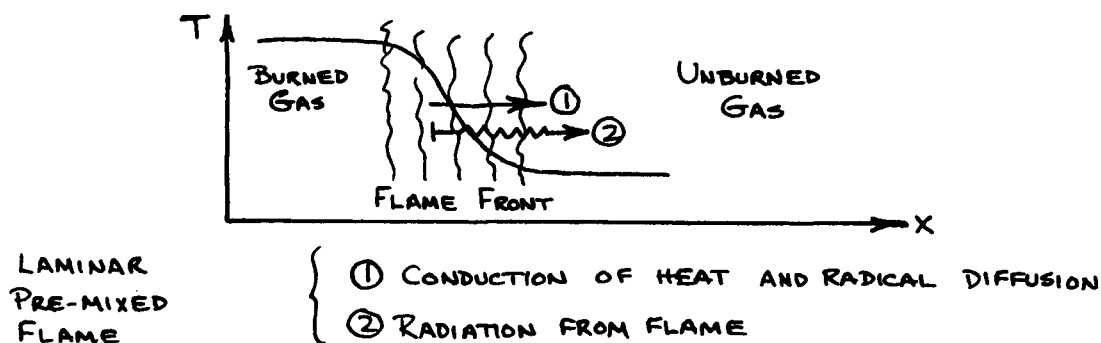
This implies that the integrated effect of exothermic heat release below, at, and above the propellant surface is assigned to the surface. This allows the nonlinear term representing the distributed heat release to be taken out of the differential equation and placed in the boundary condition. Thus, the boundary conditions on the heat diffusion equation now become

$$\begin{aligned} T(x, y, 0) &= T_0 \\ T(x, \infty, t) &= T_0 \\ \lambda_p \frac{\partial T}{\partial y} \Big|_{y=0} &= -[\dot{q}_{\text{SUR}}(x, t) + \dot{q}_{\text{GAS}}(x, t)] \end{aligned}$$

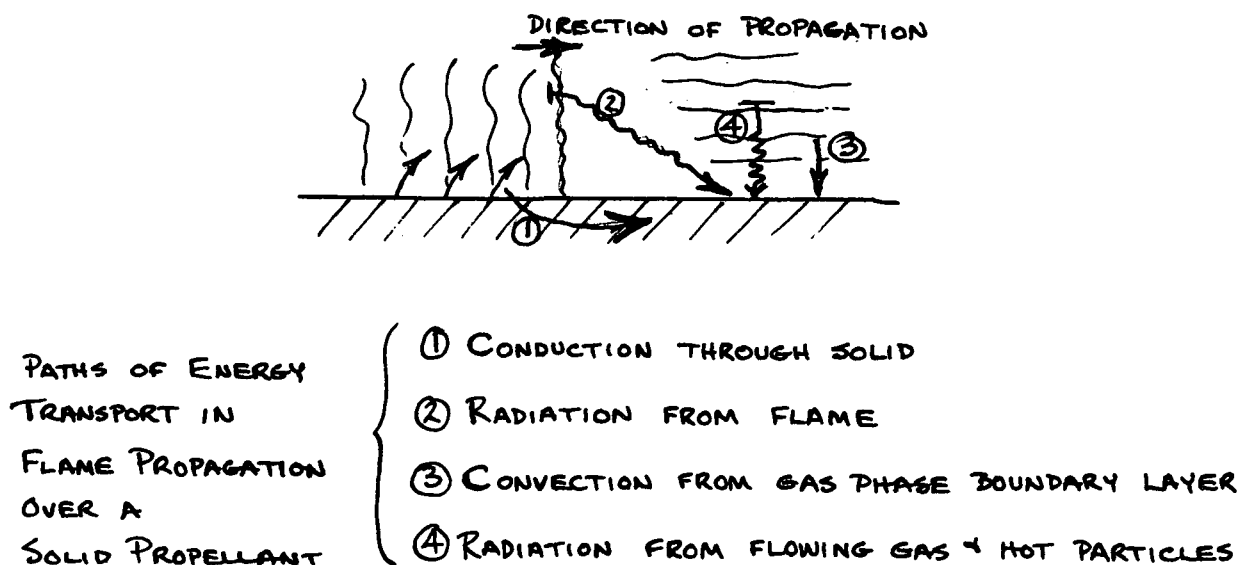
This surface heat release term will be important only in situations where the energy flux due to surface reaction becomes comparable to the energy flux from the gas above the surface.

II-B. PROPAGATION OF IGNITEDNESS. Having characterized the local ignition event and described the solid phase heat-up, the next mechanism to be considered is the propagation of ignitedness. Extensive photographic observations of rocket motors (Ref. 6, 7, 8, from this study) during the ignition transient confirms the fact that a flame front propagates progressively over the propellant grain. Although the demarcation between the ignited and unignited regions is not a sharp line, the useful concept of a flame front can be retained.

In the classical case of flame propagation through premixed gases, the available modes of energy transport to ignite the successive "layers" of gas are conduction of heat and diffusion of radicals from the burned zone to the unburned zone and radiation from the flame front itself.



In the case of flame propagation over a solid propellant, four paths of energy transport are available to ignite the propellant: conduction through the solid, radiation from the flame front, convection from the gas-phase boundary layer and radiation from the flowing gas and hot particles.



For rocket motors with gas-producing igniters located in the forward end, the dominant mode of energy transfer to the propellant surface is usually convection via the gas-phase boundary layer. Radiation, if it is to be important, will be dominated by the contribution from the flowing gas and from hot particles in the flow, not from the flame front itself. This can be reasoned from the geometry of the situation - The flame zone is perpendicular to the surface whereas the flow is adjacent to and parallel to the surface. Conduction through the solid phase is a slow energy transport path because of the low conductivity of the propellant.

Another observation which argues against the solid-phase conduction and flame front radiation paths is that the flame is occasionally observed to "jump" to a location considerably in advance of the main flame front. The interesting point is that these advance flamelets do not spread, but remain relatively stationary until overtaken by the main flame. This seems to indicate that these localized points received higher heat flux than their neighboring elements. A mechanism by which this could occur is through localized irregularities in the surface increasing the local convective heat transfer. Conduction through the solid and radiation from the flame front would heat the unignited surface more uniformly, independent of the localized character of the surface.

From this, it is hypothesized that the ignition of a given surface element depends only on the convective or radiative heat flux from the flowing gas phase and does not depend on the thermodynamic state of its neighboring elements. The ignition of a given surface element may depend on the element's position relative to the flame front, but only indirectly through the flame front's interaction with the convective boundary layer. This theory of flame spreading is not, of course, the only one which has been advanced. For example, Refs. 91 and 92 have advanced a model which views flame spreading as a continuous gas-phase ignition process driven by radiation directly from the adjacent flame front. (This model and others will be discussed in detail in Chapter III.) The model advanced here is, however, quite reasonable for situations dominated by strong convection from the flowing gases. The experimental verification of this model is given in Chapter IV.

The description of the gas phase heat convection to the propellant surface is an extremely difficult problem. This problem has received a great deal of attention and will be discussed in detail in the review section and experimental section of this paper. The flow field in any rocket motor differs from an idealized, solvable boundary layer pattern. The entering flow field is not uniform because of the igniter jet breakup and/or shock pattern. This results in a poorly defined leading edge and an unknown turbulence level and intensity. The surface over which the flow passes is rough. There is mass addition from the surface. Axial temperature gradients, and hence property gradients, are known to exist. The flow is nonsteady, particularly during the rapid part of the flame spreading interval. It is sufficient at this point simply to say that some description of the heat flux is necessary in order to evaluate the surface temperature as a function of time and position. Obviously, such a description must account for both the geometry and the boundary conditions of flow for each individual situation. For the geometry and flow conditions considered in this study the variation of the boundary layer film coefficient, h_{conv} , with the flow parameters of the hot gas stream was determined by systematic heat transfer tests. These tests were performed in a motor both with an inert grain and with a live propellant bed where the flame moved toward the

flux gauge as the mass flow rate increased. (This latter point, the possible interaction of the flame front with the gas flow, has been overlooked in many studies.) Based on these tests an empirical Nusselt number-Reynolds number correlation was produced. (Fig. 1). (The details of the experiments leading to this correlation are given later.)

$$Nu_{x+a} = 0.0734 Re_{x+a}^{0.8}$$

This leads to

$$h_{conv} = 0.0734 \left(\frac{\lambda_g}{x+a} \right) Re_{x+a}^{0.8}$$

$$\dot{q}_{conv} = h_{conv} (T_g - T_s)$$

The parameter "a" here is a leading edge term. Physically it should correspond to the point at which the boundary layer growth begins. It also serves to avoid the obvious error of predicting an infinite heat flux at the leading edge of the propellant grain, $x = 0$. The effect of "a" should disappear downstream as x becomes longer than a .

The driving potential across the boundary layer can be approximated by $(T_g - T_s) \approx T_g$ if the gas temperature is large compared to the range of surface temperatures of interest. A further approximation made in this study is that the driving temperature can be taken as constant in time and uniform in space. This point will be discussed in detail later.

It should also be pointed out that the mass flow rate appearing in the Reynolds number is not simply the mass flow rate out the rocket nozzle, as it would be in the steady flow case. The mass storage downstream, between the grain location in question and the nozzle, can be appreciable and must be considered in order to calculate the correct flow rate. Many of the heat transfer studies appearing in the literature were done with steady flow conditions where this is not important and thus this point is not usually emphasized. The correct mass flow rate should be written as

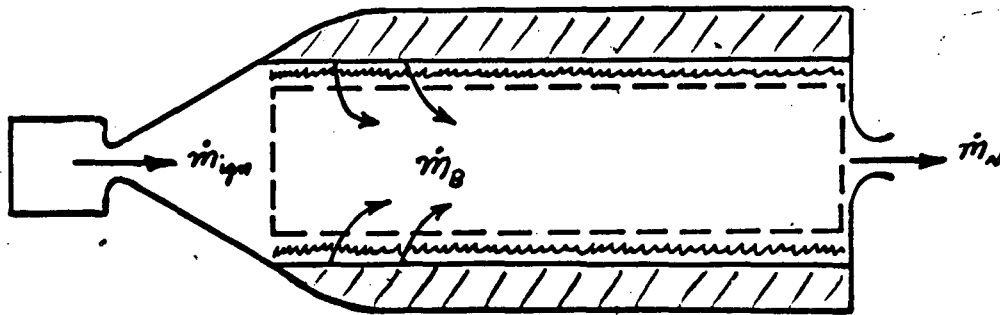
$$\dot{m}_x = \dot{m}_N + \frac{(L-x)}{L} \frac{dm_c}{dt}$$

In this way the heat transfer calculation is coupled to the bulk gas dynamic model for the free volume of the motor.

The empirical heat transfer correlation given above is in the form of a steady state correlation. It is used to represent the convective heat flux in a highly nonsteady flow field where the mass flow rate is continually varying. As indicated, the nonsteady mass balance is used to obtain the instantaneous flow rate. The steady state form of this correlation implies that the boundary layer which controls the convection is quasi-steady, adjusting to the varying conditions on a time scale small compared to the variation in mass flow and pressure. However, very simple considerations of the momentum equation for the boundary layer show that the characteristic time for adjustment of the boundary layer is the same order of magnitude as the residence time of the chamber. This implies that the boundary layer will adjust at approximately the same rate as the pressure and mass flow. Thus, an inconsistency arises and one is driven to the conclusion that nonsteady terms should appear in the heat transfer equation.

Unfortunately, there is no adequate theoretical analysis of a boundary layer flow over a rough surface with mass addition and chemical reaction. Without such an analysis, there is no guide to the nature and form of the appropriate nonsteady terms. The use of an empirical correlation in the form of a steady state equation can be justified only on experimental grounds. The experimental verification of this assumption will be discussed later.

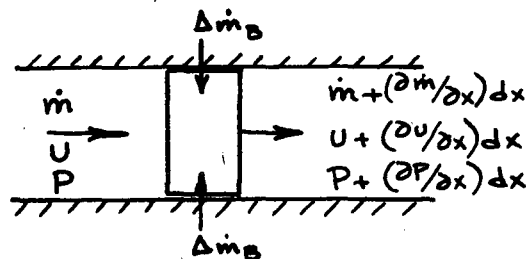
II-C. GAS DYNAMIC MODEL The analytical model of the ignition transient is completed by the gas dynamic equations. A control volume defined as the free volume of the rocket chamber is considered. The thickness of the flame above the propellant is assumed to be small compared to the dimensions of the combustion chamber. This results in a reaction-free control volume. (This assumption would not be exactly valid for aluminized propellant. The aluminum additive is known to burn in a distributed fashion throughout the combustion chamber.)



As the propellant burns, the control volume will vary with time. However, the time scale of the ignition transient is short, on the order of 200 milliseconds, and the burning rate of most propellants are low, on the order of 0.2 in/sec. Thus, the volume of propellant consumed during this interval is small enough, compared to the free volume, that the change in free volume can be ignored.

It is also assumed that the convergent section of the exhaust nozzle is short compared to the motor length. This allows the control volume to be treated without considering the rapid pressure and temperature changes associated with the nozzle.

II-C-1: MOMENTUM EQUATION In rocket motors with large port-to-throat area ratios, there is very low Mach number flow in the port. For a port-to-throat area ratio of about 6, a simple isentropic calculation shows that the Mach number at the end of the motor port (the nozzle entrance) would be less than 0.1. With this situation, the pressure gradient down the motor port would be negligibly small. This can be seen from an order of magnitude analysis of the axial momentum equation.



$$-\frac{\partial P}{\partial x} = \rho \frac{\partial u}{\partial t} + u \frac{\partial \rho}{\partial t} + u^2 \frac{\partial \rho}{\partial x} + 2\rho u \frac{\partial u}{\partial x}$$

This is nondimensionalized with respect to a characteristic chamber dimension, x^* , and a characteristic residence time, t^* .

$$\bar{x} = x/x^* \quad \bar{t} = t/t^* \quad t^* = x^*/u^*$$

$$-\frac{\partial \ln P}{\partial \bar{x}} = \frac{P}{\rho} u u^* \frac{\partial \ln u}{\partial \bar{t}} + \frac{P}{\rho} u u^* \frac{\partial \ln P}{\partial \bar{t}} + u^2 \frac{P}{\rho} \frac{\partial \ln P}{\partial \bar{x}} + 2 \frac{P}{\rho} u^2 \frac{\partial \ln u}{\partial \bar{x}}$$

For isentropic flow of a perfect gas

$$P/\rho = \frac{1}{\gamma} \left(\frac{\partial P}{\partial \rho} \right)_s = \frac{a^2}{\gamma}$$

The nondimensional momentum equation becomes

$$-\frac{\partial \ln P}{\partial \bar{x}} = \gamma M^2 \frac{u^*}{u} \frac{\partial \ln u}{\partial \bar{t}} + \gamma M^2 \frac{u^*}{u} \frac{\partial \ln P}{\partial \bar{t}} + \gamma M^2 \frac{\partial \ln P}{\partial \bar{x}} + 2 \gamma M^2 \frac{\partial \ln u}{\partial \bar{x}}$$

The leading terms in this relation are all of the order M^2 . Thus, it can be concluded that for $M \leq 0.1$ the momentum equation is simply $\nabla P = 0$. This effectively uncouples the momentum equation from the other conservation equations. This approximation would have to be reconsidered for high performance rocket motors with port-to-throat area ratios of less than 6.

II-C-2: MASS CONTINUITY EQUATION The mass continuity equation can be written as

$$\frac{dm_c}{dt} + \dot{m}_N = \dot{m}_B + \dot{m}_{ign} \quad \text{II-1}$$

On the left hand side are grouped the sink terms, the rate of mass storage and the flow rate out through the exhaust nozzle, \dot{m}_N . The mass burning rate, \dot{m}_B , and the mass addition from the igniter, \dot{m}_{ign} , are the source terms. The mass in the chamber at any instant can be written as $m_c = \rho_c V_c$ where V_c is considered to be constant.

The mass addition from the igniter depends largely upon the properties of the given igniter system. This makes a general analysis impossible. The igniter flow rate is a function of the conditions in the motor only when the igniter nozzle is unchoked; that is, when igniter operation is just beginning and when the chamber pressure has risen to the point where the igniter throat again unchokes. In these cases, the igniter flow would be coupled to the changing motor pressure through the standard unchoked nozzle equation. However, because of the small scale of the igniter compared to the main motor, the characteristic time of the igniter is small compared to that of the main motor. Thus, the igniter nozzle is choked on a time scale which is short compared to the time scale of events in the motor.

The class of igniters modeled in this study are usually operated at pressures above 1500 psia in order to attain high mass flow rates. Normal motor operating pressures are less than 1000 psia. Flame spreading, and hence the need for igniter operation, usually is complete when about half of the operating

pressure has been reached. Thus, unchoking of the igniter nozzle by the rising pressure would be encountered only after igniter burnout. At this point, in a successful ignition at least, the mass addition from the igniter would be small compared to that being generated in the main motor and could safely be neglected.

After igniter burnout the free volume of the igniter is also available to be filled by gases generated in the main motor. Thus the control volume undergoes a step change. As mentioned above, the igniter volume is usually very small compared to the motor free volume and can be safely ignored. However, these assumptions must be questioned when unusual igniter designs are considered.

The exhaust nozzle is assumed to be always choked. Igniters of the class considered generally supply a sufficient flow rate to choke the motor nozzle. The choking takes place within one or two chamber characteristic time units. This time scale is short compared to the overall transient.

The mass flow rate from the burning surface is written as $\dot{m}_b = \rho_p s_b(t) r_b$ where ρ_p is the propellant density, $s_b(t)$ is the instantaneous ignited surface area and r_b is the linear regression rate of the propellant. $s_b(t)$ changes as flame spreading takes place. The burning rate, r_b , may be a function of both the pressure and the rate of change of pressure. This will be discussed below.

These assumptions and the perfect gas law reduce the mass continuity equation to

$$\frac{V_c}{R} \frac{d(P_c/T_c)}{dt} + \frac{P_c A_t}{\sqrt{RT_c}} = \rho_p s_b(t) r_b + \dot{m}_{ign}(t) \quad \text{II-2}$$

II-C-3: ENERGY EQUATION The energy equation for the free volume of the rocket motor is:

$$\begin{aligned} \frac{\partial}{\partial t} \int_V (e + \frac{u^2}{2}) \rho dV_c + \int_S (e + \frac{u^2}{2}) \rho \vec{u} \cdot d\vec{\sigma} \\ = - \int_S P \vec{u} \cdot d\vec{\sigma} + \left(\begin{array}{c} \text{HEAT} \\ \text{ADDITION} \end{array} \right) + \left(\begin{array}{c} \text{BODY} \\ \text{WORK} \end{array} \right) \quad \text{II-3} \end{aligned}$$

The propellant combustion zone is outside the control volume, and thus there are no source terms due to chemical reaction in this equation. The heat addition term would actually be the heat loss from the flowing gases to the propellant grain in order to ignite the grain. The very purpose of an igniter is to undergo such a heat loss. However, it is assumed for now that this loss is small compared to the total energy of the gases and can be neglected. The propriety of this assumption is discussed below in those sections dealing with heat transfer. Unless the rising pressure significantly deforms the propellant grain, the body work term will be negligible compared to other terms in the energy equation.

The internal energy, e , is written in terms of the enthalpy and the

energy equation is rearranged.

$$\frac{\partial}{\partial t} \int_V \left(h + \frac{u^2}{2} \right) \rho_c dV_c + \int_S \left(h + \frac{u^2}{2} \right) \rho_c \bar{u} \cdot d\bar{\sigma} - \frac{\partial}{\partial t} \int_V P_c dV_c = 0 \quad (\text{II-4})$$

The gases within the control volume are assumed to be calorically perfect. Thus, the enthalpy is a function only of the temperature. This requires a reaction free control volume.

$$dh = \int_{T_0}^{T_c} C_p dT \quad ; \quad h = C_p T_c + (h_0 - C_p T_0)$$

It is further assumed that $C_p T_c \gg (h_0 - C_p T_0)$

In the development of the momentum equation it was shown that the class of rocket motors considered here have low Mach number flow in the port

$$M^2 = \frac{u^2}{a^2} = \frac{u^2}{\gamma R T_c} \ll 1$$

This leads to the conclusion that

$$C_p T_c \gg u^2$$

These assumptions allow the energy equation to be simplified to

$$\frac{\partial}{\partial t} \int_V C_p T_c \rho_c dV_c + \int_S C_p T_c \rho_c \bar{u} \cdot d\bar{\sigma} - \frac{\partial}{\partial t} \int_V P_c dV_c = 0 \quad \text{II-5}$$

In order to integrate this equation over the entire control volume, it must be assumed that both pressure and temperature are spatially uniform, $\nabla P_c = 0$ and $\nabla T_c = 0$. The propriety of these assumptions will be discussed below. It is sufficient at this juncture to say that the energy equation can be integrated under these assumptions.

$$\frac{d(m_c T_c)}{dt} + \dot{m}_N T_c - \dot{m}_B T_f - \dot{m}_{ign} T_{c_{ign}} - \frac{1}{C_p} \frac{d}{dt} (P_c V_c) = 0 \quad \text{II-6}$$

Using the relation $m_c = \rho_c V_c$ and the perfect gas law this equation becomes:

$$\frac{1}{\gamma} \frac{d(m_c T_c)}{dt} + \dot{m}_N T_c - \dot{m}_B T_f - \dot{m}_{ign} T_{c_{ign}} = 0$$

Now if the mass continuity equation, II-1, is multiplied by T_c and subtracted from the energy equation multiplied by γ , the result can be written in the form

$$m_c \frac{dT_c}{dt} + \dot{m}_N T_c (\gamma - 1) - \dot{m}_B (\gamma T_f - T_c) - \dot{m}_{ign} (\gamma T_{c_{ign}} - T_c) = 0 \quad \text{II-7}$$

By using the choked flow equation for \dot{m}_N , the perfect gas law for m_c , and $\rho_b S_b(t) v_b$ for \dot{m}_B , this equation can be rewritten as

$$\frac{V_c P_c}{R T_c} \frac{dT_c}{dt} + \frac{I P_c T_c (\gamma - 1)}{\gamma R T_c} - \rho_b S_b(t) v_b (\gamma T_f - T_c) - \dot{m}_{ign} (\gamma T_{c_{ign}} - T_c) = 0 \quad \text{II-8}$$

Equations II-2 and II-8 are now nondimensionalized by introducing the following dimensionless variables:

$$P = P_0/P_{0q} \quad \text{where} \quad P_{0q} = \left[\frac{\rho_0 A_B k c^*}{A_t} \right]^{1/(1-n)} \quad \text{and} \quad c^* = \frac{\sqrt{RT_f}}{\Gamma}$$

$$T = T_0/(T_f)_{0q}, \quad \bar{T} = \bar{T}_f/(T_f)_{0q}, \quad T_{ign} = T_{c,ign}/(T_f)_{0q}, \quad S = S_0/A_0$$

$$r = r_0/r_{0q}, \quad \dot{m}_{ign} = \dot{m}_{ign}/(\dot{m}_n)_{0q}, \quad \tau = t/t^* = t / \left[\frac{1}{\Gamma^2 c^*} \right]$$

The dimensionless mass continuity and energy equations are:

$$\frac{d(P/T)}{d\tau} + P/T^{1/2} - Sr - \dot{m}_{ign} = 0 \quad \text{II-9}$$

$$\frac{dT}{d\tau} + (\gamma-1)T^{3/2} + \frac{Sr}{P}(T-\gamma\bar{T}) + \dot{m}_{ign}\frac{T}{P}(\gamma T_{ign}-T) = 0 \quad \text{II-10}$$

The second equation is substituted into the first equation to eliminate $dT/d\tau$. This yields

$$\frac{dP}{d\tau} = \gamma \left[Sr\bar{T} - PT^{1/2} + \dot{m}_{ign}T_{ign} \right] \quad \text{II-11}$$

$$\frac{dT}{d\tau} = \frac{T}{P} \left[(\gamma\bar{T}-T)Sr - (\gamma-1)PT^{1/2} + \dot{m}_{ign}(\gamma T_{ign}-T) \right] \quad \text{II-12}$$

These are two nonlinear, coupled, ordinary differential equations for the chamber conditions, P and T . These equations are coupled to the ignition and flame spreading analyses through S , the nondimensional burning area. The non-dimensional burning rate, r , and the flame temperature \bar{T} , may be functions of both the instantaneous pressure and the rate of change of pressure. Thus, the equations are even more nonlinear than they first appear. r and \bar{T} as functions of p and dp/dt would have to be given by additional analysis concerned with the nonsteady burning rate mechanism⁽¹³¹⁾. Further, the nonsteady burning rate and temperature in these equations represent only a first order correction. This is because r and \bar{T} may be functions of position on the grain due to their sensitivity to the thermal profile in the solid. The heat flux-time history to each surface element is different and consequently the initial thermal profile at ignition varies with position.

Closed form analytical solutions to this complex system can be found only under severely limiting assumptions^(5,6,7). For example, if flame spreading is complete ($S = 1$), the igniter action is terminated ($\dot{m}_{ign} = 0$) and the chamber temperature is assumed to be constant, the equation for p is a Bernoulli equation which can be linearized and solved analytically for $p(t)$.

$$P = \left[1 - (1 - P_I^{1-n}) e^{-\gamma(1-n)\tau} \right]^{1/(1-n)}$$

where p_I is the initial pressure. However, the majority of interesting cases clearly fall outside the useful range of these limiting assumptions. For this reason a digital computer solution has been resorted to through this study. The computer prediction program used in this study is given in Ref. 134.

It has been assumed, largely without proof through this development, that the gas properties are spatially uniform. As was shown above, the axial pressure gradient is small for large port-to-throat area ratio motors. It is also quite

reasonable to assume that radial pressure gradients are small because there is no mechanism to support such gradients. The spatial variation of temperature is quite another matter. The purpose of the flowing igniter gas is to transfer its thermal energy to the propellant surface. If a large fraction of the energy is transferred to the propellant, axial temperature gradients will be established. Such temperature gradients have been measured in the laboratory scale motors used in this research program. These measurements are discussed in detail in the experimental section of this paper. Such temperature gradients have also been observed in larger scale motors used in some of the United Technology Center work (Ref. 25). Indeed, some of the UTC heat transfer studies have attributed the spatial variation in convective heat transfer to the changing gas temperature rather than a boundary layer development as was done in this study^(24,25,26,27). The fact that there is a center line temperature gradient implies that the boundary layer temperature profile must fully develop, i.e., the thermal boundary layer extends to the motor port centerline. Schlieren photographs, taken by Carlson and Seader⁽⁸⁵⁾, of the flow from simulated pyrogen igniters located at the head-end of the motor show the flow to be highly turbulent, despite the fact that the Reynolds numbers may be well below classical laminar-to-turbulent transition values. (The high turbulence level may, in large part, be attributed to the shock pattern or Mach disc which typically appears in the exhaust jet of pyrogen igniters.) Thus, as with many cases of turbulent flow in ducts, the velocity profile can be treated as one-dimensional.

Some authors have attempted to account for the heat loss from the flowing gas by calculating an average heat flux to the grain, \bar{q} , and multiplying by the total surface area. This correction depresses the bulk gas temperature. However, this correction is not used to calculate the axial temperature gradient. A simpler means of correcting for this heat loss has been used in this study. The losses will be most severe before first ignition and during the early stages of flame spreading when the surface area available to absorb heat is large. Thus, if an experimental c^* , i.e., temperature, is found for the igniter gas flowing in the motor port, this depressed value of T_{ign} will represent the losses. In this study, the lower value of igniter gas temperature is taken as constant in time and space.

The questions of turbulence and one-dimensionality also enter in another way. This is the question of thermal equilibrium between the igniter and propellant gases. Some authors,^(25,29,30,54) have suggested that the simple assumption of instantaneous mixing is a reasonable approximation with as much as a 500°C temperature difference between the two gases. Above this temperature difference, a mixing equation would have to be added to the analysis. In any event, the temperature difference between the gas flowing over the ignited portion of the grain and the propellant flame temperature will decrease rapidly as flame spreading takes place and the flow is increasingly dominated by mass addition from the burning surface.

The three critical assumptions which have been made in the analysis are $\nabla p = 0$, $\nabla T = 0$ and $h \gg u^2$. These assumptions cannot be removed or relaxed in any easy way. Many of the other assumptions made in this development can be relaxed in obvious ways. The assumptions of caloric perfection, perfect gas and choked nozzles could all be removed at the expense of increased computer time.

II-D. BURNING RATE BEHAVIOR Throughout the development given above the propellant burning rate has not been specified. At this point any burning rate expression, steady or nonsteady, could be coupled to the chamber gas dynamic equations. For example, Ref. 121 gives a nonsteady burning model where both the instantaneous burning rate and flame temperature are functions of the instantaneous pressure and rate of change of pressure. However, it can be shown that the nonsteady burning rate correction would be negligibly small for the rates of pressure rise covered in the class of rocket engines considered in this study, having large port-to-throat area ratios (large free volumes) and rates of pressure rise generally below about 10^4 psi/second^(5,6). This is the range of pressurization rates which have been explored in the experimental portion of this work. Thus, throughout this study, it has been assumed that the propellant burning rate is adequately described by a steady state burning rate equation. The steady state burning rate versus pressure for many solid propellants can be adequately fit over the range of interest by an expression of the form $r_s = k p_c^n$. When a steady state burning rate is assumed, it follows that the nonsteady effect on the flame temperature must also be negligible. Therefore, $\bar{T} = T_b / (T_b)_{eq} = 1$ and disappears from the equations. Substituting $r_s = k p_c^n$ into Eq. II-11 and II-12 results in the following equations:

$$\frac{dP}{dt} = \gamma [S P^n - P T^{1/2} + \dot{m}_{ign} T_{ign}] \quad \text{II-13}$$

$$\frac{dT}{dt} = \frac{T}{P} [(\gamma-1) S P^n - (\gamma-1) P T^{1/2} + \dot{m}_{ign} (\gamma T_{ign} - T)] \quad \text{II-14}$$

It is obvious, however, from Eq. II-11 and II-12 that any steady state burning law could be used if \bar{T} is set equal to one. For example, many propellants have peculiar burning rate pressure curves which cannot be fitted with a simple $r_s = k p_c^n$ law. Such burning rate behavior could even be given in tabular form and used in conjunction with an interpolation scheme.

II-E: SAMPLE THEORETICAL PREDICTION A number of features, which are characteristic of all calculations based on the analytical model, can be explained by examining a typical theoretical prediction, Fig. 2. (The details of the computer program are given in Ref. 132.)

In this calculation, the igniter was chosen to fire as a square wave, i.e., it ends instantaneously when the igniter cut-off criterion is reached. Initially at $t = 0$, the chamber pressure is 15 psia, and the gas temperature is 2600°K, the temperature of the igniter gas. The pressure then begins to rise due to the filling process, and the gas temperature rises due to compression, but as the pressure reaches its preignition equilibrium value, the temperature returns to its initial value of 2600°K. The chamber properties remain at these values (steady flow situation) until the grain begins to burn. The pressure then rises as the mass flow from the propellant becomes significant, and the temperature decreases as the cooler combustion gas of the main propellant mixes with the igniter gas.

When 30% of the grain has been ignited, mass flow from the igniter is cut off, as planned for this calculation, causing a discontinuous change in mass flow rate. Consequently, the pressure decreases momentarily; similarly, the heat transfer to the propellant surface decreases. This causes a sharp drop in flame spreading rate (almost to zero). As the flame spreading continues, the pressure, obeying the chamber filling equations, continues to rise. The

temperature, responding to the compressive effect of the steep part of the pressure rise, climbs again, but its rise is neutralized to some extent by the fact that the propellant combustion gas happens to be cooler than the igniter gas. Depending on the relative magnitudes of these two processes, the temperature may rise, fall, or remain fairly constant. As more and more of the propellant burns, the pressure rises to its equilibrium value, and the temperature begins to fall toward the equilibrium value for the main propellant.

When the flame spreading is complete, a process of feedback ensues whereby the pressure increases, thus increasing the burning rate, and thereby sending more mass into the chamber to increase the pressure further. In this manner, equilibrium conditions are reached in the chamber.

Several interesting general results can be pointed out. One is that when flame spreading is complete, the chamber pressure is usually about 50% of the design equilibrium pressure.^(5,6,7) Also, it was noticed empirically that the maximum value for (dp/dt) occurs at the very beginning of the chamber filling interval. If the maximum (dp/dt) occurs within the chamber filling interval and if the temperature is reasonably close to its equilibrium value, then it can be proved that the maximum value of the pressure rise must occur exactly at the beginning of the interval.⁽⁵⁾ However, it must remain an empirical observation so far that $(dp/dt)_{\max}$ does indeed occur during the chamber filling interval, and its value depends on the pressure level at the beginning of the interval.

III. REVIEW OF PREVIOUS LITERATURE ON THE IGNITION TRANSIENT The literature on the ignition transient can be divided into three general groups: first, there are researches attempting to describe the entire ignition transient, often conducted in conjunction with the development of a particular rocket motor. Second, there are researches into the fundamental processes involved in the ignition process, in particular induction times and flame spreading mechanisms. Third, there are the experimental studies of heat transfer to the propellant grain during ignition.

Within these primary categories many further subdivisions are useful in cataloguing the large amount of work that has been done in this field. There have been a large number of studies concerned with igniter hardware and characterization of igniter materials. These studies have sometimes been referred to as "practical" igniter design work. A great deal of this practical information has been compiled, for example, in "The Solid Propellant Igniter Design Handbook"⁽⁵⁹⁾ prepared by The Bermite Powder Company for the Navy. This reference is recommended to the reader.

A further subdivision can be made on the basis of igniter placement. Igniters placed at the head-end of the motor or distributed down the axis of the motor (as with a piccolo tube igniter) are characterized by having the dominant flow directed toward the exhaust nozzle. Within this head-end category there have been analytical studies of the entire ignition transient and correlation studies. These latter studies have attempted to find empirical and semi-empirical correlations which could be used to size the igniter and to predict the effect of igniter design alterations on the transient operation without considering the details of the associated physical processes.

Aft-end igniters are characterized by an igniter jet penetrating the motor free volume, by passing through the exhaust nozzle toward the head-end, and an opposing flow out the exhaust nozzle. It is obvious that this constitutes a

distinct category because the flow or gas dynamic model for such cases must be significantly different from the head-end type model presented above.

Ignition systems which employ hypergolic materials might be considered as a third subdivision. Hypergolic ignition obviously does not depend on the more conventional modes of energy transfer to the grain. The characterization of hypergolic ignition is considerably different from the Reynolds Number-Nusselt Number type of correlations for convective heat transfer.

III-A. CORRELATION STUDIES Many of the early attempts to describe the complete ignition transient for solid propellant rocket motors focused on isolating relatively simple groupings of a few parameters which could be used to correlate igniter properties versus motor geometry. Examples of this type of work are References 45, 46, 47 and 48 by Bryan, Lawrence and Edwards of NOL. These references represent a research effort extending over some four or five years. Considering Ref. 48 in particular, 53 rocket motors of World War II and later vintage were considered in an attempt to establish minimum motor ignition energy requirements. The 53 motors considered used double-base propellants and composite propellants with both ammonium perchlorate and potassium perchlorate. The grain configurations ranged from internal burning cylinders and cruciforms to internal-external burning cylinders. A few end-burning grains were also considered. The igniter materials included black powder, double-base and ammonium perchlorate propellants and seven different pyrotechnic compositions. This entire group of motors and igniters was correlated on the basis of Q_T , the total igniter energy, (Q_T = weight of igniter x heat release per gram) versus Aq_c . A is the total area exposed to the igniter output, including the propellant surface area and exposed liner and metal parts. q_c is the required ignition energy for the particular propellant per unit surface area. q_c was defined by the results of lock-stroke compressor studies for a 3 millisecond ignition delay. A secondary correlation of $(Q_T/q_c A)$ vs. $L\sqrt{4\pi A_p/A}$ was also proposed. Aside from marveling at the naive hope of these authors that nature would be so simple as to permit such a simple correlation of such a range of systems, we must also point out that the definition of required ignition energy, q_c , is a rather arbitrary one, and that no consideration is given to the rate of delivery of the igniter stimulus. (Later in this paper, it will be shown that the same total igniter mass delivered at progressively decreasing rate will lead to a hangfire and eventually a complete misfire.) At best, it would seem reasonable that such a correlation would be valid within a single family of motor configuration and igniter type.

The Bryan-Lawrence Correlation Equation was also used in Reference 63 (BPC, 1962) to correlate data taken in micro-motors.

$$Q_T = 38 \left[A q_c \left(L \sqrt{4\pi A_p/A} \right)^{0.59} \right]^{1.06}$$

It was reported that this gave consistently lower values of igniter weight than was required for successful ignition in the experiments. It was claimed that this equation would provide for successful ignition for only 50% of the test firings. Part of the difficulty was also attributed to the definition of q_c as given above. A new correlation was proposed:

$$Q_T = \frac{b A P_i}{\pi} \sqrt{E_{ig}/K_M}$$

where Q_T and A are the same as defined above. b is a function of the igniter material. P_i is the pressure achieved by firing the igniter in an inert motor.

K_N is the usual A_D/A_T and E_{100} is the threshold ignition energy (50% go-no-go) at 100 psig. Now at least a parameter, b , characterizing the particular igniter material appears. E_{100} , as a measure of the ignition energy of the propellant in question, is justified by saying that most ignition takes place near this pressure level. Still lacking is any consideration of the distribution of the igniter energy over the grain or its rate of delivery.

References 61 (BPC, 1964), 62 (BPC, 1965) use the equation given above in a simplified form,

$$Q_T = CA\sqrt{E_{100}}$$

where C is an empirical constant. The correlation is considered valid for an igniter whose mass is 10 grams or more. The comments given above apply here as well.

Reference 62 (BPC, 1965) also gives a correlation for the maximum pressure developed by an igniter whose weight is determined by the equation given above. In this correlation K_N is plotted against peak gauge pressure per gram of igniter material per cubic centimeter of free volume of the motor. The data necessary for this correlation was obtained from micro-motors ignited by boron-potassium nitrate pellets burned in a piccolo tube igniter chamber. It is reported that the correlation is restricted to small motors with a free volume-to-nozzle throat area ratio of less than 100. However, even within this regime the questions of mass flow rate of the igniter material and possible extension to other igniter materials or igniter configurations are not considered.

Reference 33 (Aerojet-General, 1962) presents a step-by-step igniter sizing based on several empirical correlations. First, the weight of the igniter is found from a correlation of igniter charge weight vs. motor free volume. Second, this initial value is checked against a correlation of total igniter energy divided by total surface area vs. energy delivery rate. (At last this crucial parameter is considered!) Third, the length of the motor versus igniter weight is compared to similar motors. Based on this consideration the igniter weight is increased by 45%.

This last example does contain two elements missing from the references mentioned above. It considers igniter energy delivery rate and, to some extent, the distribution of area through the motor length-igniter weight consideration. However, correlations such as these must always be viewed with great caution and skepticism. They are all attempts to simplify very complex situations. It is very questionable that they retain the essential elements, even for rocket geometries, igniter configurations and materials and propellant ignition requirements that would fit within a single "family". That such correlation can be extended across major design or propellant variations is even more doubtful. At best they are to be trusted for initial igniter sizing. This sizing can then be checked in a rational manner with an analysis similar to that given in Chapter II. In this way questions of the mode and rate of energy transfer, the impingement of the igniter jet, the distribution of propellant surface area (particularly hard-to-ignite stagnant regions) and the ignition requirements (pressure level and flux-time history) can be considered in detail. These correlations are but the first step in the igniter design, not the last.

III-B: ANALYTICAL MODELS OF THE IGNITION TRANSIENT The earliest analysis of the ignition transient was published by von Karman and Malina in 1940⁽⁶⁸⁾. This analysis makes no effort to describe the flame spreading interval. An arbitrary chamber pressure at the instant of full ignitedness was assumed. A second highly unrealistic initial condition, that the chamber temperature is at room temperature at the time of full ignitedness, was assumed. These faults, coupled with an over-simplified burning rate law ($r = k_1 + k_2 P_c$) and an error in the energy equation, negate any practical results of this analysis.

In 1962 Baker⁽¹⁸⁾ of UTC published a set of gas dynamic equations similar to those developed in Chapter II. These equations were one of the first published developments to include the dynamic compression effect on the chamber temperature. This development also appears as an appendix to Ref. 19 and was used in that work together with measured flame spreading rates. In this way the questions of an ignition criterion, flame spreading mechanism and spatial distribution of heat transfer were avoided. A steady state burning rate, $r_{ss} = kP_c^n$ was used. With these aids, good predictions of the entire ignition transient were made for a motor with a slotted cylindrical grain geometry ignited by a head-end pyrogen. In 1963 Fullman and Neilsen⁽²⁰⁾, also of UTC, again used the same gas dynamic equations. In this work the critical surface temperature ignition criterion was used in conjunction with a fully developed turbulent pipe flow heat transfer correlation, $Nu_p = 0.0234 Re_p^{0.8}$. This combination was used to predict first ignition. After first ignition, observed flame spreading rates were fitted with a linear function of time. This linear flame spreading rate took account of both the slow spreading rate into the stagnant head-end of the motor and the accelerating spreading rate downstream. A steady state burning rate law was also used in this analysis. Fullman and Neilsen also presented an isothermal analysis which neglects the energy equation. The same first ignition criterion and flame spreading description as employed for the dynamic temperature case were used. Both of these analyses were compared to experimental data. The given flame spreading rates almost guarantee reasonable agreement between theory and experiment. This is obtained for both the dynamic and isothermal analyses. The unfortunate thing is that this limited comparison for a single case is used as justification for always ignoring the dynamic energy equation. It is claimed that this assumption introduces only a 5% error. As can be easily seen in Ref. 10, the degree of error introduced is very much a function of the rate of pressurization as controlled, in part, by the motor free volume and the difference between the igniter gas temperature and propellant flame temperature.

Following these early leads, there has been a very active research program investigating various aspects of ignition and of the ignition transient by a group at UTC.^(21 through 31) Although the personnel of this group has changed over the years, a reasonably consistent theme, following the pattern established by Fullman and Neilsen, has been carried through the work. The local ignition event was characterized by a constant critical ignition temperature. The solid phase heat equation was solved with a boundary condition which includes a flux term due to heterogeneous attack on the surface by active gas species and the usual convection and radiation fluxes from the gas phase. Isothermal gas dynamics were used, i.e., T_c is not a function of time or space. Only the mass continuity equation was written. Various attempts were made to describe the heat transfer, particularly for those situations where convection dominates. The classical fully developed turbulent pipe flow heat transfer correlation based on diameter mentioned above was used to predict the film coefficient for

igniter alone, h_{ign} . The effect of mass addition from the burning propellant surface was accounted for by an empirical expression, $h_{amu} = h_{ign} (m_g + m_{ign}/m_{ign})^{0.5}$. The axial variation in heat flux was attributed to the drop in gas temperature down the propellant grain. This is inconsistent with the gas dynamic equation used.

In addition to this basic model, the UTC group has published extensive data on measured flame spreading rates and correlations of ignition delays versus flux level and pressure. (24,25,26)

An example of the comparison between a theoretical prediction and an experimental test firing from the UTC work is shown in Fig. 7. This prediction was made for a motor using a cylindrical grain. The igniter was located in the head-end of the motor and used canted nozzles and an aluminized igniter material. The isothermal gas dynamic equations were used.

Beginning in 1964, Paul, Lovine and Fong have published a series of papers dealing with various aspects of ignition and the ignition transient. The first of this series, Ref. 35 (Aerojet-General, 1964), presented a gas phase model of the local ignition event. This model requires knowledge of the reactant concentrations near the surface of the propellant. This is a difficult problem to solve in a flowing boundary layer situation and is solved only approximately for the stagnant case. Also in this same paper, the dynamic mass continuity and energy equations for the motor chamber are presented. The gas dynamic equations are essentially the same as those developed in Chapter II but include a heat loss term based on a fully developed turbulent pipe flow equation, $Nu_0 = 0.023 Re_0^{0.8}$. In Reference 36 (Aerojet-General, 1964) by the same authors, the same gas dynamic equations without the igniter term or the heat loss term are combined with a nonsteady nozzle flow equation and a nonsteady burning rate reacting to the rate of pressurization.

$$r_b = r_{ss} \left[1 + \frac{Nu_0}{r_{ss}^2} \frac{dP/dt}{P} \right]$$

This is similar to a model previously introduced by von Elbe^(111,112) and has since been shown to involve a grave conceptual error.⁽¹²¹⁾ These two nonsteady effects and the dynamic temperature result in predictions of chamber pressure overshoots where none would have previously been predicted.

A third paper by the same authors, Ref. 37 (Aerojet-General, 1964) considered the question of flame spreading. A motor configuration with the igniter jet impinging downstream of the propellant leading edge was considered. The flame spreading was treated in three parts. The area subjected directly to the igniter jet impingement was taken as being instantaneously ignited (no induction interval). The heat transfer downstream of the igniter jet impingement zone was taken as being independent of axial distance and was correlated with a classical pipe flow heat transfer equation. This correlation, coupled with the use of a critical temperature ignition criterion, results in the obvious error of predicting that the entire downstream surface area is ignited at the same time (instantaneous flame spreading). A very approximate equation was used to estimate the heat flux as a function of axial distance and time in the region upstream of the igniter jet impingement zone. This description of the flame spreading interval was coupled with a steady state burning rate law, $r_{ss} = K P_c^n$, and the coupled gas dynamic equations, but with both the

igniter source term and the heat loss term left out. The comparison between experiment and theory shown in Fig. 8 is only fair for the single case shown.

Later in 1964 Lovine and Fong published a report (Ref. 39) in which a flat plate heat transfer expression was used, $Nu_x = 0.0296 Re_x^{0.8}$. The axial variation of the gas temperature was also considered, resulting in an expression for the heat flux as a function of position. (This analysis will be considered in detail later.) This concept of a temperature gradient is not consistent with the gas dynamic equations, even though the mean heat loss is subtracted. However, if the temperature appearing in the gas dynamic equations is interpreted as a mean chamber temperature, this may be permissible. Using this heat transfer and the gas phase ignition criterion mentioned above, the time to first ignition was predicted. This was compared to motor data where first ignition was identified as the first rise of pressure from the pre-ignition level. This definition of first ignition is difficult to apply because the chamber pressure is relatively insensitive to the mass addition from the first small area ignited. However, good agreement between experiment and prediction was claimed. The case of post-ignition ballistics ($S=1$ and $\dot{m}_{ign}=0$) was treated with the full dynamic equations and the nonsteady burning rate and nozzle flow analyses mentioned above.

In Reference. 40 (Aerojet-General, 1965) Lovine and Fong attacked the heat transfer problem by solving directly the turbulent, incompressible, constant property boundary layer with zero pressure gradient. The Blasius $(1/7)^{th}$ power velocity profile was assumed. It is not obvious that this is an adequate description of the boundary layer developing from an impinging jet and, in any event, the strong axial temperature gradients tend to invalidate the incompressible assumption. That is, the boundary layer may be incompressible (energy equation uncoupled) at each location, but the strong axial temperature gradient will recouple the energy equation. The analysis could not be extended directly to the flame spreading interval because of the mass addition from the surface. This boundary layer heat transfer equation was considered in conjunction with the bulk gas dynamic equation and the gas phase ignition model mentioned above to predict first ignition. The flame spreading rate was assumed to be a given function of time for the post-first-ignition ballistics.

References 39 and 40 also include a ballistic analysis of the igniter using gas dynamic equations similar to those given above. In Ref. 40 closed form solutions are obtained for the particular cases of n , the igniter material burning rate exponent, equal to 0, $1/2$ and 1.

In 1968 Micheli and Linfor⁽⁴³⁾ presented the latest in the ignition and ignition transient research carried out at Aerojet-General. For the gas dynamics model this work treated the coupled mass continuity and energy equations with the momentum equation uncoupled, as was presented in the analysis given in Chapter II. The bulk heat loss from the igniter gas was subtracted out. This loss was reported to be on the order of 40% of the total energy of the igniter gases. Despite the fact that this loss must establish axial temperature gradients and must vary with time as ignition and flame spreading proceed, spatial uniformity and a constant loss fraction was retained. Local ignition as a function of propellant aging, core release left on the propellant surface, smoothness of the grain and hygroscopicity of the propellant was discussed in some detail. The model of ignition which was settled on was a critical surface ignition temperature but it was modified in the following way. The integral

for the surface temperature as a function of the time varying flux was written as

$$T_s = T_o + \frac{1}{\lambda_p} \sqrt{\frac{\alpha_p}{\pi}} \int_0^t \frac{\dot{q}(t-\tau)}{\sqrt{1-m}} d\tau$$

where m was determined experimentally from arc image ignition data. For the case of an inert solid, as presented above, $m=2$. Of course, it must be recognized that a wide range of values of m 's between 0 and 2 can be obtained from the arc image as a function of the flux range and the rate of change of flux.

The experimental test firings conducted in this study employed a grain geometry with a finned head-end section, a cylindrical port and a stagnant region of the grain around a sunken nozzle. The igniter was a head-end pyrogen whose jet impinged just upstream of the point at which the finned foreclosure joined the cylindrical port. The three distinct areas, stagnant head-end, cylindrical bore and stagnant aft-end, were characterized by three different heat transfer correlations. They are, respectively:

$$h_{conv} = 0.029 \frac{\lambda_g}{(L_i - x)^{0.2}} \left(\frac{\gamma \dot{P}_c}{RT_c} \frac{x}{\mu} \right)^{0.8} Pr^{0.3}$$

$$h_{conv} = 0.033 \frac{\lambda_g}{(x - L_i)^{0.2}} \left[\frac{(L - x) \dot{m}_{ign} + (x - L_i) \dot{m}_o}{\mu A_p (L_o - L_i)} \right]^{0.8}$$

$$h_{conv} = 0.029 \frac{\lambda_g}{(x - L_o)^{0.2}} \left[\frac{\gamma \dot{P}_c (L_o - x)}{\mu RT_c} \right]^{0.8} Pr^{0.3}$$

A radiation contribution was also considered. This was said to be particularly important in the stagnant regions. These heat transfer correlations will be discussed in detail later.

The burning rate used in this study was the nonsteady equation advanced by earlier Aerojet workers and mentioned above⁽³⁶⁾. Excellent agreement between experiment and theory for one test firing was shown. The theoretically predicted effects of initial grain temperature and radiation absorptivity were also shown. These results are displayed in Figures 9 and 10.

In 1964, deSoto and Friedman^(22,23) published a treatment of the entire ignition transient. This study was originally guided by the senior author of this paper and consequently developed along lines similar to those developed in Chapter II. The significant aspect of the study was that it was the first work to describe the entire ignition transient, including the flame spreading interval. This was done by adopting the flame spreading hypothesis of Summerfield⁽⁴⁾ and a constant propellant surface ignition temperature criterion. (see detail explanation in Chapter II.) The analysis was carried out only for the case of an isothermal chamber temperature. No comparison with experimental

results was given.

A theoretical analysis of the ignition transient was published by Bradley in 1964. This work presented a correct treatment of the energy equation, i.e., the response of the chamber temperature to the dynamic compression. The principal failure of this research was, in the author's words, the "naively assumed" flame spreading model relating the rate of spreading to the burning rate by a linear relationship.

An experimental and theoretical analysis of the ignition transient was carried out in 1964 by Sharn et. al.⁽⁵⁵⁾. This study used the von Elbe ignition criterion.⁽¹¹¹⁾ This model requires that not only a critical surface temperature be attained, but also that a critical thermal profile be established in the solid. The critical profile is the one associated with steady state burning at the environmental pressure. Thus, this ignition criterion is pressure dependent. This characterization of local ignition was combined with a modified pipe flow heat transfer correlation, $h_{conv} = 70 \left(\frac{\dot{m}}{A_p} \right)^{0.8} (1 + D/L)^{0.7}$ plus a radiation term to predict the average ignition time of the grain. That is, the entire grain was assumed to ignite instantaneously at some average ignition time. A steady state burning rate law was used. The chamber gas dynamics were treated by considering only the mass continuity equation, i.e., the isothermal analysis. A large part of this particular study was devoted to characterizing the output of a pyrotechnic igniter by: 1. A ballistic analysis of the igniter which is shown to be inaccurate (Ref. 42, NOL, 1962), 2. An empirical correlation for the peak igniter chamber pressure; and 3. A simple integration of the measured pressure-time curve to obtain the average igniter mass output. The entire analysis was compared to experimental data taken in a motor with a cylindrical grain and ignited by a Hi-Low pyrotechnic igniter located at the head-end. Only one comparison of experiment and theory is given in the reference. This comparison is given in Fig. 11. This single example shows excellent agreement over the early portion of the run but prediction and experiment diverge over the later portion of the transient.

In 1966 Adams^(96,96,97) published a study involving experimental test firings and the by now familiar isothermal treatment considered by the many authors mentioned above. The effective flame spreading rates were considered as input to the computer program. No attempt was made to predict the flame spreading interval. An attempt was made to include erosive burning effects by taking a single (average) value of the Mach number along with the axis of the port, but this violates the mass continuity equation. Despite this fact, the agreement between theory and experiment shown in Fig. 12 was taken as proof that "ignition spikes were caused primarily by erosive burning effects". The effect of erosive burning on the ignition transient in small port-to-throat area ratio motors was not considered in the model developed in Chapter II where the velocity in the port was assumed to be small. This mechanism may well be significant in certain situations. However, the omission from Adams' model of the dynamic chamber temperature and the axial pressure gradients which must exist in such motors weakens the basis of his conclusions.

In 1968 Peleg and Manheimer-Timmat⁽⁷⁰⁾ published a study of the ignition transient which arrived at a set of differential equations similar to those developed above in Chapter II. The only essential difference between the two models is the addition of the surface heat release term included in the analysis given in Chapter II. These two models would predict the same trends and effects

for vigorous ignition situations, provided the same heat transfer correlation was used. There are serious questions which can be raised about the quality and interpretation of the heat transfer data reported in this reference. Rather slow response thermocouples (10 msec rise time) were used in the heat transfer study. This may have affected the quality of some of the data.

Based on these data, the authors asserted that there was instantaneous flame spreading along the outer diameter of the star-shaped grain used in this study and that the flame spreading along the sides of the star points was slower, controlled by a heat transfer correlation similar to that reported in Refs. 77 and 81, $St=0.046Re_x^{-0.2}$. Ignition upstream of the igniter jet impingement point was attributed to only radiative heat transfer. It is not obvious that heat conduction and convective contribution due to large scale recirculation eddies in the "stagnant" region can be ignored. (An approximate analysis of this sort for the stagnant region by Paul, et.al. was mentioned above, Ref. 37.) The agreement between experiment and theory appears to be good but this may be misleading because of the compressed time scale used in presenting the comparisons. Comparisons of experiment and theory for a series of test firings is given in Fig. 13.

In 1968 Falkner and Kilgroe⁽⁶⁷⁾ of CETEC presented an analysis of the ignition transient. The gas dynamic model presented above in Chapter II was used. Indeed, an early version of the Princeton Ignition Transient Computer Prediction Program was used. (The most recent version of this program is presented in Ref. 134.) The critical surface temperature ignition criterion for an inert solid phase was used. A steady state burning rate equation was used. The heat transfer correlations of the form developed earlier by Kilgroe⁽³¹⁾ were used.

$$Nu_D = k_2 \left[1 + (1 - k_2) \frac{x}{D} \right] (1 - k_3) Re_D^n$$

for the stagnant region upstream of the igniter jet impingement point and

$$Nu_D = k_2 \left[1 + k_3 \exp(-k_4 \frac{x}{D}) \right] Re_D^n$$

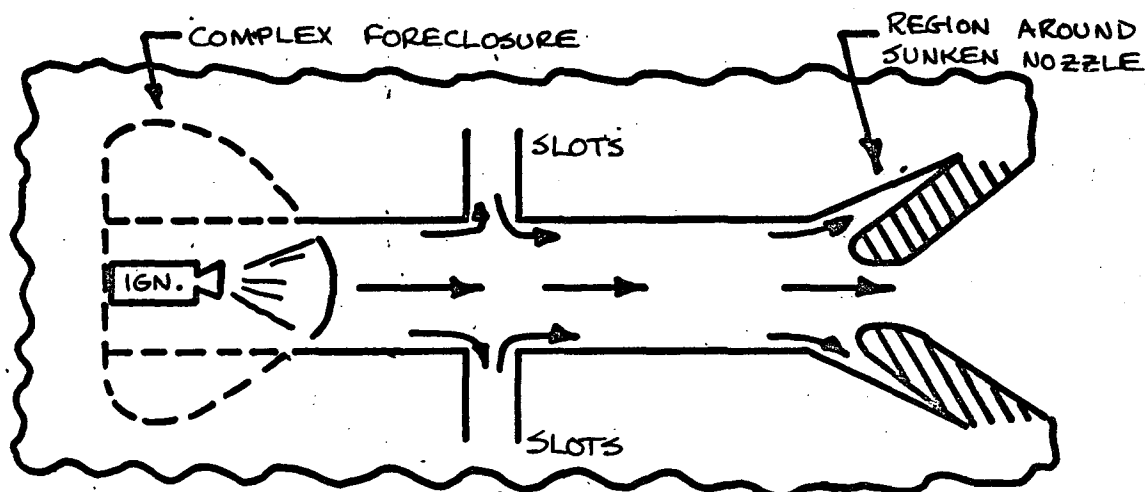
for the region downstream of the impingement point. The predicted flame spreading and ignition transient using Kilgroe's⁽³¹⁾ values for the k 's and $n = 0.8$ was compared to data given in Ref. 29. As can be seen in Fig. 14, prediction of first ignition compared well with the measured time but the predicted flame spreading rates after first ignition exceeded the measured values. Good agreement between predicted and measured flame spreading rates was achieved by changing n to 0.5 and adjusting k_2 to keep the flux level at the impingement point constant. This is shown in Fig. 15. Using these adjusted values, predictions of the transient for a large motor with a deeply slotted cylindrical grain were made. The agreement between experiment and theory shown in Fig. 15 for this motor ranged from good to fair. However, the time to full pressure was always predicted within 10%. The difficulties were attributed to the inadequacy of the heat transfer correlations for complex geometries.

This review is not complete. There are other authors who have made notable contributions to various aspects of the ignition transient problem. The references mentioned above and many others are summarized in Table I. However, the papers mentioned above give a sampling of the approaches used and the progress made in the past few years. These efforts can now be summarized.

It is believed that for the class of motors considered, the most correct gas dynamic equations which have been solved to date are those which have been formulated and tested by a number of authors (5-15, 18-20, 35, 36, 39-41, 43, 54, 65, 67, 68, 70, 71) and which are in all cases similar in principle to those presented in this paper in Chapter II. As was pointed out in that chapter, a number of limiting assumptions used in this development can be relaxed to adapt the model to other situations. The characterization of the local ignition event by a critical ignition temperature has been almost uniformly accepted, but discretion must be used in limiting situations of, for example, sub-atmospheric induction pressures. The addition of the self-heating term is a new aspect of the problem, but is quite reasonable in marginal ignition situations. The use of a steady-state burning-rate law with no erosive correction term is generally accepted, particularly for comparatively slow transients. As was pointed out above, the model does not exclude the use of a more sophisticated burning rate law. The most limiting assumption of the gas dynamic model is that of a spatially uniform temperature. The other two important gas dynamic assumptions, $\nabla P_c = 0$ and $h \gg u^2$, are indeed limiting, but are not believed to be as critical as the $\nabla T_c = 0$ assumption. Within this framework the major difficulty remains the question of the heat flux to the propellant grain.

III-C: CONVECTIVE HEAT TRANSFER There is slowly evolving extensive literature on the heat transfer to propellant grains prior to first ignition and during the subsequent flame spreading interval. As has been seen, such information is essential to the prediction of the overall pressure transient, but presents a most arduous task due to the variety of igniters, igniter configurations and motor geometries. The discussion in Chapter II pointed out that the flow in any rocket motor is far from the ideal flow which an aerodynamicist would like to deal with. The entering flow is not uniform because of the igniter jet breakup and/or shock pattern. This results in a poorly defined leading edge and an unknown turbulence level and intensity. The propellant surface over which the flow passes is rough. There is mass addition from the surface and chemical reaction within the boundary layer. Axial temperature gradients, and hence property gradients are known to exist. The flow is nonsteady, particularly during the rapid flame spreading interval.

As a useful guide, the heat transfer in a rocket motor can be divided into a number of coupled but distinct classes. The first obvious division is to consider the heat transfer before and after the first flame has appeared on the grain. The flow, and subsequent heat transfer in stagnant volumes, can be taken as an additional division. These stagnant regions can be the volumes forward of the igniter impingement, slots perpendicular to the direction of the main flow or volumes whose openings face the flow at some angle.



The convective heat transfer in the straight port region prior to first ignition has received, by an enormous degree, the greatest attention. There are two reasons for this. First, it is the simplest situation and second, it holds the promise of being tractable with classical heat transfer correlations, despite the difficulties mentioned above.

Fully developed turbulent flow in pipes has been investigated for many years by many researchers. All heat transfer text books give examples of these empirical formulas. They are generally of the form given by Dittus and Boelter:

$$Nu_{DB} = 0.0243 Re_D^{0.8} Pr^{0.4}$$

Various authors give different values for the leading coefficient but an exponent on the Reynolds number very near 0.8 is typical for all turbulent flows. In the entrance region of a pipe the momentum and thermal boundary layers are not fully developed and thus, a dependence on the axial distance from the leading edge must be introduced. This has been done in a variety of ways. A function of x can be inserted in the fully developed correlation.

$$Nu_D = a f(x) Re_D^{0.8} Pr^{0.4}$$

Alternately, one may retreat to the flat plate form. This is quite reasonable when the boundary layer is thin compared to the diameter of the tube.

$$Nu_x = b Re_x^{0.8} Pr^{0.4}$$

The typical head-end pyrogen rocket igniter introduces many variables which, obviously, do not appear in these simple correlations. The shock structure in the igniter jet induces a vorticity and an accompanying turbulence level which may not be truly characterized by a Reynolds number. That is, a Reynolds number is not a true similarity parameter downstream of a curved or other complicated shock structure. The work of Carlson and Seader^(85,86) clearly demonstrates that the heat transfer level is a function duct-to-igniter throat diameter ratio. Other parameters which could reasonably be introduced are igniter nozzle half-angle and exit diameter, igniter exit Mach number and igniter jet-to-duct pressure ratio. All of these parameters effect the igniter jet expansion and shock pattern.

With these reservations in mind, we can now examine in some detail several of the many heat transfer studies. Carlson, Seader & Wrubel (85,1965, 86,1967; 87,1967; 88,1967-Rocketdyne) have carried out an extensive study of the heat transfer from pyrogen igniters to grains of various configurations. This study used a simulated igniter of hot nitrogen flowing through thin walled stainless steel test sections at a pressure level of about 600 psia. The test section gas temperatures ranged from 615°K to 800°K. These pressures are high and the temperatures low compared to typical pyrogen igniters. The igniter nozzle types considered were axially directed supersonic and sonic and three-ported canted nozzles. The test sections simulated cylindrical, star and conocyl shape grains. The general observations concerning the flow patterns can be summarized: The initial pressurization of the port was accomplished by a nearly normal traveling shock wave. (This was accentuated by the high port-to-ambient pressure ratios achieved.) The igniter jet disintegrated after passing through a single shock wave at the plane of maximum jet diameter. Jets from sonic igniters disintegrated in a shorter distance than those from supersonic igniters.

Turbulence scale was large and varied as a function of flow rate and nozzle type. The heat transfer was generally steady with no transient behavior (see Reference 88). (Some nonsteady heat transfer behavior has been observed during the start-up of the pyrogen igniter used in the studies conducted by the authors of this paper. see Ref. 134.) From heat transfer considerations these authors concluded that axially directed sonic igniter nozzles are preferable to either axial supersonic nozzles or canted three-port nozzles. In the first case, the stagnant region upstream of the jet breakup was too large. In the latter case, the maximum heat transfer was increased but the distribution of flux was less favorable.

The heat transfer data from this study were correlated by a local Nusselt number based on diameter normalized by the Dittus-Boelter Nusselt number given above. The dependence of the heat flux on length, igniter nozzle-to-port diameter ratio and port-to-throat area ratio was given graphically. Figures 3 and 4 are examples of these data for cylindrical grains. It was also found that conocyl-shaped grains could be treated as cylindrical grains. The decrease in heat transfer due to increasing port diameter in the conical section was accounted for by the x/D_p relations developed for straight cylinders. No general correlation of star-shaped grains was achieved.

A series of investigators at UTC have carried out heat transfer studies from pyrogen igniters. If the most recent report by Kilgro (Reference 31, 1967) can be taken as summarizing, in a sense, all of the UTC work, we are presented with several empirical equations for the maximum heat transfer near the igniter jet impingement point and for the regions both up and downstream of this point. This work was carried out in a cylindrical copper duct for axial directed and canted igniter nozzles. The duct apparently was not fitted with an exhaust nozzle. The igniters burned both an unaluminized and an aluminized propellant. For the axial igniters the correlations are:

$$Nu_D = 0.033 \phi Re_D^{0.8} Pr^{0.3}$$

with

$$\phi = \left\{ \begin{array}{l} 1 + 1.23 e^{-0.418 x/D} \\ 2.23 - 0.7 x/D \end{array} \right\} \quad \begin{array}{l} \text{Downstream} \\ \text{Upstream} \end{array} \left. \vphantom{\begin{array}{l} 1 + 1.23 e^{-0.418 x/D} \\ 2.23 - 0.7 x/D \end{array}} \right\} \begin{array}{l} \text{Nonaluminized} \\ \text{igniter} \end{array}$$

$$\phi = \left\{ \begin{array}{l} 1 + 2.0 e^{-0.5 x/D} \\ 3 - 1.25 x/D \end{array} \right\} \quad \begin{array}{l} \text{Downstream} \\ \text{Upstream} \end{array} \left. \vphantom{\begin{array}{l} 1 + 2.0 e^{-0.5 x/D} \\ 3 - 1.25 x/D \end{array}} \right\} \begin{array}{l} \text{Aluminized} \\ \text{igniter} \end{array}$$

where x is measured from the impingement point. The qualifications given for these equations are that they are valid only for jet-to-duct pressure ratios from 20 to 45 and duct-to-igniter nozzle diameter ratios from 10 to 15. The peak values for (x/D) ratios of less than 2 and Reynolds numbers less than 3.6×10^4 are given by

$$Nu_{MAX} = 12.25 Re_D^{0.285} Pr^{0.3} \quad \text{Nonaluminized}$$

$$Nu_{MAX} = 0.01 Re_D Pr^{0.3} \quad \text{Aluminized}$$

In 1965 Lovine and Fong⁽³⁹⁾ presented an interesting correlation. The classical flat plate correlation was assumed to be valid.

$$Nu_x = 0.0296 Re_x^{0.8}$$

The variation of the bulk gas temperature down the port was calculated from the energy equation.

$$C_p \dot{m}_{ign} \frac{dT_g}{dx} + P \dot{q} = 0$$

where P is the perimeter of the port. The approximation was made that the driving potential across the boundary layer is $(T_g - T_s) \approx T_g$ for large gas temperatures. This was combined with the film coefficient from the flat plate correlation given above and substituted into the energy equation for \dot{q} . The differential energy equation was then solved for $T_g(x)$. This was multiplied by the film coefficient to obtain the heat flux as a function of position.

$$\dot{q}(x) = 0.0296 \Delta H_r \left(\frac{\mu}{x}\right)^{0.2} \left(\frac{\dot{m}_{ign}}{A_p}\right)^{0.8} \exp\left[-0.037 \left(\frac{\mu}{\dot{m}_{ign}}\right)^{0.2} \frac{P x^{0.8}}{A_p^{0.8}}\right]$$

where ΔH_r is the igniter propellant heat of explosion. This should then account for both the developing boundary layer and the axial temperature gradient. This certainly is a reasonable analysis and the only one which attempts to account for both factors. There is, however, an inconsistency in the analysis. The use of a flat plate heat transfer correlation implies that the boundary layer is not fully developed. That is, the boundary layer thickness is less than half of the pipe diameter. Obviously, if the thermal profile does not extend to the center line, the temperature along the center line of the port cannot vary. In this case, the driving temperature across the boundary layer remains constant within the limits of the assumption of $(T_g - T_s) \approx T_g$. A further limitation of this analysis is that in order to account for heat transfer after first ignition, the problem would have to be resolved for T_g as a function of space and time, and should, in fact, be coupled to the chamber gas dynamic equations. This analysis was compared to steady state data obtained in an instrumented inert cylinder and good agreement was achieved except near the impingement point where large scatter was encountered. When this analysis⁽³¹⁾ was compared to the correlations of Carlson et.al.,^(85,86,87,88) and Kilgroe^(15,34) and to the correlation developed in studies conducted by the authors of this paper^(15,34) the flux values were found to be a factor of between 4 and 5 smaller. This is attributed to the fact that the heat flux near the impingement point is greatly underestimated by the classical flat plate correlation.

The heat transfer correlations used by Micheli & Linfor⁽⁴³⁾ were given above. The equation for the cylindrical section of the grain can be transformed for the steady flow case in the following way: x is measured from the impingement point, \dot{m}_{ign} is the flow rate toward the exhaust nozzle at $x=0$, and the aft-end stagnant region is eliminated by taking $L_0=L$. This allows the equation for h_{conv} to be recast in the form of a steady state correlation.

$$Nu_x = 0.033 Re_x^{0.8}$$

For the dynamic case, the mass flow rate in the Reynolds number was corrected for the mass storage due to the pressurization in a manner identical to that described in Chapter II. Unfortunately, the authors of this paper are not explicit about what driving potential across the boundary layer was used with

this correlation. It is not known whether the variable gas temperature analysis of their co-workers at Aerojet-General, Lovine & Fong⁽³⁹⁾, was adopted or whether a constant mean temperature difference was used.

In 1966 Allan, Bastress and Smith^(77,78,81) of A. D. Little presented a heat transfer correlation for data obtained in simulated cylindrical motors. The igniters burned B-KNO₃ pellets and two propellants designated ADL-2 and ADL-5. The analysis considered a multiple film boundary layer in an attempt to account for chemical reactions which may be occurring at some position within the boundary layer. Thus, for the two film case, the driving potential becomes

$$\dot{q}_{\text{conv}} = h_{\text{conv}} \left[(T_g - T_s) + \frac{\Delta Y \Delta H}{C_p} \right] = h_{\text{conv}} \frac{\Delta H_{\text{total}}}{C_p}$$

where ΔY is the species change due to the reaction and ΔH is the enthalpy difference. Therefore, the bracket term represents the total enthalpy difference across the boundary layer. With this concept of driving potential, and with the assumption it is independent of x , the heat transfer correlation arrived at was of the form

$$St = 0.08 Re_x^{-0.2}$$

or, solving for film coefficient,

$$h_{\text{conv}} = 0.08 \left(\frac{\dot{m}}{A_p} \right)^{0.8} / x^{0.2}$$

for Prandtl number equal to one. This is expected to apply well downstream of the igniter so that the infinite values at $x=0$ are avoided. A similar correlation was reported by Peleg and Manheimer-Timnat⁽⁷⁰⁾ with a small change in the coefficient. The correlation was given above in Chapter III-B.

The question now becomes how to compare these various correlations. Figure 6 shows the film coefficients, h_{conv} , given by each of these correlations (except the Lovine and Fong correlation). A constant value of viscosity and gas thermal conductivity was assumed. The mass flow rate per port area and distances from the impingement or maximum flux point were scaled to the laboratory size motor used in this particular study. (See Figure 6 for details.) This may not be a completely fair means of comparing the various correlations because of the wide range of variables involved. For example, the values calculated from the work of Carlson et. al.^(85,86,87) are for single values of A_p/A_t and D_p/D_{ign} . The shock structure in the igniter jet in the case of this study was radically different since a shock-separation pattern was forced to occur in the igniter nozzle. However, if these differences are kept in mind and also the limits of the assumptions and interpretations of other work, it would appear the correlation developed in this study and that by Allan, Bastress and Smith^(77,78,81) form an upper bound on the film coefficient and the correlation used by Micheli and Linfor⁽⁴³⁾ forms a lower bound. The correlations by Carlson, Wrubel and Seader^(85,86,87,88) and Kilgroe⁽³¹⁾ fall in the middle and show good agreement. The greatest lack of agreement is in the region of the impingement point, between $x/D=0$ and $x/D=2$. Here Kilgroe adjusted to a value which is higher than that of Carlson et.al., but still below that measured in this study. Most studies have reported the greatest scatter in the heat transfer data near the impingement point, and so the largest degree of disagreement between the various studies is to be expected there. Three of the studies gave the x dependence of \dot{q} as $x^{-0.2}$ but

Kilgroe and Carlson, et. al. gave slightly higher order dependences. However, this can not be translated directly to the dependence of \dot{q} on x . This depends not only on $h_{conv}(x)$ but also on what was assumed about the driving potential as a function of x . This study and that of Allan et. al. assumed a constant driving force. Micheli and Linford do not specify what was assumed. The other two studies considered apparently measured the centerline gas temperature at the location of the flux gauge and thus, $T_g(x)$ would have to be known in order to obtain $\dot{q}(x)$. Because $T_g(x)$ decreases with increasing x , these two correlations would show the heat flux decreasing more rapidly with x than $h_{conv}(x)$ would imply.

The convective heat flux is an even more difficult problem after first ignition than during the induction interval. The flow field is now highly nonsteady since the mass flow rate and chamber pressure are varying rapidly with time in response to the increasing mass flux from the propellant. Thus, the boundary layer is continually being perturbed away from the steady state. The increasing mass flux not only gives rise to a nonsteadiness but the ratio of the mass flux from the surface to the mass flux from the igniter may also play an important role in determining whether or not the boundary layer separates from the surface. It is unfortunate that very little heat transfer work has been conducted under dynamic conditions with mass addition from, and flame spreading over, live propellant grains. To be sure, many of the correlations have been tested by using them to predict flame spreading rates. However, this is a significantly less sensitive test.

In the heat transfer studies conducted by the authors of this paper and previous co-workers, both steady state and dynamic conditions have been investigated. The dynamic case was studied by measuring the heat transfer due only to mass addition from the propellant grain with no external igniter^(5,6,7). The steady state case was examined by measuring heat transfer due only to an external pyrogen igniter^(12-15,134). It was found that the convective heat transfer in both cases could be correlated by a single equation. (See Fig. 1) The particular way in which the igniter jet shock structure and associated separation flow pattern was confined in these experiments does raise questions about the general applicability of this correlation near the leading edge or jet impingement point. However, the essential features should be valid a diameter or so downstream of the leading edge. The important point is that in both the steady and dynamic cases the correlation is of a steady state form. No nonsteady effects can be discerned within the scatter of the data. The correlation also indicates that the convective heat transfer scales according to the local instantaneous mass flux to the 0.8 power, typical of turbulent flow. (The experimental equipment used in these heat transfer studies is described in Chapter IV.)

Jensen and Cose⁽²⁹⁾ of UTC also measured convective heat transfer during the flame spreading interval. The most important conclusion of this work is that the data appear to be steady state in nature. This agrees with the results obtained by the authors of this paper and implies a quasi-steady boundary layer. Most of the data reported in this reference indicate that the heat flux scales as the mass flux to a power ranging between 0.85 and 0.75. (See Fig. 5) Some of the data indicate scaling as the mass flux to 0.55 power. The authors claimed that, since the flow is assumed to be laminar, the scaling power should be 0.5. The apparent higher powers were attributed to the changing gas temperature downstream of the flame front. The gas temperature should approach a limiting value equal to the adiabatic flame temperature as the flame front advances. After the limit has been reached, the heat flux should increase with

the mass flow rate to the 0.5 power. Unfortunately, none of the gas dynamic models are sufficiently developed to allow these two effects, nonsteady mass addition and changing temperature gradient, to be separated.

Falkner and Kilgroe⁽⁶⁷⁾ also found that their predicted flame spreading rates agreed more closely with measured values if the heat transfer was scaled according to the mass flux to the 0.5 power (Figures 14 and 15). Micheli and Linfor⁽⁴³⁾ show good agreement between predicted and experimental ignition transients with a scaling law to the 0.8 power (Figures 9 and 10). The degree of agreement would indicate reasonably accurate prediction of flame spreading rates. However, both of these last two references are indirect measurements of the accuracy of heat transfer correlations used.

Heat transfer in stagnant regions has received very little attention. The rationale for this has always been that the stagnant regions contain only a small percentage of the total area available for burning and thus should have little effect on the overall ignition transient. However, flame spreading rates into such areas are sufficiently slower than those in the direction of the flow, so that even small hidden areas can have a significant effect.

Figure 6 also shows the film coefficients from Refs. 31 and 86 for the region upstream of the impinging igniter jet. These values were calculated under the same assumptions as outlined above. Kilgroe's⁽³¹⁾ data shows a sharper peak at the impingement point. Carlson et.al.⁽⁸⁶⁾ show a flatter peak and more gentle decrease both upstream and downstream of the maximum. No general conclusion can be drawn.

The convective heat transfer correlation for stagnant regions suggested by Micheli and Linfor⁽⁴³⁾ (see above) indicates no convection unless the chamber pressure is changing. At steady igniter flow and before first ignition there would be no convective heat transfer in the stagnant regions. Although this does not agree with some measured data, it does emphasize that radiation and conduction may be the more dominate modes of heat transfer in stagnant volumes. Peleg and Manheimer-Timnat⁽⁷⁰⁾, for example, attribute flame spreading forward of the impingement point to radiation alone.

It is very difficult to summarize these heat transfer studies. This difficulty reflects the great number of variables involved and the variety of assumptions and experimental configurations which have been used. It is obvious that more heat transfer studies in stagnant volumes and in dynamic situations during flame spreading should be conducted. However, the critical question is: Can a better heat transfer correlation be found or even used within the scope of the present gas dynamic model? It is believed that much of the problem is tied to the axial temperature gradient which is a function of time, and also possibly to the nonsteady nature of the boundary layer. In regard to the temperature gradient problem, the approach of Lovine and Fong⁽³⁹⁾ of considering the gas temperature as a function of position is a good one. However, it must be carried a step further. $T_g(x,t)$ must be correctly coupled to the gas dynamic equations and the nonsteady boundary layer terms properly formulated. The obvious conclusion of this reasoning is that a more accurate gas dynamic model may be required before substantial progress can be made in the understanding of the heat transfer. This is not to deny the usefulness of the present correlations. The degree of agreement which has been achieved by a number of researchers between theoretically predicted ignition transients and experimental test firings quickly shows the value of this work to the design

engineer. However, the present level of sophistication prohibits the finding of a universal correlation for each geometry. Thus, the design engineer must understand in some detail the conditions under which the correlation was obtained and exercise caution when extrapolating to significantly different conditions.

III-D. HYPERGOLIC IGNITION The ignition of a solid propellant rocket motor by direct spraying of the propellant surface with a hypergolic material was originally thought to be an attractive concept from several viewpoints. It was originally believed that pressure overshoots above the design operating pressure, frequently associated with pyrogen or pyrotechnic igniters, could be easily avoided⁽¹⁷⁾. A hypergolic ignition system also offers easy on-and-off capabilities for restart operations. The materials which are attractive for such applications are those like the interhalogens, chlorine trifluoride, bromine trifluoride and bromine pentafluoride, which are hypergolic with propellant materials at room temperature. With no other source of external heating, the means of raising the propellant surface temperature must be direct chemical attack on the surface, at least initially. After the propellant begins to decompose actively, the reaction site may move off the surface into the gas phase. In a sense, though, hypergolic ignition can be viewed as a special case of energy transfer to the propellant. Hypergolic ignition could be incorporated into the analytical models for the overall ignition transient discussed in Chapters II and III-B. What is needed is a description of the energy release at the surface, and the distribution along the surface. The earliest researches on hypergolic ignition of solid propellants were primarily qualitative. This work, by several authors, concerned such aspects of the problem as the relative reactivity of various hypergolic materials with various propellants^(106,107), the effects of altitude on hypergolic ignition⁽¹⁰⁶⁾, and the optimum percentage of the surface initially sprayed with the hypergolic material.^(106,20)

An analytical model for hypergolic ignition was advanced in 1963 by a group of workers at UTC⁽²¹⁾. This model has progressed through a series of references (22,23,25,28) to a form which has been incorporated in an analysis of the complete ignition transient. The model was originally developed for a stagnant ignition situation but was extended to a flow environment on the basis that mass transfer in the gas phase during the preignition interval is negligible. The heat release due to the hypergolic reaction was written as

$$\dot{q}_{\text{Hypergolic}} = \Delta H_r C^{n'} \exp(-E/RT_s)$$

where ΔH_r is the heat of reaction, C is the concentration of the hypergol at the surface and n' is the reaction order. This heat generation was assigned completely to the surface and was put into the boundary condition on the solid phase heat-up equation just as the self-heating term was handled in the development given in Chapter II. The concentration at the surface is given by

$$k_m(C_m - C) = C^{n'} \exp(-E/RT_s)$$

where k_m is the mass transfer coefficient and C_m is the hypergol concentration in the main stream. Due to the consumption of the reactive material at the surface, the concentration in the main stream decreases along the motor axis.

$$-\frac{\partial C_m}{\partial x} = \frac{Pk_m(C_m - C)}{A_p U_m}$$

The boundary conditions for this equation are

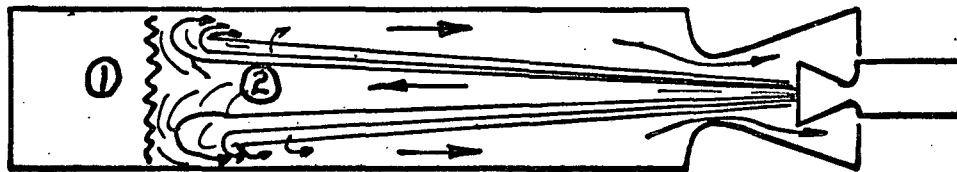
$$\text{At } x = \int_0^t \dot{r}_p dt, \quad C_m = C_m^0$$

$$\text{At } x \geq t u_m, \quad C_m = 0$$

where \dot{r}_p is the flame spreading rate and C_m^0 is the hypergol concentration leaving the ignited region. This description of the hypergolic attack on the surface was combined with a critical surface temperature ignition criterion. There are obviously no great difficulties in coupling this hypergolic ignition model with any of the analyses of the complete ignition transient given above. The boundary condition on the solid phase heat-up is, of course, nonlinear, but this can be handled by various iterative techniques. As with any simple model of ignition, the great complexities of the actual ignition are buried in some innocent appearing term. In this case it is the simple Arrhenius-type description of the heat release and the critical surface temperature ignition criterion.

The concentration of the hypergolic material at the propellant surface down the length of a rocket motor is not easily measured. This prevents a direct confirmation of the concentration as a function of x . At best, it would seem that this simple description would yield $C(x)$ or $C_m(x)$ only prior to first ignition. The mass addition from the surface, the dilution of the gases in the port by propellant combustion products and possible secondary reactions in the gas phase would require a more complete treatment of the developing boundary layer in order to obtain $C(x)$. It is also not obvious that the model is capable of explaining certain experimental data. Ciepluch et.al.(106) and Fullman and Nielsen⁽²⁰⁾ report that ignition of the motor is actually retarded when the per cent of the total surface area wetted by the injected spray of hypergolic material is increased much above 30%. Since the igniter flow rate per unit wetted area was held constant, this behavior can not be explained on the basis of the concentration of hypergolic material at the surface having been changed. It would seem that there is a mechanism for retarding ignition which is not accounted for in this hypergolic ignition model.

III-E. AFT-END IGNITION The term aft-end ignition refers to those configurations where the igniter is mounted external to the main rocket motor with the igniter exhaust jet penetrating through the motor exhaust nozzle into the motor port, and an opposing return flow out the exhaust nozzle.



① STAGNATION ZONE

② FLOW REVERSAL REGION

The igniter jet decays as it penetrates the motor cavity. In cases of incomplete penetration, the jet expands until it blocks the motor port and reverses flow direction. This creates a stagnant region of compressed cold gas ahead of the igniter jet near the head end of the motor. In most reported cases this region occupies approximately 30% of the motor length. The stagnation region remains stable until first ignition occurs. As ignition proceeds, and in response the chamber pressure increases, the stagnation zone is further compressed toward the head-end of the motor. Within this zone, the dominant modes of energy transfer to the propellant are radiation from the hot zone downstream and conduction from the surrounding gas. Convection heat transfer dominates downstream of the stagnation zone. The propellant is observed to ignite first at the point of maximum heat transfer near the aft-end of the motor. Flame spreading takes place both upstream and downstream from this point. The flame propagates faster in the downstream direction than in the upstream direction because of the higher heat transfer in that direction. Complete ignition is observed to occur at about the time the design pressure is reached in the motor⁽⁶⁶⁾. It is obvious that this flow pattern must be described by a flow model completely different from the one-dimensional flow models which have been applied to the situations where the igniter is mounted at the head-end of the motor.

Externally mounted aft-end igniter configurations have several inherent advantages over internally mounted ones. The weight of the igniter need not be carried along on the mission. This allows the use of redundant and conservative igniter designs with no weight penalty. The external mounting permits easier igniter installation and checkout. There are no pressure sealing problems such as there are around an igniter mounted in the forward chamber boss.

Three major problems are encountered with aft-mounted ignition systems: Long ignition delays, between the onset of the igniter action and the attainment of design operating conditions, can occur because of low penetration of the igniter jet into the motor port. This results in an unfavorable heat transfer distribution, and consequently, low flame spreading rates. Severe motor overpressurizations can occur due to aerodynamic blockage of the motor exhaust nozzle by the igniter jet. Significant pressure oscillations can occur in the motor exhaust nozzle. This is attributed to nonsteady interactions between the igniter jet and the counter-flow from the motor⁽⁶⁶⁾.

The complexity of the flow pattern in aft-end ignition situations has prevented the development of analytical prediction methods for the entire ignition transient in such cases. No comparisons between theoretical predictions and experimental test firings, similar to those available for head-end ignition situations, have been published. For this reason the aft-end ignition work is reviewed only briefly here.

The incomplete penetration of the igniter jet into the motor port and the formation of a stagnation zone near the head-end of the rocket motor was observed in the early experimental work with aft-end igniters^(19,20,33). It was also found that optimally expanded supersonic igniter jets resulted in the most complete penetration of the motor cavity^(19,20,31,33), and that full⁽⁵⁷⁾ penetration could be achieved if the jet did not expand to fill the port.

In 1964 Plumley published a model for the penetration of the igniter jet into the motor port prior to first ignition^(38, 1964, Aerojet). This model

is based on mass and momentum balances between the incoming igniter jet and the return flow out of the motor. The model assumes that there is no turbulent mixing or viscous dissipation between the two flows. This model permits the calculation of the stagnation point (penetration distance) and the pressure developed in the head-end of the motor. In the experimental work of Niessen (57, 1965, AFRPL) the stagnation zone was observed directly with flow visualization techniques. It was found the observed jet penetration distances agreed $\pm 10\%$ with the predictions of the Plumley model. However, Carlson & Seader (85, 1965, Rocketdyne) reported that the Plumley model agreed only moderately well with their experimental findings. They attribute the lack of agreement to the model's failure to include turbulent mixing and viscous dissipation between the two jets and heat losses from the gases via convective heat transfer.

A number of studies have been conducted on the heat transfer, and subsequent flame spreading, from aft-end igniters. Ref. 19 reported that first ignition was observed to take place near the igniter jet impingement point. The flame front then advanced toward the head-end of the motor, but the spreading rate was retarded by the compression of the stagnation zone. Ref. 27 (1965, UTC) reported that the peak heat transfer occurred 2 to 3 port diameters from the igniter exit plane. First ignition took place near that point and the flame propagated rapidly up the motor port until the stagnation zone was reached. Flame spreading into this region was very slow. Ref. 29 (1965, UTC) attempted to predict flame spreading rates based on pre-first ignition heat transfer measurements. It was found that the flame spreading rates predicted in this way were significantly slower than measured flame spreading rates. Such effects on the heat transfer by the propellant combustion products were also reported in Ref. 31 (1967, UTC). This points out the obvious - that the reaction of the igniter jet to the mass addition from the propellant grain and the consequently rapidly changing motor pressure alters the heat transfer. Ref. 108 (1966, NASA-Lewis) reported that the igniter flow penetrates the motor port only at relatively low motor chamber pressures. This gradual expulsion of the igniter jet must alter the heat transfer distribution and time history from that observed prior to first ignition.

Carlson, Seader and Wrubel (85, 1965, 86, 1967, 87, 1967, 88, 1967, Rocketdyne) have found that the heat transfer from aft-end igniters prior to first ignition can be correlated with classical heat transfer parameters, at least for cylindrical motors. The graphical correlations developed in these studies are valid only for supersonic igniters operating over a given range of $(\dot{m}_{\text{ign}}/A_p)$. Other heat transfer studies reported in References 27, 29 and 31 are in general agreement with these correlations. Carlson et. al., also found that the maximum heat transfer was achieved for a value of $\dot{m}_{\text{ign}}/A_p \approx 0.3 \text{ lbm/in}^2\text{sec}$. Above this value the heat transfer decreased. This is attributed to increased interference between the incoming and outgoing flows at the higher flow rates. Ref. 66 (1968, CETEC) reported no decrease in heat transfer rates as \dot{m}_{ign}/A_p increased, at least up to a value of $\dot{m}_{\text{ign}}/A_p = 0.56 \text{ lbm/in}^2\text{sec}$. It would seem reasonable to attribute the difference between the two studies to greater coherence in the igniter jet in the latter study. This would result in greater penetration of the igniter jet into the motor port, even at the higher flow rates.

Early in the study of aft-end igniter systems, it was recognized that an important parameter in avoiding pressure overshoots above the design operating

level is ϵ^* . This is defined as the ratio of the annular area between the igniter nozzle and the motor nozzle to the motor throat area. In References 19 and 20 it was reasoned that physical blockage of the motor exhaust nozzle, and hence pressure overshoots, would be avoided with $\epsilon^* > 1.0$. This was not critically tested in the experimental portion of these two studies because the igniter was always ejected before 85% of equilibrium chamber pressure was achieved. It was, however, observed in Ref. 20 that the time to reach operating conditions in the motor was increased by increasing ϵ^* . This would seem to indicate that the penetration of the igniter jet, and in turn the flame spreading, was affected by ϵ^* or that aerodynamic, rather than physical, blockage of the motor nozzle was occurring and thereby hastening chamber filling. Ref. 57 reported that direct flow visualization studies showed that changes in ϵ^* has little effect on preignition igniter jet penetration. This indicates that the latter argument, aerodynamic blockage, is the correct one. Other studies have confirmed this reasoning by observing pressure overshoots with ϵ^* 's as high as 1.4.

Kilgroe, Fitch and Guenther (66, 1968, CETEC) have proposed an analytical model to predict the correct ϵ^* and other design parameters, such as the igniter-to-motor pressure ratio, necessary to avoid pressure overshoots. The model postulates four basic modes of operation corresponding to four different overexpanded igniter flow regimes. The model considers a control volume within the motor exhaust nozzle expansion section. Mass and momentum balances are performed within this control volume assuming that the two counter flows are isentropic. That is, the flows in both directions are assumed to be free of shocks and viscous dissipation is ignored. Despite these simplifications, good agreement is reported between the predicted blocked-unblocked boundary and the experimental findings. The results indicate that for $\epsilon^* = 1.8$, an igniter-to-motor pressure ratio of 4 or less would insure that no aerodynamic blockage of the throat occurs. However, these authors point out that the model has been tested only for a limited range of design parameters, and thus, can not be extended to new situations without careful testing.

In summary, aft-end igniter configurations offer a number of unique advantages. Successful systems have been designed to use these advantages. However, the complexity of the flow field has prevented the development of any analytical model which can with reasonable certainty avoid the disadvantages - pressure overshoots, long delay times resulting from low igniter jet penetration and pressure oscillations in the motor exhaust nozzle - and predict the complete ignition transient.

IV. EXPERIMENTAL INVESTIGATION OF THE IGNITION TRANSIENT The degree of agreement between theoretical predictions of the ignition transient and experimental test firings obtained by a number of authors for several different theoretical models and a range of motor and igniter configurations has been presented. Models, including those using both isothermal and variable temperature gas dynamics, have been considered. Some of the examples used measured flame spreading rates as input to the theoretical prediction scheme. Others attempted to predict the entire transient, including the flame spreading interval. Some of the models considered used dynamic burning rate analyses, others used steady state burning relations. The material in this chapter is the comparison between experiment and theory for a single model tested over a range of igniter system and engine design parameters. This material is presented here for a number of reasons. First, it is important

that any potential user of these models be aware of the "range" of agreement that is obtained between theory and experiment when a single design parameter is systematically varied. This systematic variation of design parameters raises in a logical manner, other questions concerning the limitations of these models in general, and in particular, the applicability of these models in marginal ignition or hangfire situations.

The analytical model used in this work is the one which was developed in Chapter II. In particular, a constant critical ignition temperature was used. Heat release by exothermic decomposition reactions occurring below the ignition temperature and near the propellant surface was included. The heat transfer from the gas phase was described by an empirical correlation, $Nu_{x+a} = 0.0734 Re_{x+a}^{0.8}$ (See Chapter III-C for discussion of this heat transfer correlation and Ref. 134 for further details.) The flame spreading model discussed in Chapter II was used. The burning rate was always taken as steady state, and generally of the form $r_{ss} = k P_c^n$. This allowed the gas dynamic equations to be cast in the form given by Equations II-13 and II-14. These gas dynamic equations were developed on the basis of the following assumptions:

1. The control volume does not vary during the ignition transient.
2. The thickness of the flame zone is small compared to the control volume.
3. The gases are calorically perfect.
4. The heat addition and body work terms are negligible.
5. The composition of the igniter and propellant combustion gases are the same.
6. The two gases mix instantaneously.
7. The exhaust nozzle is choked throughout the ignition transient.
8. The pressure is spatially uniform. This implies low Mach numbers in the motor port.
9. The kinetic energy terms are small compared to the thermal energy terms.
10. The gas temperature is spatially uniform.

Assumptions 8, 9 and 10 are the critical assumptions which can not be relaxed in any easy way. Many of the other assumptions can be relaxed in obvious ways. The computer prediction program used in this work is given in Ref. 134.

The major portion of the experimental program consisted of firings of a two-dimensional motor which employed a gaseous igniter located at the forward end of the grain. These experiments included the measurement of igniter and motor pressures with fast response gauges, high speed photographic observation of flame initiation and flame spreading, the measurement of heat transfer rates at various parts of the grain and the measurement of temperature gradients in the motor port.

The motor was rectangular, 3/4" x 1" x 10", with one side wall being a Plexiglas window to permit photography of the flame spreading interval. (See Figure 17.) The propellant grain was a flat bed of propellant. Both aluminized and unaluminized AP-PBAA propellants were used. The propellant composition information is shown in Table II. The equilibrium chamber pressures ranged up to 500 psia and the thrust ranged correspondingly to about 15 lbs. The overall ignition transient from first application of the igniter until equilibrium operating conditions are reached was typically between 200 and 300 msec in duration for vigorous ignition situations.

The igniter source used in the major part of this program was a gas torch which burned gaseous oxygen and methane. The igniter was fed by fast acting valves and critical conditions were maintained across the injector orifices except during the igniter tailoff. The mixture ratio in the igniter was held at the stoichiometric ratio. The igniter torch operated typically at 95% C* efficiency. The igniter combustion gases flowed through a choked internozzle. In the expansion section, separation is believed to have occurred with the accompanying shock diamond. However, at the leading edge of the propellant grain the igniter flow was reattached to the channel walls. Thus the grain was exposed to a highly turbulent subsonic flow. The igniter combustion gases were subjected to a highly nonadiabatic cooling during the expansion process. The recovery temperature at the channel midline over the propellant leading edge was typically 1700°K.

The igniter mass flow in this experimental situation was not treated as a square wave as in the sample theoretical prediction discussed above. The actual onset and tailoff of the igniter were taken into account by detailed measurement of each experimental record. The volume of the igniter chamber in this laboratory scale system is a significant fraction of the main chamber volume. This additional volume was treated in an approximate manner by adding it to the total volume of the system at the time the igniter nozzle was unchoked by the rising back pressure in the main motor.

A typical experimental run is shown in Figure 18. The igniter supply valves open. The pressure across the injector rises. Ignition is achieved in the igniter chamber and the hot gases begin to flow into the main chamber. After an induction period, the pressure in the main chamber begins to respond to the flame initiation and spreading down the propellant grain. Chamber filling follows the completion of flame spreading. After a small overshoot due to the igniter tailoff, equilibrium conditions are achieved.

A. Photographic Observations Extensive photographic observations of the flame spreading process during the ignition transient were made. A few frames from one of the movies are shown in Figure 22. These high speed movies confirm the concept of a flame front **propagating over the propellant surface**. This flame front is not as sharp a dividing line as the one-dimensional description used in the analytical model would imply. Rather, the flame front is characterized by a narrow region in which there is a varying density of points of local ignition. As this narrow zone moves down the propellant surface, the flame fills in the diffuse region behind it. The hypothesized mechanism of flame spreading, originally advanced by Summerfield and mentioned in the analytical development, states that each surface element is brought to ignition as a function of the heat flux history to it and that ignition of an element is independent of the thermodynamic state of its neighbors or its position relative to the flame. Thus, it is reasoned that the diffuseness of the narrow region identified as a flame front is controlled by the local variation in heat flux due to small surface irregularities. This is verified by the observation that the length of the diffuse region of the flame front can be dramatically varied by roughening the surface with sandpaper or a wire brush.

A second observation which confirms this concept of flame propagation is that the flame can occasionally "jump" to a location as much as several inches in advance of the main flame front. The interesting point is that these advance flamelets do not spread, but remain relatively stationary until

overtaken by the main flame front. This indicates that the local point, due to an irregularity in the surface, received higher heat flux than its neighbors. Since the surrounding surface was not yet ready to ignite, no flame spreading could take place and hence, these advance flamelets do not have a significant effect on the overall ignition transient.

In summary of these observations: the useful concept of a one-dimensional flame front propagating progressively over the propellant grain can be retained as a useful approximation. The demarcation line is not sharp and the diffuseness of the flame front region is a function of surface roughness. The position of the flame front predicted on the basis of the one-dimensional approximation will be some mean location within the diffuse region. A flame can appear on the surface well ahead of the main front due to locally high heat transfer but spreading from such a point will not take place. The few advance flamelets have little effect on the overall ignition transient.

The flame spreading over an aluminized grain was also investigated photographically. (Figure 23) The effect of the molten aluminum particles liberated from the first portion of the grain to be ignited on the ignition of the remainder of the surface was studied. The hot aluminum particles were observed rising from the ignited surface and entering the gas stream. Many particles were seen actually rolling down the surface. In general, those particles that hit the unignited surface did not attach themselves there or cause any significant spread of ignition as they traveled downstream. The diffuseness of the flame front region was comparable to that observed on an unaluminized grain with the same surface roughness. In short, the flame spreading over an aluminized propellant is very similar to flame spreading over an unaluminized propellant. The quantity of hot aluminum particles liberated from the grain is not sufficient to augment significantly the spread of ignitedness.

There is a second very qualitative observation regarding the aluminized propellant. The visible radiation from the flowing gases and particles in the sensitive portion of the film's spectral response was much more intense than was observed with the unaluminized propellant. Subjectively the radiation appeared to intensify rapidly as the amount of liberated hot aluminum in the flow increased. Although this is admittedly a very qualitative observation and was not pursued further, it suggests that radiation from the hot aluminum particles would be an important means of energy transfer during the latter portion of flame spreading over heavily aluminized propellant grains.

B. Gas Temperature Measurements It was assumed in the development of the theoretical model presented in Chapter II that both the pressure and gas temperature in the motor port could be treated as spatially uniform, and varying only with time. In order to test the validity of the $\nabla T_c = 0$ assumption, the temperature of the igniter gas was measured during the induction interval. This was done by replacing the live propellant grain with an inert material of similar thermal properties. Thermocouples were mounted at several axial positions in the port across the flow direction with the junctions at the motor centerline.

These measurements indicated temperature gradients on the order of 70°K/inch along the centerline of the rectangular motor during the induction interval. This implies that the flow is fully developed, at least in the sense that the thermal profile extends to the centerline of the motor. Thus, during the

induction interval and the early portion of flame spreading interval, the assumption of $\nabla T_c = 0$ is very poor. The crudeness of this assumption is recognized, both in terms of the gas dynamic model and in terms of the heat transfer correlation used in this study where it was assumed that the temperature difference across the boundary layer $\Delta T = (T_g - T_s) \approx T_g = \text{constant}$. However, the approximation improves for the gas dynamic model as the ignition transient progresses. As flame spreading proceeds, the mass flow in the port increases. Consequently, the total energy content of the gases increases. The area available for heat losses decreased rapidly, going to nearly zero at the end of flame spreading. Thus, the approximation improves as the ignition transient proceeds and should be completely valid after flame spreading is complete. This is fortunate because it is during the end of the flame spreading interval and the beginning of the chamber filling interval that the most significant gas dynamic processes are observed to occur - the maximum rate of pressurization and the accompanying maximum dynamic temperature change (5,10,132).

It is interesting to note that the measured axial gradient in gas temperature is not sufficient in itself to explain the observed difference in heat flux rates between the two ends of the propellant grain. If the boundary layer film coefficient were constant down the length of the port, the ratio of the heat flux at two axial locations on the grain should equal the ratio of the gas temperature over those locations.

$$\dot{q} = h_{\text{conv}} \Delta T \approx h_{\text{conv}} T_g$$

$$\therefore \dot{q}_1 / \dot{q}_2 = (T_g)_1 / (T_g)_2$$

where the subscripts 1 and 2 refer to axial positions. The experimental results are:

$$(T_g)_1 / (T_g)_2 = 1.4 \text{ to } 1.7 \quad ; \quad \dot{q}_1 / \dot{q}_2 = 3.5 \text{ to } 3.7$$

This indicates that two mechanisms are at work, heat losses establishing a temperature gradient and a changing boundary layer altering h_{conv} .

C. Pressure Measurements The experimental test firings of the rectangular motor included in this paper consists of five series. In each series a single experimental parameter was systematically varied with all other parameters held constant. In Series A the exhaust nozzle was varied, in Series B the igniter duration was varied, and in Series C the igniter mass flow rate was varied with the total igniter mass held constant. Series D is a study of marginal igniter duration and Series E shows the effect of aluminum addition to the propellant.

Series A - Exhaust Nozzle Varied. The pressure transients for Series A are shown in Fig. 24. Duplicate firings with identical conditions were made for each one of these tests. The repeatability of these tests was excellent and, therefore, the duplicate firings are not shown. The pressure overshoots above the design operating conditions are due to extended igniter durations. The small triangle on each trace indicates the time at which the igniter feed valves were closed. If the igniter action had terminated sharply at this time, the prefiring computer predictions indicated that the igniter would have been properly tailored. The overshoots, then, were due to the capacitance decay of the igniter and its feed lines.

The agreement between the theoretical predictions using the experimental igniter tailoff and the complete experimental firings for these nonmarginal, vigorous ignition situations is illustrated in Figures 25 and 26. (The reason for the qualifications on this statement will become apparent later.) Figure 25 is typical of the good agreement that has been obtained for these vigorous ignition situations and Figure 26 represents the greatest lack of agreement. The agreement between theory and experiment for all of the test firings in Series A and B (Figure 27) was within these limits.

It has been suggested that the degree of agreement between the theoretical predictions and the experimental test firings shown in Figures 25 and 26 would not be anticipated on the basis of the scatter in the heat transfer data shown in Figure 1. The greatest degree of scatter in Figure 1 is for the data taken during flame spreading over live propellant grains. Further, the greatest degree of scatter in these runs occurs when only a small percentage of the surface is ignited, and consequently, the mass flow rate is relatively small. The scatter in the data reduces as the mass flux increases. The comparatively large mass flow rates provided by the pyrogen igniter also resulted in less scatter in the heat transfer data. These two factors result in better characterization of the heat transfer, and consequently better agreement between prediction and test firing, than would be judged from an initial examination of Fig. 1.

It should be emphasized that the pressure overshoots observed in Series A are not due to nonsteady burning rate effects on the mass addition from the propellant. It was stated in the theoretical development that it can be shown that nonsteady burning rates are not important at these rates of pressurization.^(5,6) The fact that the overshoots observed in Series A can be calculated from the igniter characteristics is experimental verification of the absence of such effects.

Series B - Igniter Duration Varied. The pressure transients for Series B are shown in Figure 27. This series illustrates that the pressure overshoots observed in Series A can be eliminated by progressively reducing the igniter durations. Not only are the overshoots eliminated, but the rate of pressurization is decreased in a predictable manner. Both the peak pressure and the rate of pressurization are of interest to the structural designer. The ability to predict, without the aid of an extensive experimental firing program, the effects of design changes in the igniter on these parameters is of critical importance. It is clearly apparent that decreasing the igniter duration is not a linear effect and could not be extrapolated in any obvious way from a single test firing. By comparing Runs B-3 and B-4 of Series B, it would appear that some sort of limit is being approached. This will be discussed later.

Series C - Igniter Flow Rate Varied. A hangfire is characterized by there being a long delay in reaching the motor operating conditions. The motor generally appears to be completely inactive during this interval, as if the igniter had never fired. This situation can arise when the igniter stimulus is capable of igniting only a small portion of the propellant grain. The amount of mass produced by the ignited portion of the grain is insufficient to supply the heat transfer necessary to continue rapid ignition.

It can be easily shown that, for the heat transfer correlation used in this study ($Nu_{x+a} \sim Re_{x+a}^{0.8}$), the rise in surface temperature of the propellant is

proportional to $(\dot{m}_{\text{ign}})^{0.3}$, for an igniter of constant total mass. Thus, it can be seen that, although a given igniter may contain enough total mass for a successful ignition transient, if it is fired at too low a mass rate of flow, a misfire or hangfire may occur. In practice, such a reduction in igniter flow rate could occur because the igniter material is at a low ambient pressure or because the igniter nozzle throat is enlarged. Series C (Figure 28) demonstrates this interesting type of hangfire.

Between Firings C-1 and C-4, the mass flow rate was reduced by a factor of 3.7 with the total igniter mass held constant. The time to reach operating conditions was increased by a factor of better than 7. This series was not carried to the obvious conclusion of a complete nonfire because of experimental difficulties. Combustion in the igniter chamber could not be maintained at flow rates below that used in Firing C-4.

The high speed movies of a long delay firing are very interesting. As an example of such a run, Figure 29 shows the details of the pressure-time trace and Figure 34 shows a few frames from the movie. This run is similar to Firing C-4 shown in Figure 28. In the run shown in Figure 30 a neutral density filter was placed across part of the motor window. The "unfiltered" portion of the window is the leading edge of the grain where first ignition occurs. This filter was added so that the weak first flame could be observed and proper exposure still maintained as the flame intensified as it propagated downstream. The low heat transfer rate associated with the low igniter flow resulted in the first flame appearing on the grain at 335 msec into the run. As the igniter action continued, rapid flame spreading took place over the leading 25% of the propellant grain. At this point the igniter action ended and the flame spreading rate dropped to almost zero. This occurred at 625 milliseconds into the run. For the next 725 milliseconds the flame front location barely moved. During this long interval, the chamber pressure was almost at the ambient pressure, but the low mass flow produced by the ignited 25% of the grain continued to heat the remainder of the grain. Finally, at 1350 milliseconds into the run the flame front began to advance rapidly down the surface. The flame spread over the unignited 75% of the grain in 125 milliseconds. This portion of the firing appeared just like a normal, vigorous ignition transient. Figure 29 shows that the rate of pressurization is about the same as observed in the more vigorous situations.

Firing C-4 also shows an interesting pressure overshoot. The pressure overshoots seen in Series A and B (Figure 24 and 27) and Firing C-1 (Figure 28) are due to extended igniter durations. The overshoot observed in Firing C-4 is due to the preheating in depth of the unignited portion of the propellant during the long delay between the start of igniter firing and the final rapid phase of flame spreading. At these low heating rates, the thermal wave has penetrated far enough into the solid so that there is a layer of propellant which burns with an increased rate due to the higher initial temperature of the propellant. The increased burning rate of this thin layer results in a pressure overshoot. No other explanation seems possible. The igniter has been turned off for a long time before the operating conditions are approached and hence, could not cause the overshoot. The overshoot can not be attributed to nonsteady burning effects, in the sense that the burning rate is a function of the rate of pressurization, because no overshoots were observed in Firings C-2 and C-3 which experience similar rates of pressurization.

When Series C was initially done, it was found that the quality of the computer predictions degenerated for increasingly marginal ignition situations, although the correct trends were predicted. The theoretical predictions indicated marginal ignition, but consistently yielded longer hangfires than were observed experimentally. This indicated that some source of energy input to the grain had not been included in the model. This led to the inclusion of the self heating term discussed in the theoretical development, $\dot{q}_{surf} = p_p q r = p_p q A \exp(-E/RT_s)$. The effect of this term is dramatically shown in Figure 31 for a marginal ignition situation. The values of the activation energy, E_s , and the heat release parameter were obtained by selecting those values which brought the theoretical predictions into agreement with the experimental firings for Runs C-1, C-2 and C-3. This may appear to be a crude approach. However, it can be justified on two bases. First, it is apparent from the experimental work that an energy source, important only in marginal ignition situations, was missing from the model. A heat release at or near the surface is the only physically reasonable place to look for it. Secondly, the necessary physical parameters are not well known for steady state cases, and certainly are not available for incipient transient cases. Thus, a certain amount of curve fitting is justified. The activation energy and surface heat release found this way are within approximately 10% of the quoted steady state values.⁽¹³³⁾ The values, which gave the best fit for all three runs, C-1, C-2 and C-3, are activation energy, $E_s = 13,700$ cal/mole, and heat release parameter, $Q = 250$ cal/gram. Using this value of E_s , the correct value for A was calculated by matching the calculated burning rate to the measured one with T_s taken as 900°K ⁽¹³³⁾.

It is important to re-emphasize that, even without this self heating term, the proper trends were predicted. Thus, the designer would be warned that the igniter is marginal, even if detailed agreement between the prediction and a test firing is not achieved.

Series D - Marginal Igniter Durations. Series D (Figure 32) was originally intended to display the effects of varying the size of the motor exhaust nozzle systematically, while other design parameters were held constant. This is similar to Series A. The difference was to be that the pressure overshoots observed in Series A would be eliminated. A choice was made of the magnitude and duration of the igniter flow, and these were held constant.

This systematic variation of nozzle throat diameter, from small to large, was expected to show corresponding systematic changes in the final equilibrium pressure, from high to low. It can be seen in the pressure-time traces of this series, that this expectation was fulfilled.

However, some irregular behavior showed up in the traces for the firings with the largest nozzles. Upon examination of this situation, it was concluded that this resulted from the choice of an igniter input (mass flow and duration) that was very close to the marginal requirement for prompt ignition. Under such circumstances, while the firings with the smaller nozzles resulted in acceptable pressure-time traces, the firings with the larger nozzles showed erratic behavior indicative of an ignition input that is marginal.

Further verification of the interpretation, that this particular choice of igniter flow and duration was marginal, was provided by the appearance of some unexpected hangfires in the Series during the test firing program. These unexpected hangfires are shown in Figure 33. There was no change in the firing

conditions for the traces shown in Figure 33 as compared with the traces shown in Figure 32. The interpretation is clear, that the ignition exposure was marginal. As may be expected in a marginal situation, the firing behavior is sometimes normal, and in such normal situations, it was found that the experimental firing trace came close to the theoretical prediction for that situation. Such agreement is shown in Figure 34.

That the chosen exposure was indeed marginal was demonstrated theoretically by carrying out the computer prediction with a 10% smaller igniter mass flow than that standardized for Series D. The drastic effect of so small a reduction in the igniter mass flow is shown in Figure 35. The standard exposure is computed to produce a normal ignition; however, the 10% weaker exposure results in a hangfire. It is obvious that the chosen mass flow and duration were marginal for this motor.

From observation of the normal-appearing curves in Figure 32, it appears that enlargement of the exhaust nozzle does not stretch out the induction period, but it slows down the rise of pressure from the start of the grain burning to the final equilibrium level. That the induction period is unaffected by enlargement of the exhaust nozzle follows theoretically from the fact that the heat flux in the preignition interval is not dependent on the pressure level. Rather, it is a function of the flow rate divided by the port area ($Re_{*} = \dot{m}(x+d)/A_p \mu$). This is kept constant. The slowing down of the rise of pressure after the induction interval results from the lower rate of burning associated with the enlarged exhaust nozzle.

The drastic effect of so small a reduction in the igniter mass flow raises the question of the sensitivity of the model to such parameters as the ignition temperature and the thermal conductivity of the propellant. It was mentioned in the theoretical development that the thermal conductivity of the solid is assumed not to vary as the propellant heats up. This introduces an additional uncertainty which varies with time. As might be anticipated, the model is more sensitive to small uncertainties in the parameters in marginal situations than in vigorous ignition cases. The standard deviation in the experimental determination of the ignition temperature was $\pm 15^{\circ}\text{C}$. In order to test the effect of this uncertainty, the results of varying the ignition temperature by $\pm 20^{\circ}\text{C}$, for both vigorous and marginal cases, are shown in Figure 36. The effects of varying the thermal conductivity by $\pm 10\%$ for both cases are shown in Figure 37. The relative insensitivity to variations in thermal conductivity in the vigorous ignition case is justification for taking solid phase properties as constant in the analysis. However, the extreme sensitivity of the model to the ignition temperature and the conductivity must be kept in mind when it is apparent that a marginal situation is being approached.

Series E - Effects of Aluminum Addition. One way in which the addition of aluminum to the propellant could conceivably affect the ignition transient would be for the molten aluminum, liberated from the first portion of the grain to be ignited, to enhance the flame spreading rate downstream by impinging on the unignited portion of the grain. This possibility was discussed in the section on Photographic Observation. In short, the aluminum particles do not augment flame spreading and thus flame spreading over an aluminized propellant is very similar to flame spreading over an unaluminized propellant.

If one sets aside, for the moment, possible unpredictable combustion effects caused by aluminum, the presence of powdered aluminum may be expected to affect the pressure-time trace in several predictable ways. The first, and most obvious, is that the presence of powdered aluminum increases the thermal diffusivity of the solid propellant; this would act to slow down the rise of surface temperature at any given point on the propellant grain, and thus, slow down the rate of flame spreading. In addition, the presence of aluminum changes both the burning rate and the pressure exponent. What these changes are, depends on whether the aluminum is added at the expense of ammonium perchlorate, at the expense of fuel, or at the expense of both. For the comparative firings reported in this paper (Fig. 38), the aluminum was added largely at the expense of the perchlorate, although some of the fuel was also removed. The percentages of the three components for the two propellants are given in Table II. The burning rate exponent was depressed from 0.40 to 0.27 in the range of pressure applicable to this transient. At the same time, a significant change was observed in the burning rate of the propellant (measured in a strand burner), the value rising from 0.09 in/sec at the preignition pressure of 40 psia to 0.12 in/sec at the same pressure. Thus, the addition of aluminum made the propellant burn more actively in the lower range of pressure corresponding to the preignition interval.

In the particular test firing comparison reported here, the effects of both increased thermal diffusivity and increased burning rate are observed (Fig. 38). As seen from the theoretical predictions shown in Figure 39, the induction period is lengthened for the aluminized propellant but the higher burning rate results in a greater dp/dt . Thus, equilibrium conditions are reached earlier despite the later start. Time did not permit more elaborate tests to isolate these two effects. An excellent test of the effect of the increased thermal diffusivity of the aluminized propellant would be in the hangfire or long delay fire limit. Under such conditions, the thermal diffusivity of the propellant becomes very critical, as is shown in Figure 37.

In general, the agreement between the theoretical predictions and the experimental test firings (Fig. 38) for the aluminized propellant is similar to the agreement obtained for the unaluminized propellant. However, Firing E-1 requires some additional explanation. The larger-than-normal divergence between the theoretically predicted and experimentally observed behavior is not due to any breakdown of the model because of the presence of aluminum. The earlier-than-expected pressure rise is attributed to progressive plugging of this small nozzle as the aluminum oxides condensed on the nozzle. It was difficult to identify an equilibrium pressure on the firing trace because the pressure continued to rise rapidly until the grain was consumed. After the test firing, an aluminum oxide "mold" of the nozzle was found in the motor. This confirmed the suspicion that the effective throat area was varying during the test firing. Repeated test firings failed to eliminate this difficulty. This behavior was not observed in test firings with larger nozzle throat diameters.

Series F - Application of Prediction Method to Practical Motor Configurations. Experimental test firings also were carried out for several rocket engines of more practical configurations than the two-dimensional motor. These experiments involved laboratory-size rocket motors with a solid propellant igniter located at the forward end of the motor^(9,10). (Fig. 19) The igniter used a CMDB type propellant. The motor grains were an AP-PBAA unaluminized composition weighing

up to 0.33 lbs. Various hollow cylinders and star-shaped grain designs were fired. Companion predictions were made for these test firings, using the same equations and heat transfer correlation developed for the two-dimensional motor described above.

The quality of the predictions can be judged in Figure 40, which compares the experimental and theoretical curves for a star grain motor. The same gas dynamic equations and heat transfer correlation developed for the rectangular motor were used. Although there is good agreement between the theoretically predicted and experimental trends, certain consistent differences are observed. In Figure 40, the experimental trace begins to deviate from the pre-ignition pressure level earlier than was predicted. This is attributed to more rapid flame spreading down the points of the star grain than was predicted from the flat plate heat transfer correlation. Once flame spreading began in the case of the theoretical prediction, it took place more rapidly than in the experimental case due to the longer pre-heating of the surface. It was found, in the computer study conducted by diLauro⁽¹⁰⁾, that the maximum rate of pressurization is altered by the pressure level which is achieved at the end of flame spreading. In this case, the predicted pressure at the end of flame spreading is low because of the prediction of rapid flame spreading. This results in a prediction of a higher maximum rate of pressurization. This effect, coupled with the possibly slower than predicted flame spreading along the sides of the star points, is believed to account for the high rate of pressurization predicted by the model.

The elimination of these consistent differences would require a detailed study of the heat transfer along the points of the star. This has not been done.

Series G - Hot Particle Igniter Test Firing. The second set of experiments with practical configurations involved a rocket engine which uses a pyrotechnic igniter. (Figure 20) This motor was selected because of the great difference between the previously studied pyrogen igniters and this hot particle system.

The simplest assumption that can be made to adapt the present model to this obviously different situation is to assume that the flame spreading is instantaneous. This particular motor is singularly suited to this assumption since the igniter tube extends the entire length of the grain. This brings most of the propellant surface area under direct impingement. Experiments were performed to gain knowledge of the percentage of the propellant surface which was initially covered by impinging igniter products. These tests, done by firing the igniter on to an inert grain, confirmed that most of the surface was indeed subjected to direct impingement, except for a small region in the head end of the motor. This uncovered area constituted approximately 12% of the total area. The quality of the limiting assumption of instantaneous flame spreading can be judged by comparison of the theoretical prediction and an experimental test firing of a live grain.

Another necessary piece of information was the flow rate versus time characteristics of the piccolo tube two-phase flow igniter. This information was obtained by firing the igniter into an inert chamber.

The comparison of the theoretical prediction and an experimental test firing is shown in Figure 41. The agreement is surprisingly good. The assumption of instantaneous flame spreading dictates that the initial rate of pressurization should be higher than observed experimentally since $(dp/dt)_{\max}$ is known

to occur at the end of flame spreading.⁽⁵⁾ This assumption also dictates that the theoretical dP/dt must be lower at some later time than the experimental value. This behavior is, in fact, seen in Figure 41.

The error in predicting the time of maximum pressure and the "saddle" in the experimental curve can be attributed to the flame spreading into the stagnant region mentioned above. The 3% difference between the theoretical and experimental peak pressure is due to a probable under-estimate of the pressure contribution of the vapor - particle mixture during live motor firings, as compared to the firing of the igniter into an inert chamber.

The encouraging result of this study is that useful theoretical predictions of the ignition transient can be made for complex engines by using even the simplest assumptions, providing the gas dynamics are adequately described.

V. CONCLUSIONS AND PROBLEMS FOR FUTURE WORK

A. Conclusions. A physically rational theory has been developed that can predict motor ignition transients for the class of rocket motors with head-end pyrogen igniters and with large port-to-throat area ratios. Within this theory the complete ignition transient, including the flame spreading interval, is predictable, provided some description of the heat transfer to the propellant grain is available. Additionally, the model is capable of dealing with at least portions of the thrust transient for a much wider range of rocket engine types, and ways can be seen for extending it eventually to cover the entire transient of such complex engines. The validity of the gas dynamics of the model and the characterization of the local ignition and flame spreading process have been adequately confirmed experimentally in a wide variety of situations.

The model assumes that local ignition can be characterized by a simple critical surface temperature criterion. This has been shown to be generally adequate, except in marginal ignition situations where a propellant grain self-heating term must be included.

Three critical assumptions are made in the gas dynamic model: $\nabla P = 0$, $h \gg U^2$, $\nabla T = 0$. The first two assumptions were shown experimentally to be good approximations for the class of motors investigated (large port-to-throat area ratio.) The assumption of $\nabla T = 0$ was shown to be a poor approximation, however, at least during the preignition interval and the early portion of flame spreading. Fortunately, the degree of error introduced by this approximation does not seem to degrade too much the agreement between the theoretical predictions and the experiments.

A number of empirical engineering-type heat transfer correlations have been developed for the flow in the motor port during the induction and flame spreading intervals. It is very difficult to summarize these correlations because of the many igniter design variables involved and the wide variety of assumptions and experimental configurations which have been used. The flow in a rocket motor is far from any ideal flow of the kind that can be treated on a firm theoretical basis. This makes it impossible to extrapolate the empirical heat transfer correlations to situations significantly different from those actually tested. However, this is not to deny the usefulness of the present correlations. The degree of agreement which has been achieved by a number of researchers between their theoretically predicted ignition transients and experimental test firings quickly

shows the value of this work to the design engineer. Nevertheless, because a universal heat-transfer correlation for each geometry is not possible, the design engineer must understand in some detail the conditions under which each particular correlation was obtained and exercise caution when extrapolating it to significantly different conditions.

Photographic observations confirm the existence of a narrow, diffuse region which can be identified as a flame front during flame spreading. These observations, and the ability to predict the flame spreading rates quantitatively on the basis of measured convective heat transfer correlations, confirm the hypothesis that ignition of a surface element is a function only of the heat flux history to the element and does not depend on the element's position relative to the flame nor on the thermodynamic state of the surrounding elements.

The theoretical model was tested over a wide range of experimental parameters. Good agreement between the theoretical predictions and the experimental test firings was obtained in all cases involving normal, vigorous ignition.

It was demonstrated that pressure overshoots above the design operating condition can be caused by a number of igniter effects. Too vigorous an igniter, for example, which provides too great a mass flow or which continues to fire beyond the chamber filling interval, will cause a pressure overshoot. An overshoot can also be caused by a slow, long duration igniter leading to extensive in-depth pre-heating of the propellant before the completion of flame spreading. This results in a higher than normal burning rate in the latter part of the transient until the pre-heated layer of the propellant is consumed.

A marginal igniter can lead to a hangfire if only a small portion of the propellant surface (e.g. 20%) is ignited during the igniter action. It was shown both experimentally and theoretically that the boundary between a satisfactory igniter design and an unsatisfactory one is very narrow. The divergence between the two is very abrupt. The capability of the propellant to generate heat at or near the surface by exothermic decomposition during the induction period, as the surface slowly heats up, which is described in the analysis by means of a self-heating term, becomes critically important for accurate predictions near the boundary. Without this term, the predictions at the boundary become much too pessimistic; with it, they are much more accurate. The theoretical model is very sensitive to the accuracy of such parameters as the ignition temperature and the propellant thermal conductivity near the boundary, but it is relatively insensitive to these parameters for vigorous ignition cases. This question of the boundary between ignition failure and ignition success, and the prediction of hangfires, is one of the most important practical results of this line of research.

Photographic observations of flame spreading over an aluminized propellant grain have shown, surprisingly, that the hot burning aluminum liberated from ignited portions of the grain does not augment the spread of ignitedness downstream. Thus, the flame spreading model is not any different from that of the unaluminized propellant case. Of course, the addition of aluminum to a propellant tends to stretch out the induction period by increasing the thermal cooling at the propellant surface. Also, there are combustion effects of the added aluminum, related to the measured normal burning rate curve. For example, the aluminized propellant used in this study had a higher burning rate than the unaluminized propellant, and so this shortened the overall transient by steepening the rate of pressure rise. This obviously, is not a general result, but the

effect is predictable.

It was also shown that the analytical model can be used with just simple assumptions to make useful approximate predictions of the ignition transient for even a more complex engine, such as the one with the pyrotechnic igniter system reported in this paper. The model provides a rational basis for evaluating these assumptions and suggests means of improving the igniter. This in itself is a valuable guide to the design engineer.

B. Problems for Future Work. Future work on the prediction theory for the ignition transient should be directed toward a more comprehensive gas dynamic description that would permit the relaxing of the limiting assumptions of the present gas dynamic model, $\nabla P = 0$, $\nabla T = 0$ and $h \gg u^2$. The $\nabla T_c = 0$ assumption has been shown to break down even in motors with large port-to-throat area ratios. The other two assumptions will break down in the case of motors with high volumetric loading. The removal of these limiting assumptions requires the development of more comprehensive gas dynamic equations.

In high volumetric loading motors, erosive burning contributions will become important. In order to treat this adequately, detailed knowledge about the velocity profile down the motor port will be needed. The rates of pressurization are generally higher in such motors than those treated by the present models. A correct nonsteady burning rate analysis will have to be incorporated into the ignition transient model to account for this effect.

The present models should be tested in and extended to new situations, such as those involving gas-less (hot particle) igniters and igniters with intense radiation. The heat transfer and accompanying flame spreading into stagnant regions is a greatly neglected problem that should receive attention. Motors with complex port geometries and motors with more than one port cannot be treated by present methods with accuracy. And motors with igniter flow discharges positioned at places other than the forward end of the grain will have to be considered in future work.

The extension of the present approach to these additional motor and igniter design situations can probably be achieved with reasonable success, once the diagnostic work on flow patterns and heat transfer distributions is done.

ACKNOWLEDGEMENTS

A number of workers in the Guggenheim Laboratories at Princeton University contributed to this work. Mr. Peter L. Stang and Mr. Bruce W. MacDonald have contributed actively and extensively to the experimental portion of the program. Mr. MacDonald also participated in the computer work which led to the theoretical predictions contained in this paper. Mr. C. R. Felsheim carried out the processing of the solid propellant used in the program and collaborated with the authors in the development of the experimental equipment. Advice on matters of instrumentation and assistance with the experimental firing program was given by Mr. S. O. Morris. Credit for the photographic work and related areas goes to Mr. E. R. Crosby. Mr. J. H. Semler was instrumental in the fabrication of the experimental equipment.

This research was sponsored by the Office of Advanced Research and Technology, National Aeronautics and Space Administration, under NASA Grant NGR 31-001-109, supervised by Langley Research Center.

REFERENCES

The following references are included in Table I.

1. Lancaster, R. W., and Summerfield, M., "Experimental Investigation of the Ignition Process of Solid Propellants in a Practical Motor Configuration", Aeronautical Engineering Report 548, Princeton University, Princeton, N. J., May, 1961.
2. Grant, Jr., E. H., Wenograd, J., and Summerfield, M., "Research on Solid Propellant Ignitability and Igniter Characteristic", Aeronautical Engineering Report 662, Princeton University, Princeton, N. J., October, 1963.
3. Grant, Jr., E. H., Lancaster, R. W., Wenograd, J., and Summerfield, M., "A Study of the Ignition of Solid Propellants in a Small Rocket Motor", (Princeton University), AIAA Preprint 64-153, January, 1964.
4. Parker, K. H., Wenograd, J., and Summerfield, M., "The Ignition Transient in Solid Propellant Rocket Motors", (Princeton University), AIAA Preprint 64-126, January, 1964.
5. Parker, K. H., "The Ignition Transient in Solid Propellant Rocket Motors", Ph.D. Thesis, Princeton University, Princeton, N. J., January, 1966.
6. Summerfield, M., Parker, K. H., and Most, W. J., "The Ignition Transient in Solid Propellant Rocket Motors", Aerospace and Mechanical Sciences Report 769, Princeton University, Princeton, New Jersey, February, 1966.
7. Parker, K. H., Most, W. J., and Summerfield, M., "The Ignition Transient in Solid Propellant Motors", AIAA Second Propulsion Joint Specialist Conference, June, 1966, AIAA Preprint 66-166, published in Astronautica Acta, July-August, 1966.
8. Summerfield, M., Stang, P. L., Most, W. J., and diLauro, G. F., "The Ignition Transient of a Solid Propellant Rocket Motor", presented before the ICRPG Design Automation Group, CPIA Publication 122, July, 1966.
9. Lukenas, L. A., Most, W. J., Stang, P. L., and Summerfield, M., "The Ignition Transient in Small Solid Propellant Rocket Motors of Practical Configuration", Aerospace and Mechanical Sciences Report 801, Princeton University, Princeton, New Jersey, July, 1967.
10. diLauro, G. F., Linden, L. H., Most, W. J., and Summerfield, M., "Theoretically Predicted Ignition Transients in Solid Propellant Rocket Motors", Aerospace and Mechanical Sciences Report 802, Princeton University, Princeton, New Jersey, July, 1967.

REFERENCES - cont'd.

11. Most, W. J., Linden, L. H., diLauro, G. F., Lukenas, L. A., MacDonald, B. W., Stang, P. L., and Summerfield, M., "Effects of Igniter and Motor Characteristics on the Ignition Transient of a Solid Rocket Engine: Computer Predictions and Test Firings", presented at the Fourth ICRPG Combustion Conference, October, 1967, CPIA Publication 162, Vol. 1, December, 1967.
12. Most, W. J., Linden, L. H., diLauro, G. F., Lukenas, L. A., MacDonald, B. W., Stang, P. L., and Summerfield, M., "Effects of Igniter and Motor Characteristics on the Ignition Transient of a Solid Rocket Engine: Computer Predictions and Test Firings", Aerospace and Mechanical Sciences Report 809, Princeton University, Princeton, New Jersey, October, 1967.
13. Most, W. J., MacDonald, B. W., Stang, P. L., and Summerfield, M., "Thrust Transient Prediction and Control of Solid Rocket Engines", presented at the Third ICRPG/AIAA Solid Propulsion Conference, CPIA Publication 167, April, 1968.
14. Most, W. J., MacDonald, B. W., Stang, P. L., and Summerfield, M., "Thrust Transient Prediction and Control of Solid Rocket Engines", Aerospace and Mechanical Sciences Report 837, Princeton University, Princeton, New Jersey, June, 1968.
15. Most, W. J., MacDonald, B. W., Stang, P. L., and Summerfield, M., "Thrust Transient Prediction and Control of Solid Rocket Engines", presented at the Fall Meeting of the Western States Section of the Combustion Institute, Paper No. 68-33, October, 1968.
16. Altman, D., "The Characteristics of Gasless Igniters", UTC, Bulletin of Second Ad Hoc Ignitability Panel Meeting, October, 1956. (CONFIDENTIAL)
17. Priapi, J. J., "Advanced Ignition System for Solid Propellant Rocket Motors", UTC, ARS J, Vol. 31, No. 7, p. 1029-1031, July, 1961.
18. Baker, D. L., "Method for Predicting Chamber Pressure Transients During the Ignition of Solid Propellant Rocket Motors", UTC Technical Memorandum TM-14-62-UZ, March, 1962.
19. Grens, W. B., "Ignition Techniques for Very Large Solid Propellant Motors", UTC, Second Technical Note, Contract No. AF 04(611)-7559, July, 1962. (CONFIDENTIAL)
20. Fullman, C. H., and Neilsen, F. B., "Theoretical and Experimental Investigation of Ignition Systems for Very Large Solid Propellant Motors", UTC, Final Report RTD-TDR-61-10, Contract No. AF 04(611)-7559, May, 1963. (CONFIDENTIAL)

REFERENCES - cont'd.

21. Anderson, R., "Fundamental Investigation of Hypergolic Ignition for Solid Propellants", UTC, Semiannual Technical Reports No. 1 and 2, Contract No. NOW 62-1006-C, June, 1963. (CONFIDENTIAL)
22. Anderson, R., Brown, R. S., Thompson, G. T., and Ebeling, R. W., "Theory of Hypergolic Ignition of Solid Propellants", UTC, AIAA Preprint 63-514, December, 1963.
23. Anderson, R., Brown, R. S., and Shannon, L. J., "Theory of Hypergolic Ignition of Solid Propellants", UTC, AIAA Preprint 64-156 January, 1964.
24. Brown, R. S., Wirrick, T. K., and Anderson, R., "Theory of Ignition and Ignition Propagation of Solid Propellants in a Flow Environment", UTC, AIAA Preprint 64-157.
25. Brown, R. S., Jensen, G. E., and Anderson, R., "Investigation of Fundamental Ignition Phenomena Under Dynamic Flow Environments", UTC, Final Report, Contract No. NAS 7-156, February, 1965.
26. Beyer, R. B., MacLaren, R. O., and Anderson, R., "Ignition of Solid Propellant Motors Under Vacuum", UTC, Final Report, Contract No. AF 04(611)-9701, April, 1965.
27. Mullis, B., and Channapragada, R. S., "Heat Transfer Studies of Solid Rocket Igniters", UTC, Final Report, Contract No. NAS 7-320, September, 1965.
28. Anderson, R., "Fundamental Investigation of Hypergolic Ignition of Solid Propellants", UTC, Final Report, Volumes I and II, Contract No. NOW 64-0209-C, October, 1965. (CONFIDENTIAL)
29. Jensen, G. E., Brown, R. S., Anderson, R., and Cose, D. A., "Studies in Ignition and Flame Propagation of Solid Propellants", UTC, Final Report, Contract No. NAS 7-329, June, 1966.
30. Jensen, G. E., Brown, R. S., Cose, D. A., and Anderson, R., "Ignition and Ignition Propagation in Solid Propellant Motors", UTC, AIAA Preprint 66-677, June, 1966.
31. Kilgroe, J. D., "Studies on Ignition and Flame Propagation of Solid Propellants", UTC, Final Report, Contract No. NAS 7-479, August, 1967.
32. Slavin, J., & Billheimer, J. S., "Ignition Systems for Composite Solid Propellants", Aerojet-General Corp., Report No. 1255-6, Contract No. AF 33(616)-3072, February, 1957. (CONFIDENTIAL)

REFERENCES - cont'd.

33. Nachbar, D., Wilson, D., Taback, H., Lavinski, C. T., and Plumley, A., "Final Report: Aft End Ignition Large Solid Rocket Program, Phase II", Aerojet-General Corp., Technical Report No. SSD-TDR-62-103, Contract No. AF 04(611)-08012, September, 1962.
34. Coleal, W. A., and Pelette, L. W., Technical Memorandum 233, Aerojet-General Corp., September, 1963.
35. Paul, B. E., Lovine, R. L., and Fong, L. Y., "Diffusional Analysis of Composite Propellant Ignition, and its Application to Solid Rocket Ignition", Aerojet-General Corp., AIAA preprint No. 64-117, January, 1964.
36. Paul, B. E., Lovine, R. L., and Fong, L. Y., "A Ballistic Explanation of the Ignition Pressure Peak", Aerojet-General Corp., AIAA Preprint No. 64-121, January, 1964.
37. Paul, B. E., Lovine, R. L., and Fong, L. Y., "Propellant Surface Flame Propagation in Rocket Motors", Aerojet-General Corp., AIAA Preprint No. 64-125, January, 1964.
38. Plumley, A. G., "Development of an Analytical Model to Determine Aft-end Ignition Design Parameters", Aerojet-General Corp., Technical Paper 136SPP, Contract No. AF 04(695)-350, March, 1964.
39. Lovine, R. L., and Fong, L. Y., "Wing VI Minuteman Ignition Study, Final Report", Aerojet-General Corp., Technical Memorandum 249 SRP, Contract No. AF 04(694)-258, April, 1964.
40. Paul, B. E., and Lovine, R. L., "Ignition Problems in Solid Propellant Rockets", Aerojet-General Corp., February, 1965.
41. Cohen, N. S., and Lovine, R. L., "Fulfillment of Solid Propellant Ignition Requirements by Pyrogen Igniters", Aerojet-General, Fourth ICRPG Combustion Conference, CPIA Publication No. 162, December, 1967.
42. Mecheli, P. L., "A Stop-Start Study of Solid Propellants", Aerojet-General Corp., Contract No. NAS 1-6600.
43. Micheli, P. L., and Linfor, J. J., "The Empirical and Analytic Modeling of the Role of the Propellant in Ignition", Aerojet-General Corp., Western States Section of the Combustion Institute, Paper 68-34, October, 1968.
44. Cohen, N. S., "Additional Igniter Flow Studies: I, Analytical Developments; II, Experimental Results, Analysis and Information for Igniter Design", Aerojet-General Corp., TM-1 SRO, TM-125RO, December, 1964.

REFERENCES - cont'd.

45. Bryan, G. J., and Edwards, G. D., "A Method for Predicting Ignition Requirements of Practical Propellant Systems - Part I", NOL, NAVORD 4189, December, 1955. (CONFIDENTIAL)
46. Bryan, G. J., and Lawrence, E. K., "Application of Fundamental Data to Gun and Rocket Ignition", NOL, Bulletin of the Second Symposium on Solid Propellant Ignition, Vol. I, SPIA, 1956. (CONFIDENTIAL)
47. Bryan, G. J., and Lawrence, E. K., "A Method for Predicting Ignition Energy Requirements of Practical Propellant Systems - Part II, Guns", NOL, NAVORD 5750, December, 1957. (CONFIDENTIAL)
48. Bryan, G. J., and Lawrence, E. K., "A Method for Predicting Ignition Energy Requirements of Practical Propellant Systems - Part III, Rockets", NOL, NAVORD 6134, February, 1959. (CONFIDENTIAL)
49. Larrick, B. F., Beauregard, R. L., ZOVKO, C. T., and Amster, A. B., "Rocket Motor Ignition Systems: I. A Rocket for Studying the Variables Affecting Pressure During Ignition", NOL, NAVORD 6851, 1960. (CONFIDENTIAL)
50. Sharn, C. F., "Solid Propellant Rocket Ignition Systems. III. A Research Program for the Scientific Design of Igniters, NOL, NOLTR 61-110, October, 1961.
51. Price, E. W., "Technical Recommendations for the Ignition Research Program of the Bureau of Naval Weapons", NOTS, NAWEPS 7923, NOTS TP 2947, June, 1962.
52. Sharn, C. F., "Solid Propellant Ignition Systems. IV. Evaluation of the NOL 'Hi-Lo' (Rocket-in-Rocket) Igniter, NOL, NOLTR 62-189, November, 1962.
53. Price, E. W., "Annotated Ignition Bibliography and Information Retrieval System", NOTS, NAWEPS 8365, NOTS TP 3263, September, 1963. (CONFIDENTIAL)
54. Bradley, H. H., "Theory of a Homogeneous Model of Rocket Motor Ignition Transients", NOTS, AIAA Preprint 64-127, 1964.
55. Sharn, C. F., Beauregard, R. L., Ferguson, J. D., Lawrence, E. K., Ragsdale, W. C., and Zovko, C.T., "Solid Propellant Rocket Ignition Research (Final Report)", NOL NOLTR 64-107, July, 1964.
56. Shook, G. B., "Measurement of Some Properties of Solid Propellants Pertinent to Ignition and Combustion Studies", NOTS, NAVORD 1949, NOTS 503, March, 1952.

REFERENCES - cont'd.

57. Niessen, W. R., "Solid Propellant Rocket Ignition Test and Evaluation (SPRITE) Program", AFRPL TR 65-23, January, 1965.
58. Turner, S. W., "Electrical Control of Composite Solid Propellant Flame Spread Rates", AFRPL, Third ICRPG/AIAA Solid Propulsion Conference, June, 1968.
59. Lowry, E. M., "Solid Propellant Igniter Design Handbook", BPC, NAVWEPS 8015, April, 1961, (CONFIDENTIAL)
60. Lowry, E. M., "1963 Supplement to Solid Propellant Igniter Design Handbook", BPC Report No. 361, Contract No. NOW 62-0236-C, December, 1963. (CONFIDENTIAL)
61. Fleming, R. W., "Ignition, Studies, Final Report", BPC Report No. 383, Contract NOW 62-0236-C, March, 1964. (CONFIDENTIAL)
62. Fleming, R. W., "Ignition Studies", BPC, Final Report, Contract No. NOW 64-0357-C, May, 1965. (CONFIDENTIAL)
63. Lowry, E. M., "Ignition Studies", BPC Report No. 290, December, 1962. (CONFIDENTIAL)
64. LoFiego, L., "Practical Aspects of Igniter Design", BPC, Western States Section of the Combustion Institute, Paper 68-32, October, 1968.
65. Falkner, C. E., "Analytical Igniter Design Handbook for Solid Propellant Rocket Motor", CETEC Corp., Contract No. AF 04611-67-C-0083, 1968.
66. Kilgroe, J. D., Fitch, R. E., and Guenther, J. D., "An Evaluation of Aft-End Ignition for Solid Propellant Rocket Motor", CETEC Corp., Final Report, Contract No. NASA CR-72447, September, 1968.
67. Falkner, C. E., and Kilgroe, J. D., "Ignition Models - Solid Propellant Rocket Motors", CETEC Corp., Western States Section of the Combustion Institute, Paper 68-35, October, 1968.
68. von Karman, K., and Malina, F. J., "Characteristics of the Ideal Solid Propellant Rocket Motor", Jet Propulsion Laboratory, Calif. Inst. of Tech. Report No. 1-4, 1940. Reprinted in Collected Works of Theodore von Karman, Vol. IV, 1940-1951, Butterworth, London, 1956.
69. Lee, T. P., "Ignition System for the ATS Rocket Motor", Jet Propulsion Laboratory Technical Memorandum 33-317, February, 1967.

REFERENCES - cont'd.

70. Peleg, I., and Manheimer-Timnat, Y., "A Study of Solid Propellant Rocket Motor Ignition", Israel Institute of Technology, Israel Journal of Technology, Vol. 6, No. 1-2, p. 32-45, 1968.
71. Barrere, M., "L'Allumage des Propergols Solides Considerations Generales", ONERA, La Recherche Aerospatiale, No. 123, March-April, 1968.
72. La Rue, P., "Dispositif Experimental D Etude de L'Allumage d'un Bloc de Propergol Solide de Grandes Dimensions", ONERA, La Recherche Aerospatiale, No. 123, March-April, 1968.
73. Scagnetti, M., and Crabol, J., "Mesure des Flux de Chaleur Pendant la Phase D'Allumage d'un Propergol Solide", ONERA, La Recherche Aerospatiale, No. 123, March-April, 1968.
74. Sineau, J., "Etude sur Calculateur Analogique de la Phase D'Allumage d'un Propulseur a Propergol Solide", ONERA, La Recherche Aerospatiale, No. 123, March-April, 1968.
75. Godai, T., "Flame Propagation into the Gap of Solid Propellant Grain", National Aerospace Laboratory, Tokyo, Japan, NASA-TM-X-60 559, July, 1967.
76. Yamazaki, K., Iwama, A., Hayashi, M., and Kishi, K., "Erosivity of a Composite Propellant with Extreme Slow Burning Rate and Depression of the Ignition Transient Pressure with Partial Restriction of the Flow Channel", Aerospace Research Institute, University of Tokyo, Report No. 2, No. 2(B), June, 1966.
77. Allan, D. S., Bastress, E. K., and Smith, K. A., "Heat Transfer Processes During Ignition of Solid Propellant Rockets", A. D. Little, Inc., AIAA Preprint 66-66, January, 1966.
78. Niessen, W. R., and Bastress, E. K., "Solid Propellant Ignition Studies", A. D. Little, Inc., Final Report, Contract No. AF 04(611)-10741, Tech. Report No. AFRPL-TR-66-32, February, 1966.
79. Bastress, E. K., and Niessen, W. R., "Solid Propellant Ignition by Convective Heating", A. D. Little, Inc., Final Report, Contract AF 49(638)-1120, AFOSR 67-0932, October, 1966.
80. Bastress, E. K., "Boundary Layer Effects on Solid Propellant Ignition under Convective Heating", A. D. Little, Inc., Third Combustion Conference, CPIA Publication No. 138, Vol. I, p. 141, October, 1966.

REFERENCES - cont'd.

81. Allan, D. S., Bastress, E. K., and Smith, K. A., "Heat Transfer Processes During Ignition of Solid Propellant Rockets", A. D. Little, Inc., J. of Spacecraft and Rockets, Vol. 4, No. 1, January, 1967.
82. Bastress, E. K., "A Boundary Layer Model of Composite Solid Propellant Ignition", Northern Research and Engineering Corp., Third ICRPG/AIAA Solid Propulsion Conference, June, 1968.
83. DeSoto, S., and Friedman, H. A., "Flame-spreading and Ignition Transients in Solid Grain Propellants", Rocketdyne, AIAA Preprint No. 64-122, January, 1964.
84. DeSoto, S., and Friedman, H. A., "Flame Spreading and Ignition Transients in Solid Grain Propellants", Rocketdyne, AIAA J. 3, 405-412 (1965).
85. Carlson, L. W., and Seader, J. D., "A Study of the Heat Transfer Characteristics of Hot Gas Ignition", Rocketdyne, Technical Report AFRPL-TR-65-158, June, 1965.
86. Carlson, L. W., and Seader, J. D., "A Study of Heat Transfer Characteristics of Hot Gas Ignition", Rocketdyne, AIAA Preprint 66-67, January, 1967.
87. Carlson, L. W., and Seader, J. D., "Heat Transfer Characteristics of Hot Gas Ignition", Rocketdyne, AIAA J., Vol. 5, No. 7, July, 1967.
88. Wrubel, J. A., and Carlson, L. W., "Study of Heat Transfer Characteristics of Hot Gas Igniters", Rocketdyne, Technical Report AFRPL-TR-67-267, July, 1967.
89. Barrett, D. H., and Jones, Sr., R. A., "Design of Igniters for Air-Launched Missile Solid Propellant Systems", Rocketdyne, Third Combustion Conference, CPIA Publication No. 138, Vol. I, p. 149, October, 1966.
90. Barrett, D. H., "Design Criteria Monograph for Solid Rocket Igniters", Rocketdyne, Contract No. NAS 3-11181, April, 1968.
91. McAlevy, III, R. F., Magee, R. S., and Wrubel, J. A., "Flame Spreading over the Surface of Double Bas Propellants", Stevens Inst. of Tech., AIAA Preprint 64-109.
92. McAlevy, III, R. F., Magee, R. S., Wrubel, J. A., and Horowitz, F. A., "Flame Spreading over the Surface of Igniting Solid Rocket Propellants and Propellant Ingredients", Stevens Inst. of Tech., AIAA J., Vol. 5, No. 2, February, 1967.

REFERENCES - cont'd.

93. Guth, E. D. and Dubrow, B., "An Approach to the Calculation and Evaluation of Ignition Transients for Large Rocket Motors", STL Technical Report No. 6121-6432-TC-000, March, 1963. (CONFIDENTIAL)
94. Dubrow, B., Guth, E. D., and Wong, M. W., "Ballistics of Solid Propellants During Thrust Modulation", TRW/STL, AIAA Preprint 64-130.
95. Adams, D. M., "Analysis of Igniter Performance in Solid Propellant Rocket Motors", Thiokol, Special Report No. U-65-373, September, 1965.
96. Adams, D. M., "Igniter Performance in Solid Propellant Rocket Motors", Thiokol, AIAA Preprint 66-680, June, 1966.
97. Adams, D. M., "Igniter Performance in Solid Propellant Rocket Motors", Thiokol, J. Spacecraft and Rockets, Vol. 4, p. 1024, August, 1967.
98. Baer, A. D., Ryan, N. W., and Salt, D. L., "Propellant Ignition by High Convective Heating Fluxes", Solid Propellant Rocket Research, Vol. I of the ARS Progress Series, Academic Press, New York, p. 653, 1960.
99. Mitchell, R. C., "Flame Spreading on Solid Propellants", Ph.D. Thesis, University of Utah, 1963.
100. Mitchell, R. C., and Ryan, N. W., "Flame Spreading on Solid Propellant", University of Utah, AIAA Preprint 64-128, January, 1964.
101. Mitchell, R. C., and Ryan, N. W., "Flame Spread on Solid Propellant", University of Utah, J. Spacecraft and Rockets, Vol. 2, No. 4, p. 610, July-August, 1965.
102. Keller, J. A., "Studies on Ignition of Ammonium Perchlorate-Based Propellants by Convective Heating", Ph.D. Thesis, University of Utah, August, 1965.
103. Keller, J. A., and Ryan, N. W., "Measurements of Heat Flux from Initiators for Solid Propellants", University of Utah, ARS J., p. 1375, October, 1961.
104. Keller, J. A., Ryan, N. W., and Baier, A. D., "Ignition of Ammonium Perchlorate-Based Propellants by Convective Heating", University of Utah, Technical Report, Grant AF AFOSR 40-63 and 64, August, 1966.
105. Keller, J. A., Baer, A. D., and Ryan, N. W., "Ignition of Ammonium Perchlorate Composite Propellants by Convective Heating", University of Utah, AIAA J., Vol. 4, No. 8, p. 1358-1365, August, 1966.

REFERENCES - cont'd.

106. Ciepluch, C. C., Allen, H., and Fletcher, E. A., "Ignition of Solid Propellant Rocket Motors by Injection of Hypergolic Fluids", NASA Lewis, ARS J, 31.514, 1961.
107. Allen, Jr., H., and Pinns, M. L., "Relative Ignitability of Typical Solid Propellants with Chlorine Trifluoride", NASA Lewis, NASA TN D-1533, January, 1963.
108. Salmi, R. J., "Compressed-Air Model Investigation of Solid Rocket Overpressures Due to Interference from Aft-End Ignition Rockets", NASA Lewis, NASA TN-D-3537, August, 1966.
109. Judge, J. F., "Titan III=C Strap-on Performance Detailed", Technology Week, p. 26-28, August, 1966.
110. Wallis, F. R., "Initial Pressure Peaks in Rocket Motors and Interruption by Venting", Imperial Metal Industry, Ltd., Kidderminster, England, J. of Spacecraft and Rockets, Vol. 5, No. 4, p. 481-483, April, 1968.
111. von Elbe, G., "Theory of Solid Propellant Ignition and Response to Pressure Transients", (unclassified), Bulletin of the Interagency Solid Propulsion Meeting, Vol. III (classified), p. 95, July, 1963.
112. von Elbe, G., "Solid Propellant Ignition and Response of Combustion to Pressure Transients", Atlantic Research Corp., AIAA Preprint 66-668, June, 1966.
113. Churchill, S. W., Kruggel, R. W., and Brien, J. C., "Ignition of Solid Propellants by Forced Convection", A. I. Ch. E.J. p. 568, December, 1956.
114. Roth, J. F., and Wachtell, G. P., "Heat Transfer and Chemical Kinetics in the Ignition of Solid Propellants", Ind. Eng. Chem. Fundamentals, 1, No. 1, 62, February, 1962.
- 114-A. Gale, H. G., "Digital Computer Investigation of Ignition, Pressurizing and Performance of Solid Rocket Motors", Air Force Institute of Technology, August, 1967.

The following references are cited in the text but are not included in Table I.

- 115 Price, E. W., Bradley, H. H., Jr., Dehority, G. L., and Ibiricu, M. M., "Theory of Ignition of Solid Propellants", NOTS, AIAA J., Vol. 4, No. 7, p. 1153-1181, July, 1966.
- 116 Ohlemiller, T. J., and Summerfield, M., "A Critical Analysis of Arc Image Ignition of Solid Propellants", Princeton University, AIAA J., Vol. 6, No. 5, p. 878-886, May, 1968.
- 117 Ohlemiller, T. J., "Radiative Ignition of Polymeric Fuels in an Oxidizing Gas", Ph.D. Thesis, Princeton University, February, 1969.
- 118 McAlevy, R. F., III, Cowan, P. A., and Summerfield, M., "The Mechanism of Ignition of Composite Solid Propellants by Hot Gases", Princeton University, Solid Propellant Rocket Research, Vol. I of the ARS Progress Series, p. 623, Academic Press, New York, 1960.
- 119 Williams, F. A., "Theory of Propellant Ignition by Heterogeneous Reaction", University of California, AIAA J., Vol. 4, No. 8, p. 1354-1357, August, 1966.
- 120 Kashiwagi, T., Waldman, C. H., Rothman, R. B., Stang, P. L. and Summerfield, M., "Ignition of Polymers in Hot Oxidizing Gas", Princeton University, presented at the 1968 Fall Technical Meeting of the Eastern States Section of the Combustion Institute, October, 1968.
- 121 Krier, H., T'ien, J. S., Sirignano, W. A. and Summerfield, M., "Nonsteady Burning Phenomena of Solid Propellants: Theory and Experiments", Princeton University, AIAA J., Vol. 6, No. 2, p. 278-285, February, 1968.
- 122 Vidal, R. J., "Model Instrumentation Techniques for Heat Transfer and Force Measurements in a Hypersonic Shock Tunnel", Cornell Aeronautical Laboratories, Report No. AD-917-A-1, February, 1956.
- 123 Krieger, F. J., "Calculation of the Viscosity of Gas Mixtures", RAND Report No. RM 649, July, 1951.
- 124 Krieger, F. J., "The Viscosity of Polar Gases", RAND Report No. RM 646, July, 1951.
- 125 Barrere, M., Jaumotte, A., Fraeijs de Verbeke, B., Vundenkerckhave, J., Rocket Propulsion, Elsevier, Amsterdam, 1960, p. 424.
- 126 Hirshfelder, J. O., Bird, R. B., and Curtiss, C. F., "Molecular Theory of Gases and Liquids", John Wiley & Sons, New York, 1954, p. 528.

REFERENCES - cont'd

- 127 Bastress, E. K., "Modification of the Burning Rate of Ammonium Perchlorate Solid Propellants by Particle Size Control", Ph.D. Thesis, Princeton University, January, 1961.
- 128 Thomas, J. P., and Layton, J. P., "Summary Technical Report on Transient Pressure Measuring Methods Research", Aeronautical Engineering Report No. 595p, Princeton University, Princeton, N. J., November, 1965.
- 129 Carslaw, H. S., and Jaeger, J. C., Conduction of Heat in Solids, Oxford University Press, London, 1959, p. 75.
- 130 Eckert, E. R. G., and Drake, R. M., Jr., Heat and Mass Transfer, McGraw-Hill Book Company, Inc., New York, 1959, p. 211.
- 131 Hermance, C. R., "Solid Propellant Ignition Studies: Ignition of the Reaction Field Adjacent to the Surface of a Solid Propellant", Ph.D. Thesis, Princeton University, December, 1963.
- 132 Waesche, R. H. W., and Wenograd, J., "Calculation of Solid Propellant Burning Rates from Condensed-phase Decomposition Kinetics", AIAA Paper No. 69-145, January, 1969.
- 133 Steinz, J. A., "The Burning Mechanism of Ammonium Perchlorate-Based Composite Solid Propellants", Ph.D. Thesis, Princeton University, February, 1969.
- 134 Most, W. J., "Ignition Transient Prediction and Control of Solid Rocket Engines", Ph.D. Thesis, Princeton University, June 1969.

TABLE 1 PREVIOUS ANALYSES AND TEST FIRING PROGRAMS
RELATED TO IGNITION AND IGNITION TRANSIENTS

ASPECTS OF THEORETICAL MODEL

REF. NO.	DATE	AUTHOR / INSTITUTION	C/U	IGNITION CRITERION	MECHANISM OF FLAME SPREADING	HEAT TRANSFER	DYNAMIC TEMPERATURE	BURNING RATE	OTHER IMPORTANT ASPECTS
1	1961	Lancaster and Summerfield Princeton	U						
2	1963	Grant, Wenograd and Summerfield. Princeton	U						
3	1964	Grant, Lancaster, Wenograd and Summerfield Princeton	U						
4	1964	Parker, Wenograd and Summerfield Princeton	U	T_{crit}	Successive ignitions	$M_{1/2} = C R_{1/2}^{0.7} R_p^{0.3}$ Laminar flat plate	NO	$r_b = A r_p^{0.7}$	
5	1966	Parker	U	T_{crit}	Successive ignitions	Flat plate $N_{1/2} = .09 R_{1/2}^{0.8}$	Yes	"	
6	1966	Parker, Most and Summerfield Princeton	U	T_{crit}	Successive ignitions	"	"	"	
7	1966	Parker, Most and Summerfield Princeton	U	"	"	"	"	"	
8	1966	Summerfield, Stang Most and diLauro Princeton	U	"	"	"	"	"	
9	1966	Lukenas, Most Stang and Summerfield Princeton	U	"	"	"	"	"	
10	1967	diLauro, Linden, Most Stang and Summerfield Princeton	U	"	"	"	"	"	
11 12	1967 1967	Most, Linden, diLauro Lukenas, MacDonald, Stang and Summerfield Princeton	U	"	"	Flat Plate $N_{1/2} = .073 R_{1/2}^{0.8}$	"	"	
13 14	1968	Most MacDonald, Stang and Summerfield Princeton	U	$T_{crit} +$ Self heating	"	"	"	"	Inclusion of heating term important in marginal ignition cases.
15	1968	Most, MacDonald, Stang and Summerfield Princeton	U	"	"	"	"	"	"
16	1956	Altman	C	T_{crit}	None	"Gasless Ignition" convection, conduction radiation and conden- sation.	"	"	Analysis shows condensation of metals and metal oxides to be dominate mode of heat transfer.
17	1961	Priepel	U						
18	1962	Baker	U	None	A given function of time.	None	Yes	$r_{1/2} = A r_p^{0.7}$	
19	1962	Grens	C	None	A given function of time.	None	Yes	"	

ASPECTS OF EXPERIMENTAL PROGRAM

REF. NO.	TYPE(S) OF EXPERIMENTS	TYPE(S) OF IGNITERS	TEST CONFIGURATION	COMPARISON WITH THEORY	OTHER IMPORTANT ASPECTS	COMMENTS
1	Live motor firings.	Head-end pyrogen.	Cylindrical grains.	None attempted		
2	Live motor firings.	Head-end pyrogen.	Cylindrical grains.	None attempted	Showed effect of free oxygen in igniter gas decreasing ignition delay.	
3	Live motor firings.	Head-end pyrogen.	Cylindrical grains.	None attempted	Showed effect of free oxygen in igniter gas decreasing ignition delay.	
4	Live motor firings.	Direct hot wire.	Flat bed of propellant	Correct shapes and trends but no detailed agreement.		
5	Live motor firings and heat transfer studies	"	"	"		
6	"	"	"	"		
7	"	"	"	"		
8	Live motor firings.	Head-end pyrogen.	Flat bed of propellant	Good agreement.		See text. Chapter IV-D
9	Live motor firings.	Head-end pyrogen.	Cylindrical and star grains.	Good agreement.		See text for an example. Chapter IV-D
10						A theoretical computer study.
11 12	Live Motor firings.	Head-end pyrogen.	Flat bed, cylindrical and star grains.	Good agreement.		
13 14	Live motor firings.	Head-end pyrogen.	Flat bed, cylindrical and star grains. Aluminized and unaluminized propellants.	Good agreement.		Movies of flame spreading over aluminized propellant show behavior similar to unaluminized propellant. Flame spreading model is unaltered.
15	"	"	"	"		"
16	Closed-bomb.		Combustion of gasless igniter materials. Calculation of peak pressure, etc.		Importance of both intensity and duration of heat transfer.	"Gasless" igniters.
17	Live motor firings.	Hypergolic			Demonstration of intensity of hypergolic ignition of motors. Measured motor pressure during transient.	Early hypergolic ignition feasibility work.
18						Full dynamic equations. No experimental work.
19	Live motor firings.	Head-end pyrogen.	Slotted cylindrical grains.	Good agreement using observed flame spreading rates as input data.		

ASPECTS OF THEORETICAL MODEL

REF. NO.	DATE	AUTHOR / INSTITUTION	C/U	IGNITION CRITERION	MECHANISM OF FLAME SPREADING	HEAT TRANSFER CORRELATION	DYNAMIC TEMPERATURE	BURNING RATE CORRELATION	OTHER IMPORTANT ASPECTS
20	1963	Fullan and Neilson	UTC	T_{crit}	Linear function of time.	$Nu_D = .023 Re_D^{1/2} Pr^{1/4}$ + radiation + conduction.	Both isothermal and dynamic.	$V_b = A P^{1/2}$	
21	1963	Anderson	UTC	T_{crit}	Not applicable	$\dot{q} = \Delta H C^* Z e^{-E/RT}$			A hypergolic ignition theory.
22	1963	Anderson, Brown, Thompson and Ebeling	UTC	T_{crit}	Not applicable	"			A hypergolic ignition theory.
23	1964	Anderson, Brown and Shannon	UTC						A comparison of local ignition theories.
24	1964	Brown, Wirrick and Anderson	UTC	T_{crit}	Successive ignitions	Used Martens's eqn. for blowing from the surface + hypergolic + radiation.	No	$V_b = A P^{1/2}$	2-D heat conduction in solid phase. Concentration of hypergolic as fcn. of x by a simple mass balance.
25	1965	Brown, Jensen and Cose.	UTC	"	"	Convection + radiation + hypergolic. $T = f(x)$. $C = f(x)$. $\dot{q}_{cond} = h_{hyp} (T_{hyp} - T_{wall})$	"	"	Axial variation in heat transfer attributed to only gas phase temperature gradient.
26	1965	Beyer, McLaren and Anderson	UTC						
27	1965	Mullis and Channarayana	UTC						
28	1965	Anderson	UTC	T_{crit}	Not applicable	$\dot{q} = \Delta H C^* Z e^{-E/RT}$			A hypergolic ignition theory.
29	1966	Jensen and Cose	UTC	T_{crit}	Successive ignitions	$Nu_D = C Re_D^{1/2} Pr^{1/4}$ $h_{hyp} = h_{hyp} \left(\frac{m_{hyp} \dot{q}_{hyp}}{m_{air} \dot{q}_{air}} \right)$	No	$V_b = A P^{1/2}$	Axial variation in heat transfer attributed to only gas phase temperature gradient.
30			UTC						
31	1967	Kilgroe	UTC						
32	1966	Slavin and Billheimer	UTC						
33	1962	Nachbar, Wilson, Taback, Lovinski and Plumley	Aerojet						
34	1963	Coleal and Pelette	UTC						
35	1964	Paul, Lovine and Pong	Aerojet	Stationary gas-phase diffusion model.	None	$Nu_D = .023 Re_D^{1/2} Pr^{1/4}$ Used only to account for heat losses.	Yes		Concentrated more with ignition model than with motor predictions. Model requires knowledge of vapor conc. above surface.
36	1964	Paul, Lovine and Pong	Aerojet	"	"	None	Yes	Nonsteady $V \sim t^{1/2} [1 + \alpha \frac{t}{\tau}]$	Nonsteady nozzle flow. No igniter term. Plot of initial P and T from which overshoots are possible.
37	1964	Paul, Lovine and Pong	Aerojet	T_{crit}	Instantaneous at impingement region. Step fcn. downstream. Propagation into headend.	$Nu_D = .023 Re_D^{1/2} Pr^{1/4}$ + radiation	No	$V_b = A P^{1/2}$	For head end: Modify heat transfer to match experimental quadratic fit to $S(t) = a + bt + ct^2$.
38	1964	Plumley	Aerojet	None					Model for penetration of aft-end igniter jet to form stagnation zone. Based on simple momentum balance.

ASPECTS OF EXPERIMENTAL PROGRAM

REF. NO.	TYPE(S) OF EXPERIMENTS	TYPE(S) OF IGNITERS	TEST CONFIGURATION	COMPARISON WITH THEORY	OTHER IMPORTANT ASPECTS	COMMENTS
20	Live motor firings.	Head-end pyrogen and hypergolic.	Slotted cylindrical grains.	Good agreement using observed flame spreading rates as input data.		
21	Small samples exposed to hypergolic liquids.			Good agreement for nonflow cases studied.		
22	Small samples exposed to hypergolic liquids.			Good agreement for nonflow cases studied.		
23						A comparison of local ignition theories.
24					Used experimental data from Ref. 98	
25						Authors claim that trends predicted by the model are consistent with observed experimental trends of UTC data. $\dot{Q}_p \sim \sqrt{t/A}$
26	Live motor firings.	Head-end pyrogen, pyrotechnic, hypergolic, conductive	Cylindrical grains	Not applicable	First ignition for pyrogen and pyrotechnic cases: For hypergolic case:	as a function of pressure and flux level plotted for several propellants.
27	Heat transfer, flow visualization.	Head and aft-end pyrogens.	Inert cylinder.	Not applicable	Graphical heat transfer correlation similar to Ref. 86. Examples of Ref. 86 given in text.	
28						
29	Heat transfer, flame spreading rates.	Head-end pyrogen.	Flat bed and cylindrical grains.	Poor to fair agreement. Limited data given. Use model to back calculate to get $S(t)$ for some motor		Authors claim agreement between predicted and experimental flame spreading rates within experimental error.
30						
31	Heat transfer.	Head-end pyrogen, axial and canted. Aft-end pyrogen.	Inert copper duct.	Not applicable	$Nu_D = A_1 (1 + A_2 \dot{Q}_p^{0.5}) R_0^{0.5} A_p^{0.5}$ $Nu_D = A_2 (A_3 - A_4 \dot{Q}_p) R_0^{0.5} A_p^{0.5}$	Heat transfer correlations given in text. Chapter III-8
32	Heat transfer	Head-end ALCLD basket	Cylindrical duct.	Not applicable	Correlat total energy delivered vs. L, D, A_c distance from igniter, and igniter weight. $\dot{Q}_{\text{burn}}/A \sim W^{0.5} \dot{Q}_p^{0.5} A_p^{0.5}$	
33	Igniter development test firings	Head and aft-end pyrogens.			Data on pressure distribution for aft-end pyrogen.	A development program: Scale up of a head-end igniter by using a correlation of igniter to motor free volume and total igniter energy/area vs. igniter delivery rate. Attempt to scale an aft-end igniter using similar correlations.
34						This study recognized the importance of stagnant flux regions in controlling the overall ignition transient.
35						
36						See text for alternative explanation of some pressure overshoots. Chapter IV-B-4-a and b
37	Live motor firings.	Head-end pyrogen.	Cylindrical grains.	Fair agreement for limited case considered.	Only limited data given.	No igniter term is included in the theoretical model.
38						

ASPECTS OF THEORETICAL MODEL

REF. NO.	DATE	AUTHOR / INSTITUTION	C/U	IGNITION CRITERION	MECHANISM OF FLAME SPREADING	HEAT TRANSFER CORRELATION	DYNAMIC TEMPERATURE	BURNING RATE CORRELATION	OTHER IMPORTANT ASPECTS
39	1964	Lovine and Fong Aerojet	U	Stationary gas-phase diffusion model.	None	Flat plate	Yes	Nonsteady See Ref. 36	x measured from igniter impingement point in heat transfer correlation. Average heat loss to walls included.
40	1965	Lovine and Fong	U		A given function of time		Yes	Nonsteady See Ref. 36	No igniter term is considered in the post-first-ignition ballistics. Erosive burning is considered.
41	1967	Cohen and Lovine Aerojet	U		None	Flat plate $Nu_x = 0.0246 Re_x^{0.8}$	Yes	None	Only time to first ignition predicted. Includes gas phase convective heat transfer.
42		Michell Aerojet	U						A model for the start-stop operation of a solid motor.
43	1968	Price and Linfor Aerojet	U	T _{crit} modified by experimental ignition data.	Successive ignitions	$Nu_x = 0.035 Re_x^{0.8}$ For cylindrical bore. See text for others.	Yes	Nonsteady See Ref. 36	
44	1964	C.	U						
45	1955	Bryan and Price Aerojet	C						A correlation study. See text. Chapter III-A
46	1956	Bryan and Lawrence	C						Correlation studies. See text. Chapter III-A
47	1957		C						
48	1959		C						
50	1961	Sharn NOL	U						
51	1962	Price NMC	U						A description of the sequence of events during the ignition transient.
52	1962	Sharn NOL	U						A ballistic analysis of a "Hi-Low" (rocket type) igniter.
53	1963	Price NMC	C						Annotated Ignition Bibliograph and Information Retrieval System.
54	1964	Bradley NMC	U	None	A linear function of time.	None	Yes	$t_{01} = k P_0^m$ See text. Chapter III-B	
55	1964	Sharn, regard, Price, Lawrence, Rydholm and Zovko NOL	U	T _{crit}	Simultaneous ignition of entire grain. Ignition delay based on average heat flux.	$t_{01} = 70 \left(\frac{P_0}{P_a} \right)^{0.9} \left[1 + \left(\frac{P_0}{P_a} \right)^{0.3} \right]$	No	"	Also gives a correlation for maximum igniter pressure. $P_0 = P_{max} \frac{W}{V}$
56	1952	Shook NOL	U						
57	1965	Hieszen NOL	U						
58	1968	Turner AFI	C						Control of flame spreading rates with electric fields.
59	1961	Lovry BPC	C						Practical igniter information. See text. Chapter III-A

ASPECTS OF EXPERIMENTAL PROGRAM

REF. NO.	TYPE(S) OF EXPERIMENTS	TYPE(S) OF IGNITERS	TEST CONFIGURATION	COMPARISON WITH THEORY	OTHER IMPORTANT ASPECTS	COMMENTS
39	Live motor firings, heat transfer studies.	Head-end pyrogen.	Cylindrical grains. Heat transfer studies done in inert duct.	Overshoots can be predicted. No detailed comparison given.		See Ref. 37 for comments.
40						
41	Live motor firings.	Head-end pyro-technic - ALCLAD	Small 5 - 10 lb. class motors. Minuteman 2nd stage.	Good agreement for limited case of predicting first ignition.		
42						
43	Live motor firings.	Head-end pyrogen.	Finned foreclosures, cylindrical bore, sunken nozzle.	Good agreement.		See text for comments. Chapter III-3
44	Heat transfer	Head-end pyrogen and pyrotechnic.	Cylindrical duct.	Not applicable	Flat plate correlation $\frac{q}{A} \sim (G/\rho \mu)^{1/4}$ Radiation important for pyrotechnic materials.	
45						Correlation of 53 rocket motors with various types of propellants, grains and igniters. Total heat release by igniter vs. total surface area times ignition requirements per unit area. $(G \sim A_{gr})$
46						Correlation studies.
47						A correlation study.
48						A correlation study.
49						A correlation study.
50						A description of the sequence of events during the ignition transient.
51						
52						
53						Annotated Ignition Bibliography and Information Retrieval System.
54						
55	Live motor firings, heat transfer studies.	Head-end pyrotechnic.	Cylindrical grains.	Good agreement over part of the transient. Limited data.		Theoretical model uses the von Elbe ignition model.
56						Measurements of C, (T), k(T) and radiative absorption constants for various propellants over a temperature range of 25 - 95 °C.
57	Aft-end flow visualization.	Aft-end pyrogen.	Inert cylindrical grain with windows.	Comparison of data with model given in Ref. 38. Agreement $\pm 10\%$.		Confirmed the existence of a stagnation zone formed by an aft-end igniter jet.
58						Control of flame spreading rates with electric fields.
59						Practical igniter information: Igniter types, igniter materials, igniter hardware.
60						

ASPECTS OF THEORETICAL MODEL

REF. NO.	DATE	AUTHOR / INSTITUTION	C/U	IGNITION CRITERION	MECHANISM OF FLAME SPREADING	HEAT TRANSFER CORRELATION	DYNAMIC TEMPERATURE	BURNING RATE CORRELATION	OTHER IMPORTANT ASPECTS
61	1964	Fleming	C						Local ignition studies, characterization of igniter materials and correlation work.
62	1965	Fleming	C						
63	1962	Lowry	BPC						Discussion of practical igniter systems, designs and problems.
64	1968	LoFiego	U						
65	?	Falkner	U	T_{crit}	Successive ignitions.	Similar to Ref. 31 but with $R_{0.8}^{0.5}$ instead of $R_{0.8}^{0.8}$ and the leading coefficient adjusted.	Yes	$r_{ss} = R_0^{0.8}$	Used the Princeton Ignition Transient Computer Prediction Program.
66	1968	Kilgroe, Fitch and Falkner	U			Art-end correlations similar to those given in References 85-88		"	An attempt to model the penetration and aerodynamic throat blockage of an aft-end igniter jet.
67	1968	Falkner and Kilgroe	U	T_{crit}	Successive ignitions.	See Ref. 65	Yes		See Ref. 65. Model the same as Princeton work except for heat transfer correlation. See Ref. 66.
68	1940	von Karman and Malina	U	None	None	None	Yes, but there is an error in the energy eqn.	$r_{ss} = R_0 + R_0^{0.8}$	Solved for unrealistic initial conditions.
69	1967	Lee	U						An example of a typical igniter development program.
70	1968	Peleg and Manheimer-Tinnat	C	T_{crit}	Successive ignitions.	$Sr = \alpha R_{0.8}^{0.8} + \text{radiation.}$ Similar to Ref. 77	Yes	$r_{ss} = R_0^{0.8}$	
71	1968	Barrere	U	T_{crit}	Successive ignitions	Several suggested	Both isothermal and dynamic.		A general discussion of several models.
72	1968	LaRue	U			$Nu_x = 0.19 Re_x^{0.8}$			
73	1968	Scagnetti and Crabot	U						
74	1968	Sineau	U	None	Flame spreading rates taken as input data.	None	Yes	$r = \alpha R_0^{0.8} [1 + R_0^{0.8} - R_0^{0.8}]$	Analog computer study. No comparison with experiment.
75	1967	Godal	U						Flame propagation into a grain crack. Threshold gap is a function of propellant composition and temperature, as well as burning rate.
76	1966	Yamazaki, Inama, Hayashi, and Kishi	U						
77	1966	Alan Bastress and Smith	U			$Sr = 0.08 Re_x^{0.8}$			
78	1966	Niessen and Bastress	U	Gas phase, T or C_x controlling.					
79	1966	Bastress and Niessen	U						
80	1966	Bastress A. D. Little	U						
82	1968	Bastress	U						Boundary layer model of ignition.
83	1964	DeSoto and Friedman	U	T_{crit}	Successive ignitions.	$Nu_x \sim Re_x^{0.8} Pr^{0.1} \left(\frac{I}{T} \right)^{0.18}$	No	$r_{ss} = R_0^{0.8}$	No igniter term. Closed form analytic solutions
84	1964	Rocketdyne	U						

ASPECTS OF EXPERIMENTAL PROGRAM

REF. NO.	TYPE(S) OF EXPERIMENTS	TYPE(S) OF IGNITERS	TEST CONFIGURATION	COMPARISON WITH THEORY	OTHER IMPORTANT ASPECTS	COMMENTS
61						Correlation studies: $Q = C A \sqrt{P}$. Also a correlation for peak pre-ignition pressure.
62						
63						
64						Discussion of practical igniter systems, designs and problems.
65						
66	Live motor firings and igniter studies	Aluminum pyrotechnic	Cylindrical port and star head closure.	Igniter parameters to avoid over pressurization can be predicted.	Previously unobserved pressure oscillations in nozzle. Attributed to interaction of igniter and main motor flow.	A partially complete model for predicting the penetration of the aft-end igniter jet was also presented.
67	Live motor firings.	Head-end pyrogen.	Slotted cylindrical grain.	Good to fair agreement - time to operating pressure predicted $\pm 10\%$.		This model is the same as the Princeton work except for the heat transfer correlation.
68	Operational igniter development.	Head-end ALCLAD basket.	Complex grain geometry.	None attempted.		An example of a typical igniter development program.
69						
70	Live motor firings, heat transfer with inert.	Head-end pyrogen.	Star grain. Aluminized and unaluminized propellants.	Good agreement	Photographs of lateral flame spreading down sides of star grain.	See text. Chapter III-B
71						A general discussion of several models for the ignition transient.
72	Live motor firings, heat transfer measurements	Head-end pyrogen	Star grain, thin propellant layer on inert backing.	None attempted	$Nu_g = 0.19 Re_g^{0.8}$	Recommends the thin propellant layer bonded to an inert backing as an inexpensive way of testing igniters for large motors.
73	Heat transfer	Head-end pyrogen	Cylindrical grain	Not applicable	$Nu_g = 0.19 Re_g^{0.8}$	Concludes that radiation and convection are the dominant modes of energy transfer.
74						
75						Flame propagation into a crack in a propellant grain. The threshold gap is a function of the propellant composition, the propellant temperature and the local pressure, as well as a strong function of the burning rate.
76	Live motor firings.	Head-end pyrotechnic.	Cylindrical and star grains.	None attempted		An attempt to control the ignition transient, particularly the rate of pressurization and overshoots, by inhibiting portions of the propellant grain.
77	Heat transfer	Head-end pyrogen and pyrotechnic.	Cylindrical duct.	Not applicable	Convection correlation	Convection heat transfer correlation similar to Ref. 70.
78	Convective ignition of small samples	Hot gas generator.	Flat samples $\sim 1"$ long.	Not applicable		It was found that increasing the flow velocity increases the ignition time. This occurred for $Re \geq 0.4$. The ignition time was found to decrease with increasing sample length.
79						
80						
81						
82						
83						
84						

ASPECTS OF THEORETICAL MODEL

REF. NO.	DATE	AUTHOR / INSTITUTION	C/U	IGNITION CRITERION	MECHANISM OF FLAME SPREADING	HEAT TRANSFER	DYNAMIC TEMPERATURE	BURNING RATE CORRELATION	OTHER IMPORTANT ASPECTS
85 86	1965 1966	Carlson and Seader Rocketdyne	U U						
87	1967	Carlson and Seader Rocketdyne	U						
88	1967	Wrubel and Carlson Rocketdyne	U						
89	1966	Barrett and Jones Rocketdyne	U	T_{crit}	None	None	No	$r_{ss} = A \cdot t^{0.8}$	Analog computer solution of the 1-D mass continuity equation.
90	1968	Barrett Rocketdyne	T						Igniter design monograph - in preparation.
91 92	1964 1967	McAlevy, Magee and Wrubel McAlevy, Magee, Wrubel and Horowitz SIT	U U	T_{crit} in gas phase.	1-D gas phase flame spreading mechanism.	Not applicable	Not applicable		A model for flame spreading over propellant surfaces in a quiescent atmosphere.
93 94	1963 1964	Guth and Dubrow Dubrow Guth and Wong SIL/TRW	C U	None	None	None	No	$r_{ss} = A \cdot t^{0.8}$ $r_{ss} = \frac{Q}{\rho \cdot L} \cdot \frac{1}{t^{0.8}}$	
95 96 97	1965 1966 1967	Adams Thiokol	U	None	A given function of time.	None	No	Nonsteady Erosive	Careful consideration of output from an igniter which burns cylindrical pellets.
	1964	Gibby Thiokol	U						
99 100 101	1963 1964 1965	Mitchell Mitchell and Ryan Utah	U U U	T_{crit}	Successive ignitions.	$p(x,y) = (1+xy)^{-n}$ y = distance from flame front to x .	Not applicable	Not applicable	
98	1960	Baer, Ryan and Salt Utah	U						
102	1965	Keller Utah	U	T_{crit}					
103	1961	Keller and Ryan Utah	U						
104 105	1966 1966	Keller, Baer and Ryan Utah	U	T_{crit}	Not applicable	Not applicable			
106	1961	Ciepluch, Allen, and Fletcher NASA Lewis/U. of Minnesota	U						
107	1963	Allen and Pinns NASA Lewis	U						
108	1966	Salmi NASA Lewis	U						
109	1966	Judge	U						

ASPECTS OF EXPERIMENTAL PROGRAM

REF. NO.	TYPE(S) OF EXPERIMENTS	TYPE(S) OF IGNITERS	TEST CONFIGURATION	COMPARISON WITH THEORY	OTHER IMPORTANT ASPECTS	COMMENTS
85 86	Heat transfer	Head and aft-end pyrogens.	Cylindrical and circumferentially slotted cylindrical grains.	Not applicable	All data taken with inert grains.	Head-end: A turbulent pipe flow correlation modified by a graphical X/D relation. 0.4 is plotted vs. X/D . Aft-end: $Re_D = P_r$
87	Heat transfer and live motor firings.	Head and aft-end pyrogens.	Three pointed star and conocyl grains.	Not applicable		The conocyl grains were found to obey the same heat transfer correlations as the cylindrical grains studied in Ref. 85. No general correlation was found for the star grains.
88	Heat transfer, live motor firing and flow visualization studies.	Head and aft-end pyrogens.	Conocyl and star grains.	Not applicable	Demonstration firings to show correlation of predicted and calculated first ignition.	See References 85, 86 and 87.
89						
90						
91 92	Flame spreading rates.	Direct hot wire	Flat sample in a quiescent atmosphere.	General trends predicted by gas phase model are observed experimentally.		This model is not applicable in motor ignition transients.
93 94	Live motor firings, thrust modulation.		End burning cylinder.		Thrust modulation by rapidly varying nozzle size.	
95 96 97	Live motor and separate igniter firings.	Head-end pyrotechnic pellets.	Star and slotted cylindrical grains.	Pair to good agreement. Difficult to evaluate on scale presented.		Overhoots attributed to erosive burning effects. The erosive correction was based on an average port Mach number, $M = M/2$.
	Live motor firings.					The effects on the ignition transient of inhibiting various parts and percentages of the propellant grain were studied. See also Ref. 76
99 100 101	Local convective ignition studies.	Hot gas flow parallel to the surface.	Flat propellant sample in a constant pressure flow.	Result correlate with solid phase heat-up.	Observation of diffuse flame front.	This study concludes that given the heat transfer distribution, flame spreading can be correlated with the solid phase heat-up to an auto ignition temperature.
98	Local or convective ignition studies.	Hot gas flow parallel to the surface.	Flat propellant sample in a constant pressure flow.	Results correlate with solid phase heat-up.	Pronounced effect of oxygen in the heating gas.	
102				Data supports simple thermal theory of ignition in range of fluxes tested: 20-60 cal/cm ² sec		
103	Heat transfer	Head-end pyrogen and pyrotechnic.	Cylindrical duct.	Not applicable		This reference concludes that independent igniter and propellant ignition studies can be correlated.
104 105	Convective heating of propellant samples.	Hot gas flow.	Flow parallel to surface - shock tunnel.	Not applicable		Most of the experimental data was correlated by the simple thermal ignition theory. Local hot spots complicated the situation.
106	Live motor firings.	Hypergolic injection at head-end.	Cylindrical grains, double base and composite propellants	None attempted	Effects of simulated altitude on ignition studied.	CIF was found to be the most reactive hypergolic material between the three, CIF ₃ , BR ₃ and BR ₄ . Double base and composite propellants were found to ignite about the same at sea level but the double base propellants were harder to ignite at altitude.
107	Small samples.	Hypergolic CIF ₃	Small samples in an ignition test chamber.	Not applicable		This study rated the relative ignitability of several propellants. Double base propellants were found harder to ignite than composite propellants. The ignition delay increased with increasing AP loading and decreasing Al loading.
108	Motor simulation	Aft-end pyrogen.	Hot gas simulation of 260" diam. motor and aft-end igniter.	Not applicable		It was found that severe overpressurizations could be caused by interference due to the aft-end igniter. This was found to be a function of the igniter-to-booster pressure ratio, the igniter diam. and the igniter mass flow rate.
109	Live motor firings.	Head-end pyrogen.	The 120" diam. motor.	None attempted		An example of igniter and ignition transient design specifications.

ASPECTS OF THEORETICAL MODEL

REF. NO.	DATE	AUTHOR / INSTITUTION	C/U	IGNITION CRITERION	MECHANISM OF FLAME SPREADING	HEAT TRANSFER CORRELATION	DYNAMIC TEMPERATURE	BURNING RATE CORRELATION	OTHER IMPORTANT ASPECTS
110	1968	Wallis Imperial Metals Industry	U	None	Assumes fully ignited surface.	None	No	Nonsteady	See comments.
111	1963	von Elbe	U	T_{crit} + critical solid phase	Not applicable	Not applicable	Not applicable	Nonsteady	See text. Chapter III-B
112	1966	ARC	U	thermal profile	Not applicable		Not applicable		
113	1956	Churchill, Kruegel and Brien Univ. of Michigan	U	Gas phase ignition model	Not applicable		Not applicable		
114	1962	Roth and Wachtell Franklin Institute	U	Primary ignition in solid phase	Not applicable	Not applicable	Not applicable		
114-A	1967	Gale AFIT	U	T_{crit} + minimum ignition energy	Successive ignitions	Radiation + pipe flow convection with variable T_s	Polytropic	$P_{ss} = k \frac{dP}{dx}$	

ASPECTS OF EXPERIMENTAL PROGRAM

REF. NO.	TYPE(S) OF EXPERIMENTS	TYPE(S) OF IGNITERS	TEST CONFIGURATION	COMPARISON WITH THEORY	OTHER IMPORTANT ASPECTS	COMMENTS
110						This model uses a steady state burning rate law of the form $\dot{m} = A_p \sqrt{P}$ and makes the burning rate nonsteady through the heat transfer film coefficient and the solid phase thermal profile.
111 112						
113	Ignition of small samples	Hot gas flow	Cylindrical samples extending into flow	Good agreement	Pyrocellulose and double-base propellants	
114	Ignition of small samples	Nonflowing hot gas	Pressurized furnace		Nitrate ester propellants	Observation of multistage ignition
114-A	Live motor firings	Head-end pyrogen	End burning and center perforated grains.	None given		

TABLE II

Table of Experimental Parameters
and Propellant PropertiesRectangular Rocket Motor

$$\begin{aligned}V_c &= 140 \text{ cm}^3 \\A_B &= 46 \text{ cm}^2 \\l &= 24.1 \text{ cm} \\A_p &= 4.0 \text{ cm}\end{aligned}$$

Star Grain Rocket Motor

$$\begin{aligned}V_c &= 79.3 \text{ cm}^3 \\A_B &= 241 \text{ cm}^2 \\l &= 24.1 \text{ cm} \\A_p &= 2.14 \text{ cm}^2\end{aligned}$$

Pyrotechnic Igniter Motor

$$\begin{aligned}V_c &= 302 \text{ cm}^3 \\A_B &= 311 \text{ cm}^2 \\l &= 19.1 \text{ cm} \\A_p &= 15.8 \text{ cm}^2 \\d_t &= 4.5 \text{ mm (4 nozzles)}\end{aligned}$$

PropellantsI Unaluminized Composition

PBAA	17
Epon 828	3
AP Fine (15 μ)	24
AP Coarse (180 μ)	56
	<u>100</u>

$$\begin{aligned}\rho_p &= 1.6 \text{ g/cm}^3 \\C_p &= 0.3 \text{ cal/g } ^\circ\text{C} \\\lambda_p &= 9 \times 10^{-4} \text{ cal/cm sec. } ^\circ\text{C} \\T_{ign} &= 420^\circ\text{C} \\T_f &= 2078^\circ\text{K} \\C^* &\begin{cases} \text{(frozen)} = 4386 \text{ ft/sec} \\ \text{(equilibrium)} = 4397 \text{ ft/sec} \end{cases} \\C_g &= 0.441 \text{ cal/g } ^\circ\text{C} \\\gamma &= 1.26 \\m_g &= 22.23 \\\mu_g &\begin{cases} (2000^\circ\text{K}) = 6.6 \times 10^{-4} \text{ g/cm sec (123, 124, 125, 126)} \\ (1200^\circ\text{K}) = 4.9 \times 10^{-4} \text{ g/cm sec (123, 124, 125, 126)} \end{cases} \\\lambda_g &\begin{cases} (2000^\circ\text{K}) = 3.6 \times 10^{-4} \text{ cal/cm sec } ^\circ\text{C (125, 126)} \\ (1200^\circ\text{K}) = 2.4 \times 10^{-4} \text{ cal/cm sec } ^\circ\text{C (125, 126)} \end{cases}\end{aligned}$$

II Aluminized Composition

PBAA	15
Epon 828	2
AP Fine (15μ)	19
AP Coarse (180μ)	49
Al (10μ)	15
	<u>100</u>

$$n = .274, k = .014 \frac{\text{in}}{\text{sec}} \frac{1}{(\text{psia})^{.274}}$$

$$\rho_p = 1.69 \text{ g/cm}^3$$

$$C_p = .286 \text{ cal/g } ^\circ\text{C}$$

$$\lambda_p = 9.3 \times 10^{-4} \text{ cal/cm sec } ^\circ\text{C}$$

$$T_{\text{ign}} = 420^\circ\text{C}$$

$$T_s = 2914^\circ\text{K}$$

$$C^* \left\{ \begin{array}{l} (\text{frozen}) = 4886 \text{ ft/sec} \\ (\text{equilibrium}) = 4948 \text{ ft/sec} \end{array} \right\} \text{ at } 300 \text{ psia}$$

$$C_g = 0.673 \text{ cal/g } ^\circ\text{C}$$

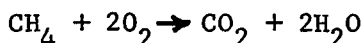
$$\gamma = 1.20$$

$$m_g = 25.85$$

$$\mu_g \left\{ \begin{array}{l} (2000^\circ\text{K}) = 9.5 \times 10^{-4} \text{ g/cm sec (123, 124, 125, 126)} \\ (1200^\circ\text{K}) = 6.9 \times 10^{-4} \text{ g/cm sec (123, 124, 125, 126)} \end{array} \right.$$

$$\lambda_g \left\{ \begin{array}{l} (2000^\circ\text{K}) = 5.16 \times 10^{-4} \text{ cal/cm sec } ^\circ\text{C (125, 126)} \\ (1200^\circ\text{K}) = 3.75 \times 10^{-4} \text{ cal/cm sec } ^\circ\text{C (125, 126)} \end{array} \right.$$

Igniter Gases



$$T_s = 3400^\circ\text{K at } 250 \text{ psia}$$

$$\gamma = 1.2$$

$$m_g = 26.67$$

$$\mu_g \left\{ \begin{array}{l} (2000^\circ\text{K}) = 6.0 \times 10^{-4} \text{ g/cm sec (123, 124, 125, 126)} \\ (1200^\circ\text{K}) = 4.36 \times 10^{-4} \text{ g/cm sec (123, 124, 125, 126)} \end{array} \right.$$

$$\lambda_g \left\{ \begin{array}{l} (2000^\circ\text{K}) = 3.02 \times 10^{-4} \text{ cal/cm sec } ^\circ\text{C (125, 126)} \\ (1200^\circ\text{K}) = 2.20 \times 10^{-4} \text{ cal/cm sec } ^\circ\text{C (125, 126)} \end{array} \right.$$

Heat Transfer Gauge

Gauge Material: Pyrex 7740

$$\lambda_o = 2.63 \times 10^{-3} \text{ cal/cm sec } ^\circ\text{C}$$

$$\rho_o = 2.23 \text{ g/cm}^3$$

$$C_o = 0.20 \text{ cal/g } ^\circ\text{C}$$

$$\text{Film thickness} \approx 10^{-6} \text{ cm (122)}$$

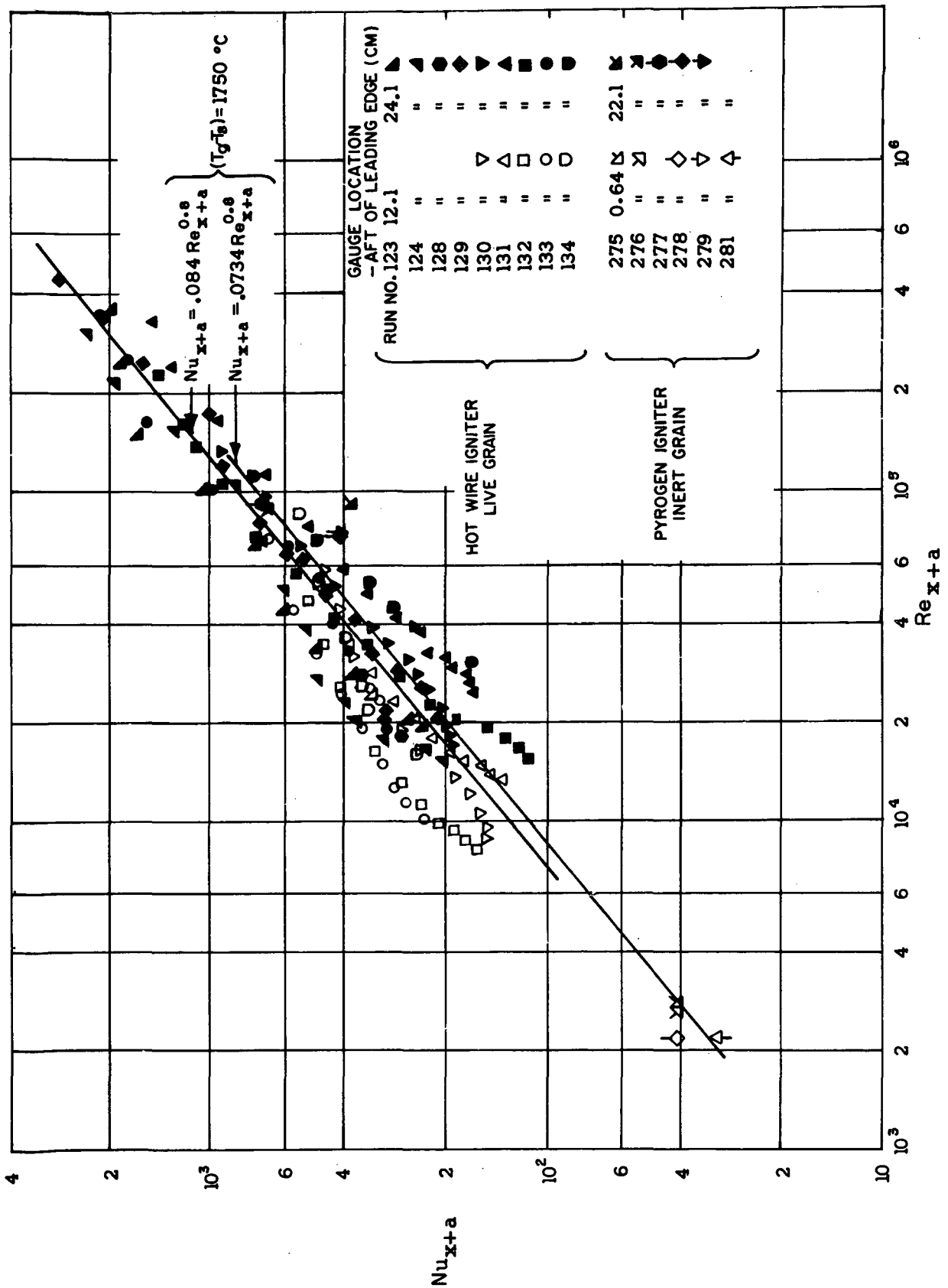


FIGURE 1

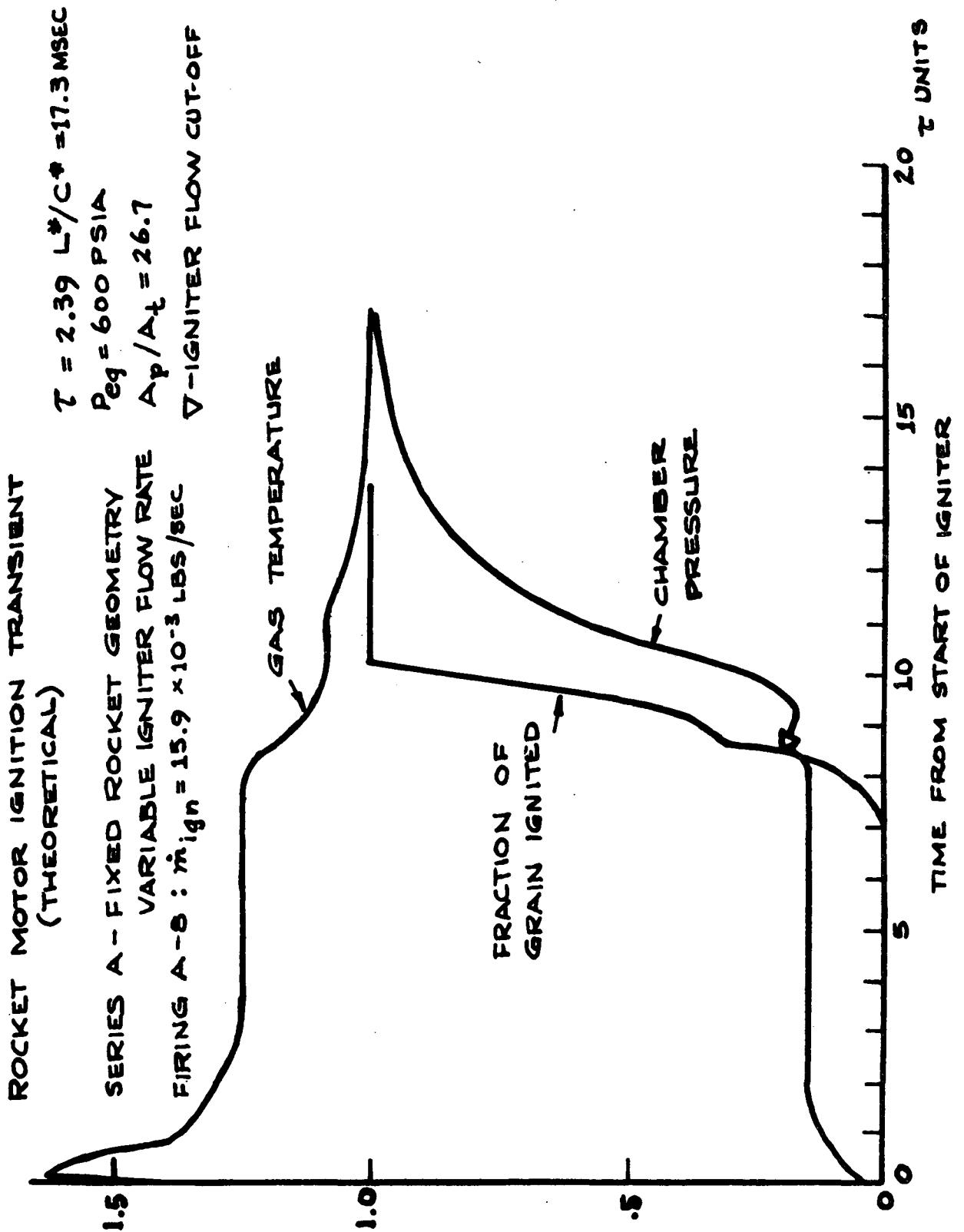


FIGURE 2

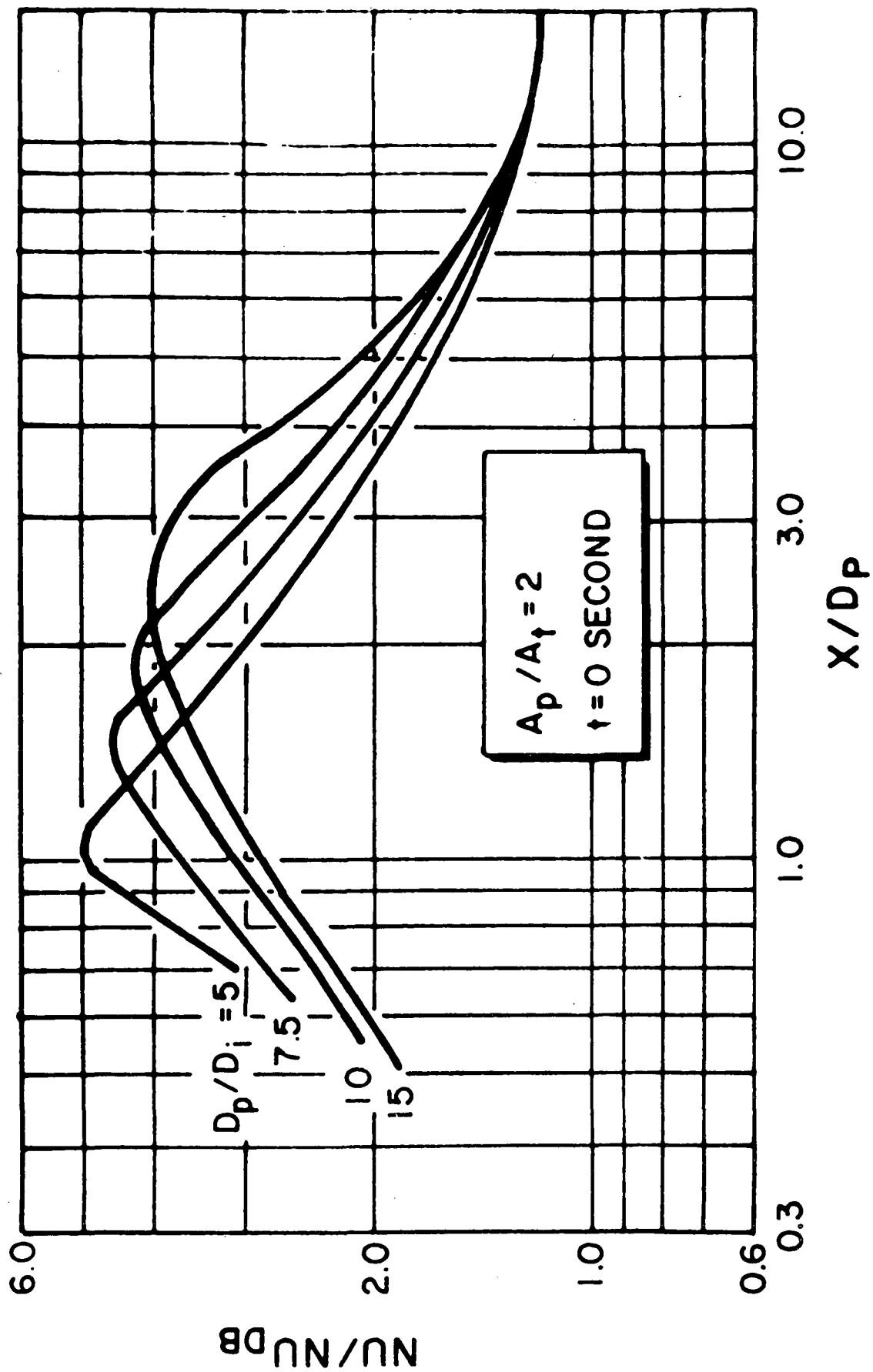


FIGURE 3

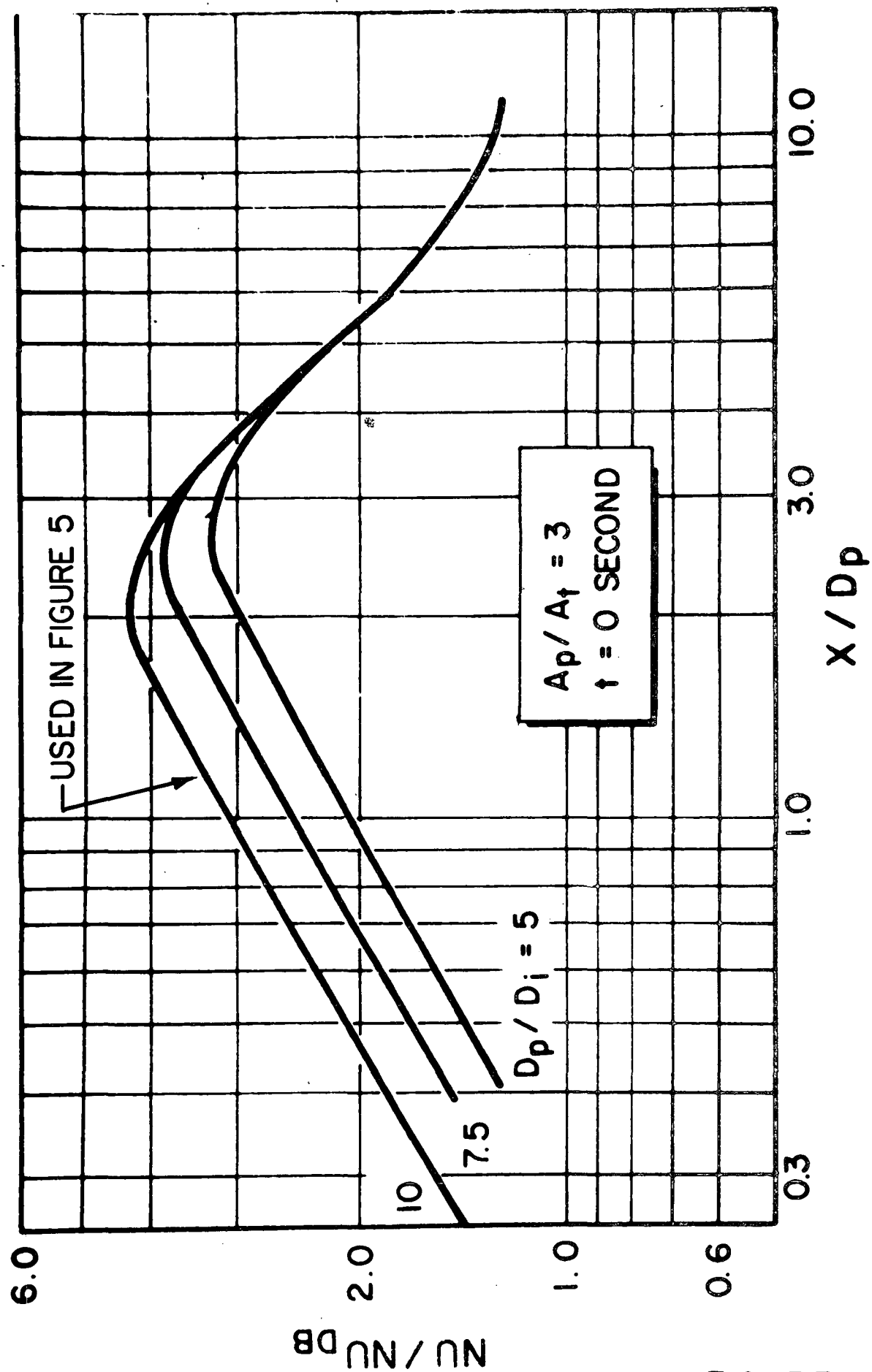
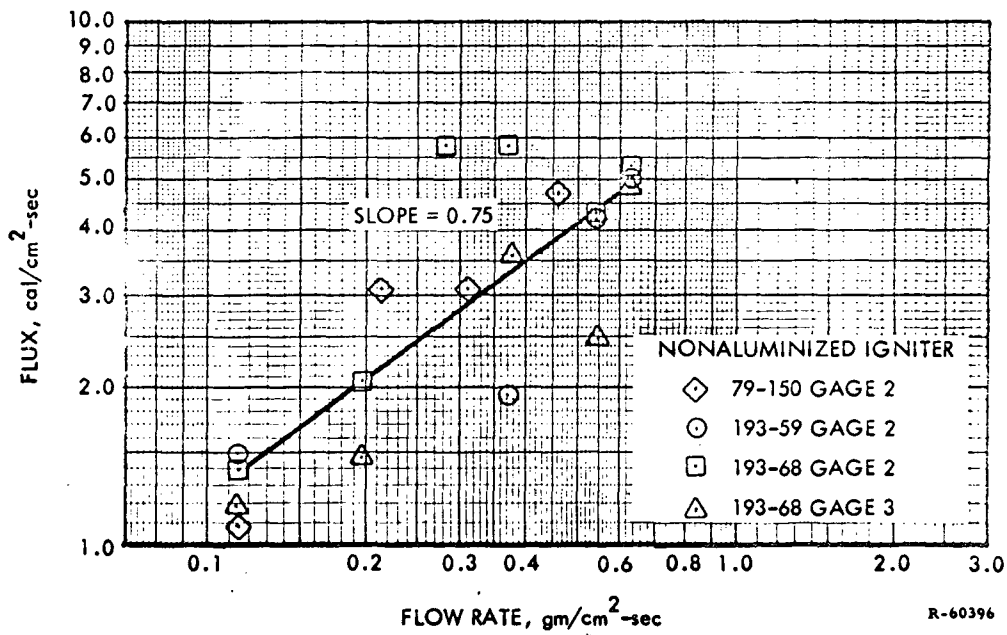
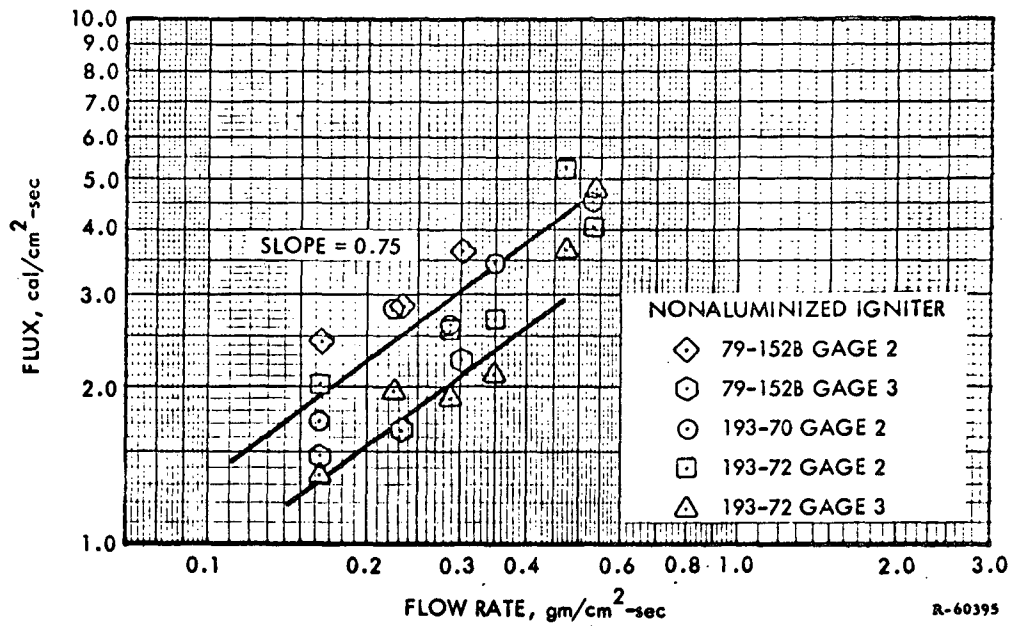


FIGURE 4

FROM REFERENCE 29



Heat Transfer During Flame Spreading Over
a Flat Bed of Propellant

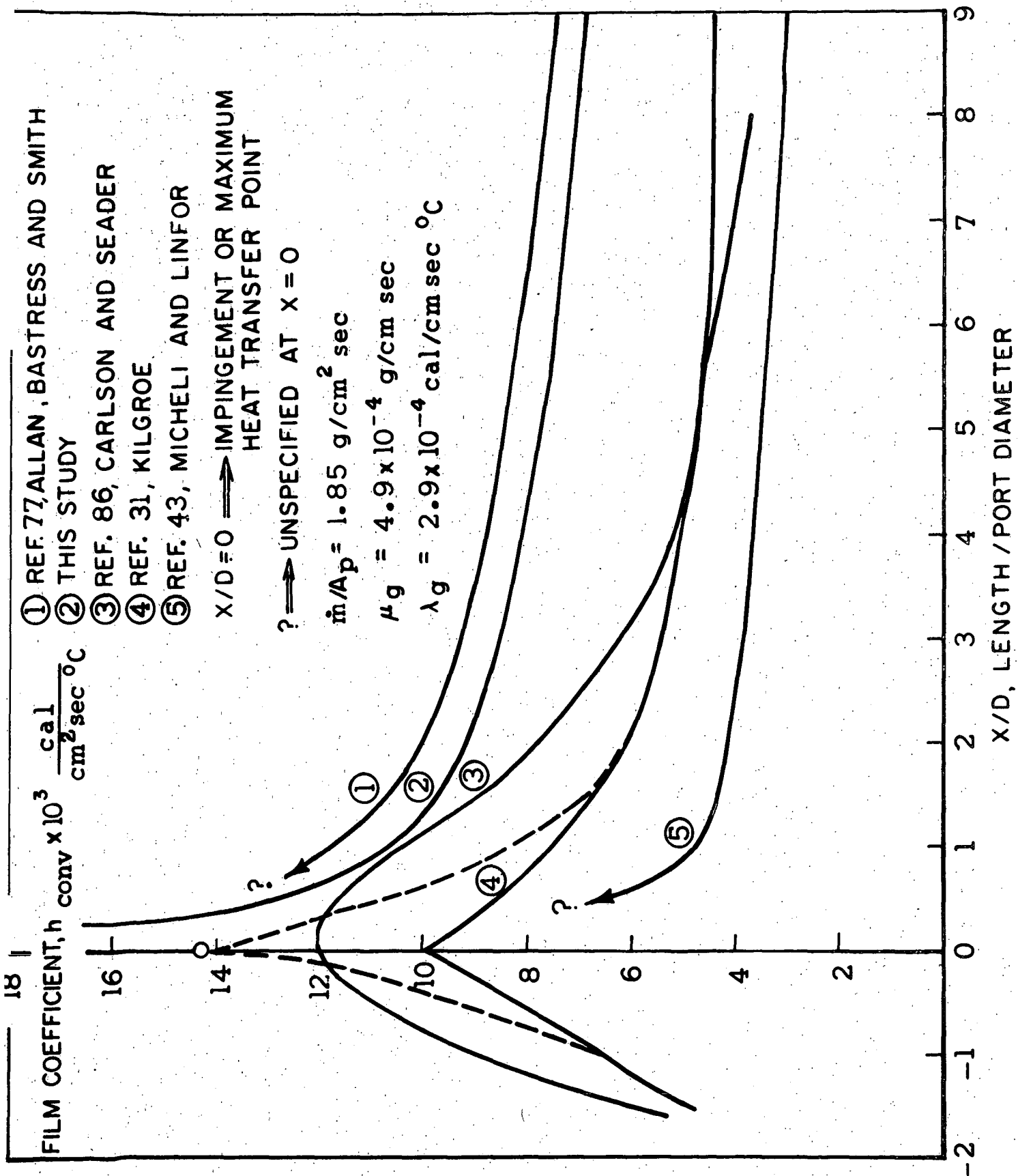
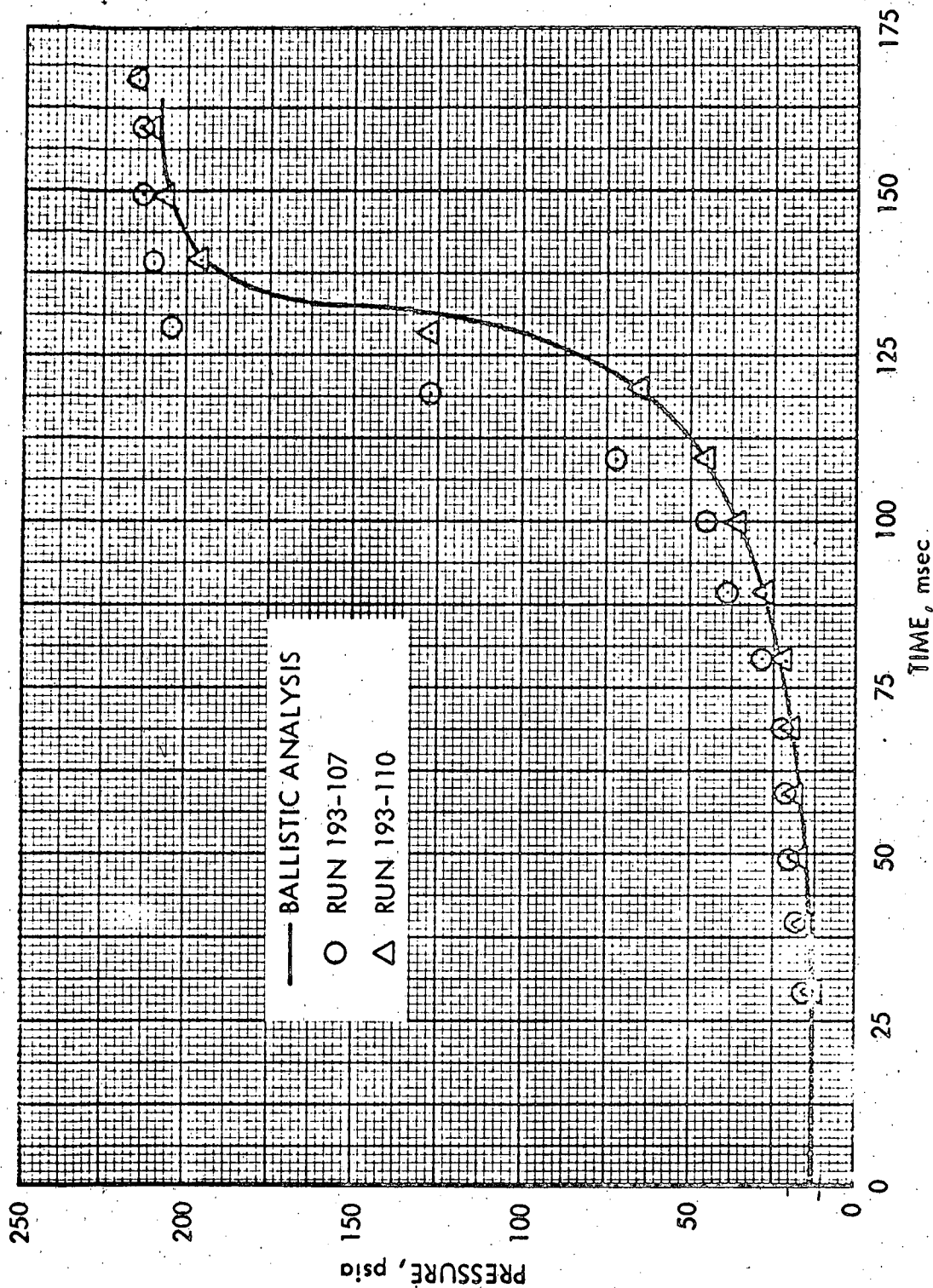


FIGURE 6



Comparison of Predicted and Experimental Pressure Transients

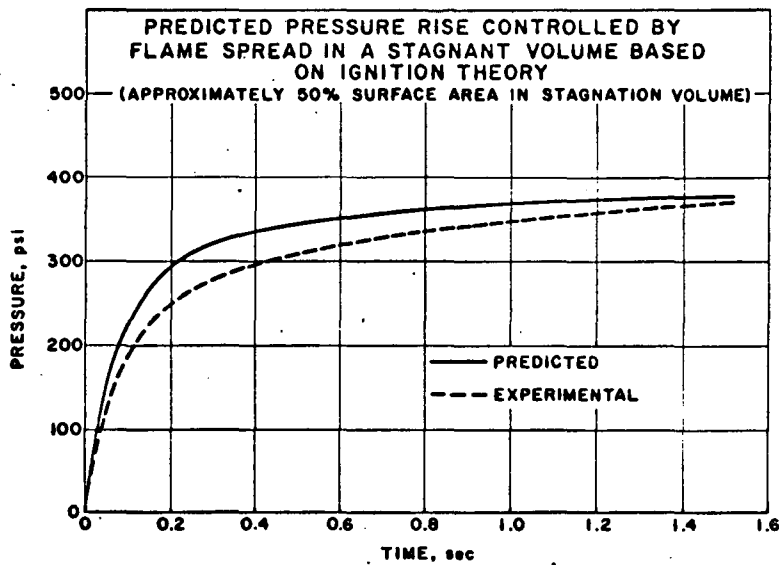
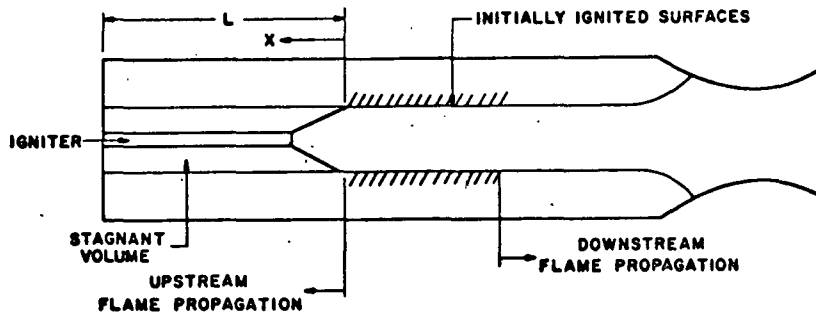
Motor: Cylindrical grain, Canted igniter nozzles, Aluminized igniter material.

Model: Measured flame spreading rates as input data.
Isothermal Gas Dynamics.

$$r_{fs} = k p_c^n$$

FROM REFERENCE 37

MOTOR SCHEMATIC



Model: T_{crit}

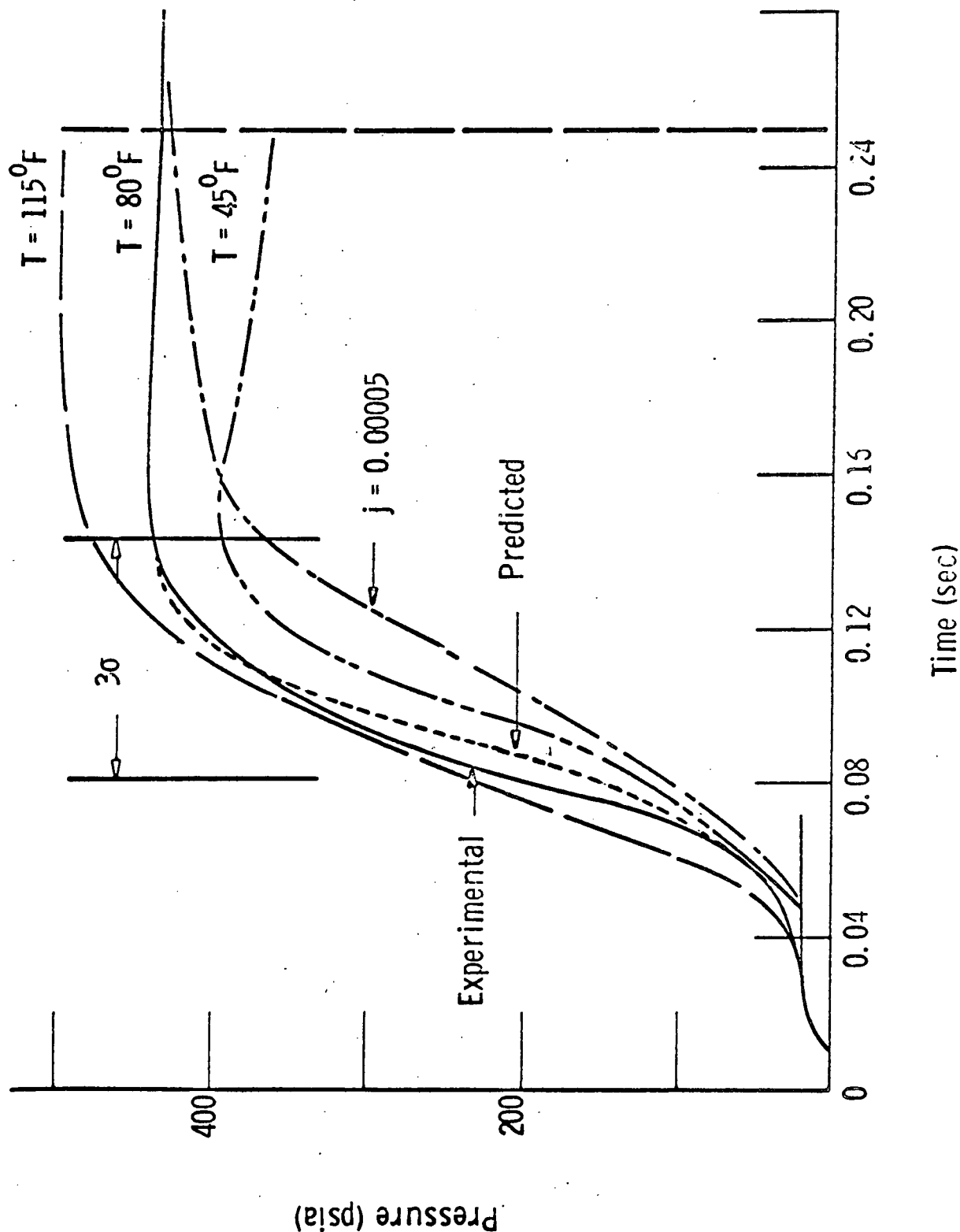
Flame Spreading: Instantaneous ignition in impingement region. Step function in downstream region. Propagation into head-end stagnant region according to a quadratic₂ fit of experimental data, $S(t) = a+bt+ct^2$.

Isothermal Gas Dynamics

$$r_{ss} = k \cdot 10^n$$

Heat Transfer - $Nu_D \sim Re_D^{0.8} + \text{Radiation}$

Effect of Temperature and Radiation Absorptivity



Motor: Cylindrical bore, Finned head section, Sunken nozzle.

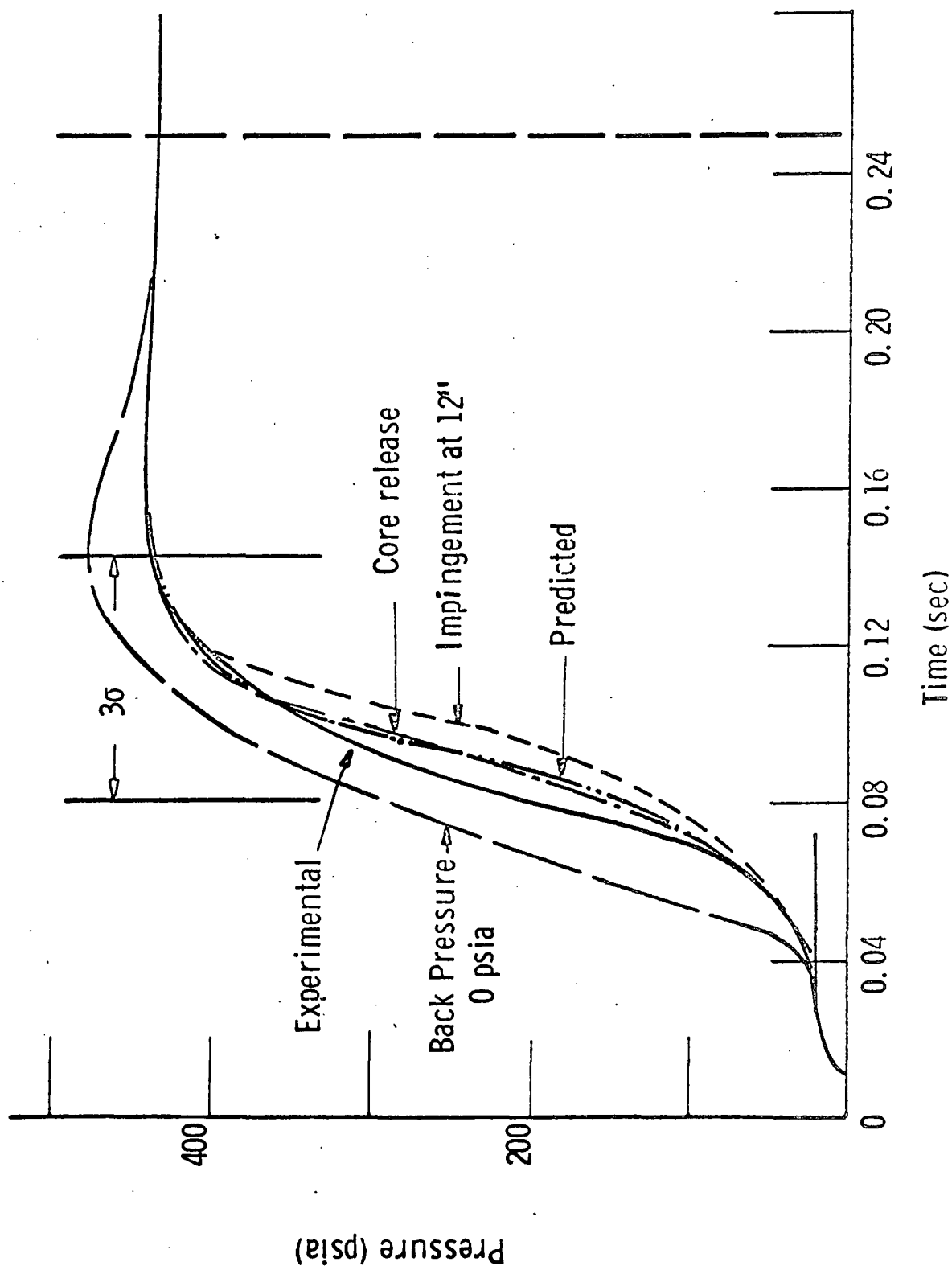
Model: $T_s \sim \int_0^t \frac{\dot{q}(t-\tau) d\tau}{r^{1-\frac{1}{n}}}$

Successive Ignitions

Dynamic Temperature

$T_b = T_{ss} (1 + \alpha_p p / r_{ss}^2 p)$

Heat Transfer - See text, Chapter III, Section C.



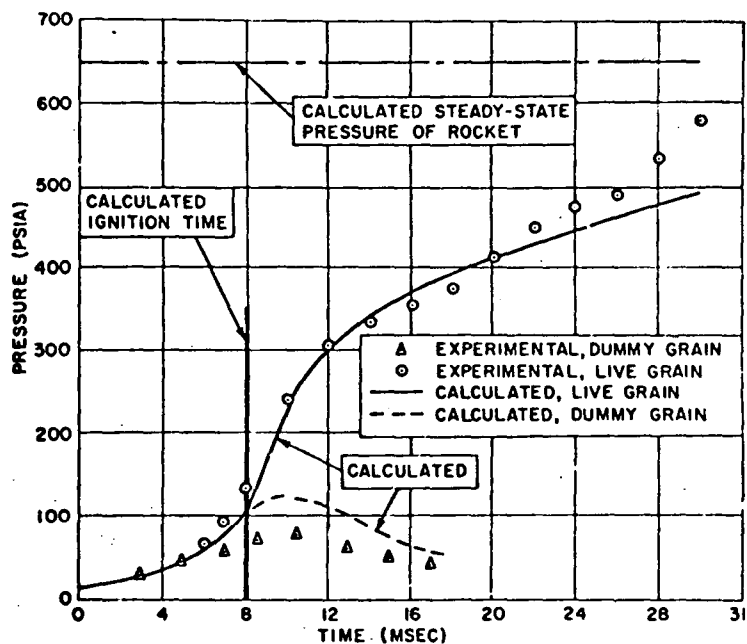
Motor: Cylindrical bore, Finned head section, Sunken nozzle.

Model:

Successive Ignitions
Dynamic Temperature

Heat Transfer -- See text, Chapter III, Section C.

FROM REFERENCE 55



COMPARISON OF CALCULATED AND EXPERIMENTAL DUMMY-
GRAIN PRESSURIZATION AND PRESSURIZATION OF ROCKET
BY IGNITER OUTPUT AND PROPELLANT COMBUSTION PRODUCTS

Motor: Cylindrical grain, Head-end pyrogen.

Model: von Elbe Ignition Model.
Simultaneous ignition of entire grain.
Isothermal Gas Dynamics.

$$r_{ss} = k p_c^n$$

Heat Transfer -
$$h_{conv} = 70 \left(\frac{\dot{m}_{ign}}{A_p} \right)^{0.8} \left[1 + \left(\frac{D}{L} \right)^{0.7} \right]$$

--- Analytical

***** Analytical - Erosive Burning and Pressurization Rate Correction

— Experimental Data

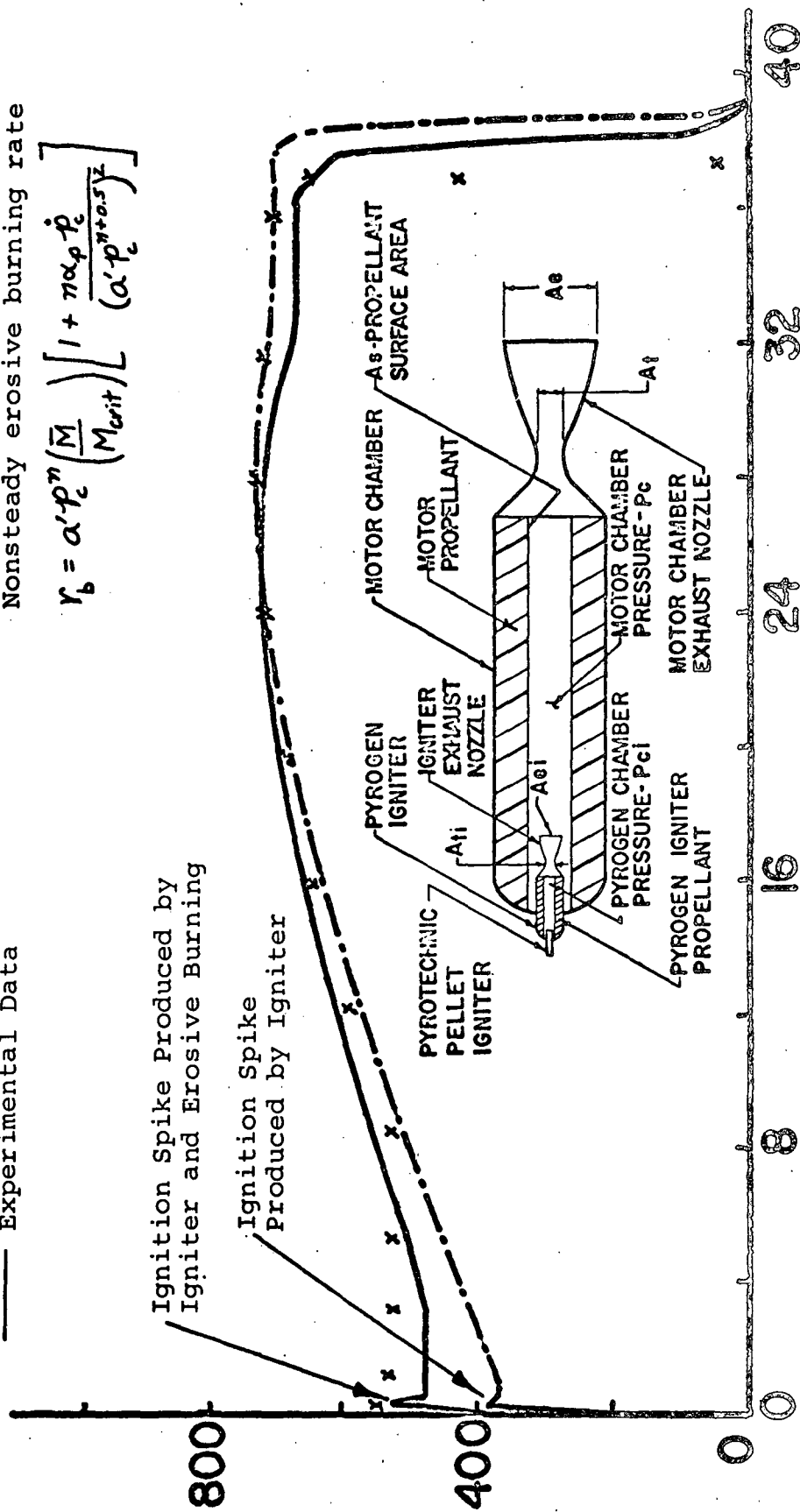
Isothermal Gas Dynamics

Flame Spreading: a given function of time

Nonsteady erosive burning rate

$$r_b = a' p_c^n \left(\frac{\bar{M}}{M_{crit}} \right) \left[1 + \frac{n \alpha_p \dot{p}_c}{(a' p_c^{n+0.5})^2} \right]$$

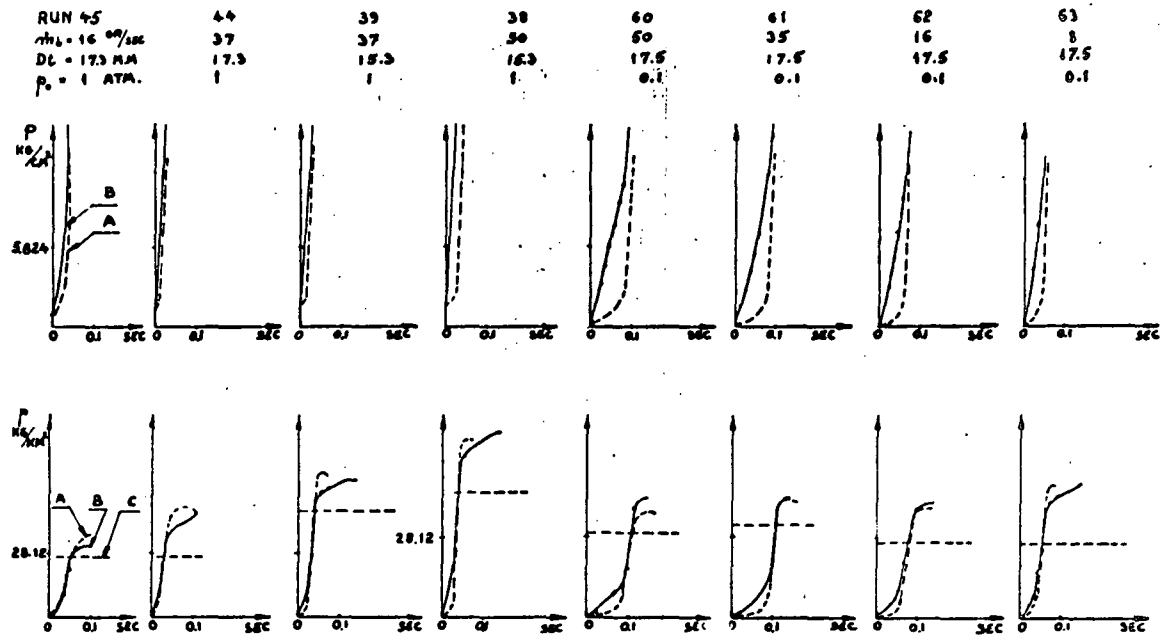
P_c CHAMBER PRESSURE, LBf/in²



t-TIME, SECOND

CHAMBER PRESSURE TRANSIENTS FOR COMBINED CYLINDRICAL PELLET IGNITER & PYROGEN IGNITER OPERATION IN A SLOTTED TUBE MOTOR

FROM REFERENCE 70



Pressure build up in 8 motors; upper half trace III, lower half trace II. A experimental, B theoretical
C steady-state (measured)

Motor: Star Grains

Model: T_{crit}

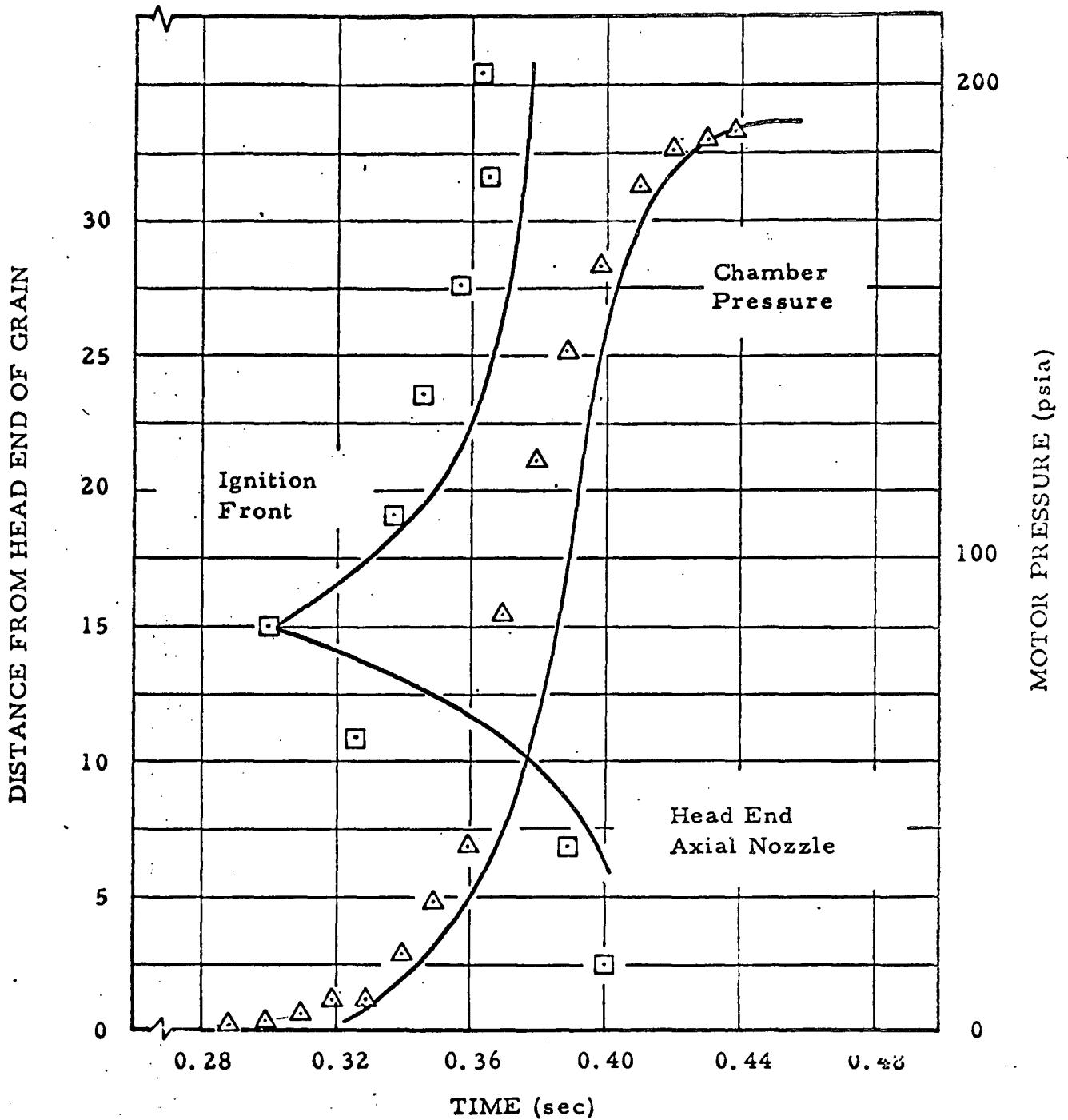
Successive Ignitions

Dynamic Temperature

$$r_{ss} = k p_e^n$$

$$\text{Heat Transfer} - St = a Re_x^{0.2} + \text{Radiation}$$

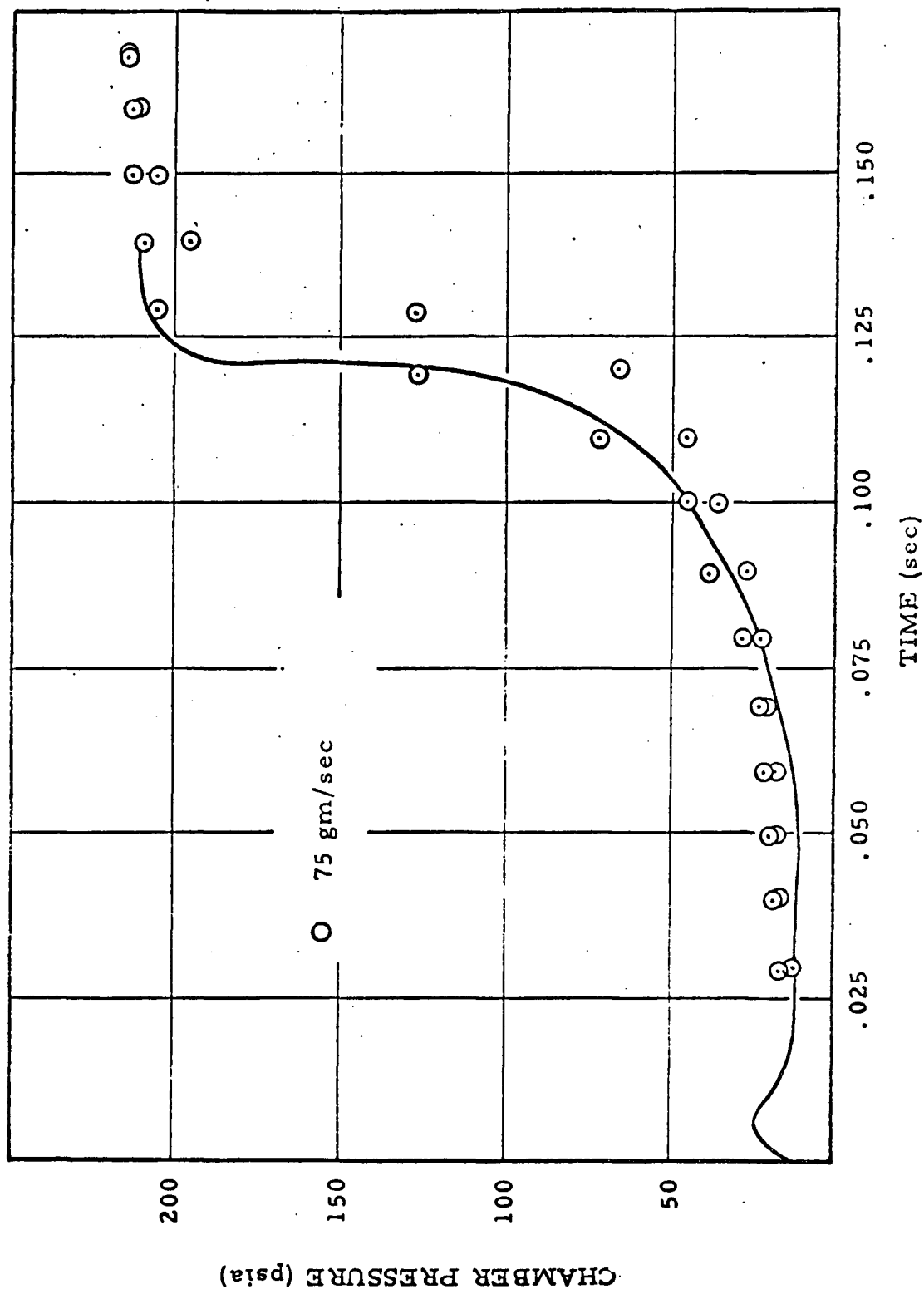
FROM REFERENCE 67
(Experimental data from Reference 29)



Ignition Front and Pressure Versus Time
for Test Motor

Model: T_{crit}
 Successive Ignitions
 Dynamic Temperature
 $\gamma_{ss} = k p_c^n$
 Heat transfer correlation from Ref. 31

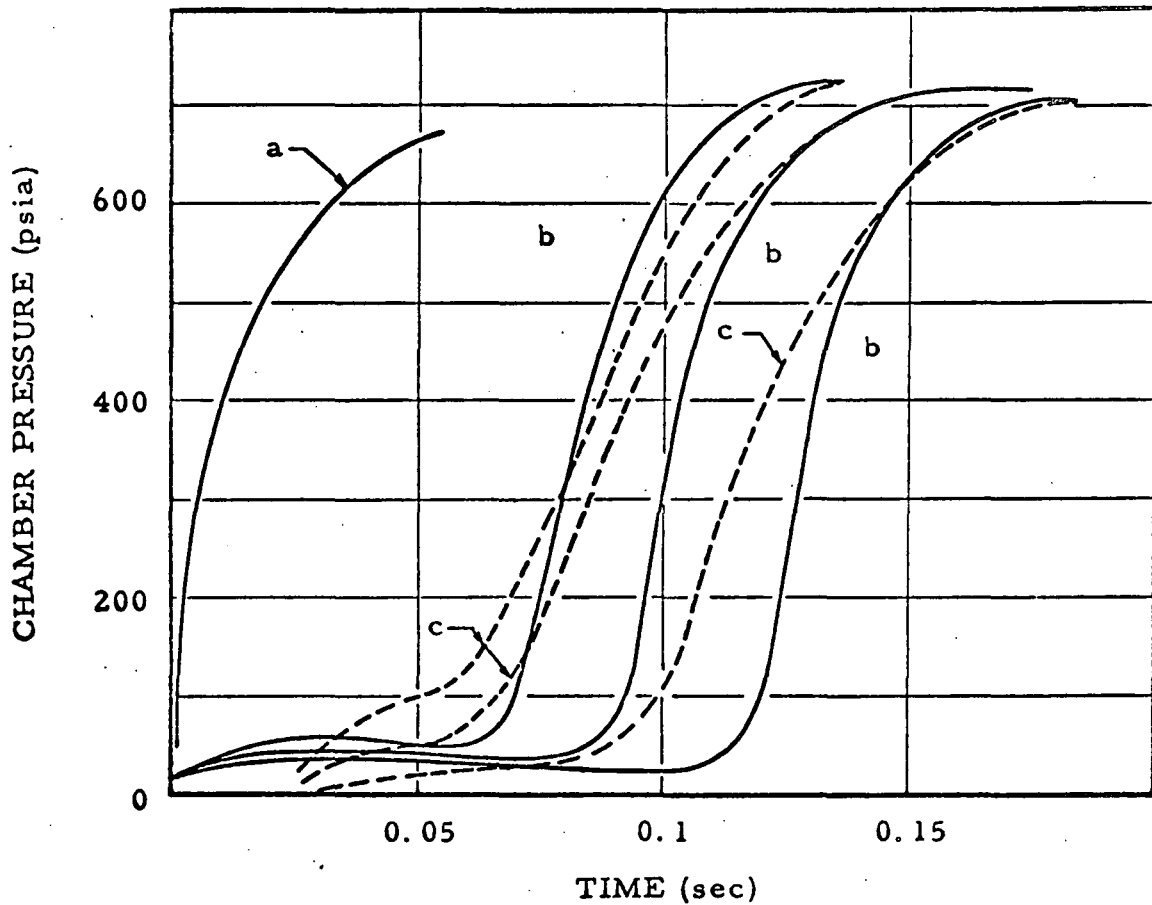
FROM REFERENCE 67
(Experimental data from Reference 29)



Comparison of Predicted Transient with Data

Model: T_{crit}
 Successive Ignitions
 Dynamic Temperature
 $r_s = k p_c^n$
 Heat transfer correlation from Ref. 31 adjusted
 to fit measured flame spreading data.

FROM REFERENCE 67



Ignition Pressure Transient for Large Test
Motor with Slots in Propellant Grain

- a: Assumes instantaneous ignition (predicted).
- b: Predicted using heat transfer correlations given in text.
- c: Experimental data - \dot{m}_{ig} varied.

Motor: Internal burning cylinder with deep slots.

Model: T_{crit}
Successive Ignitions
Dynamic Temperature
 $r_{in} = k r_c^n$
Heat transfer correlations from Ref. 31 with
adjusted coefficients.

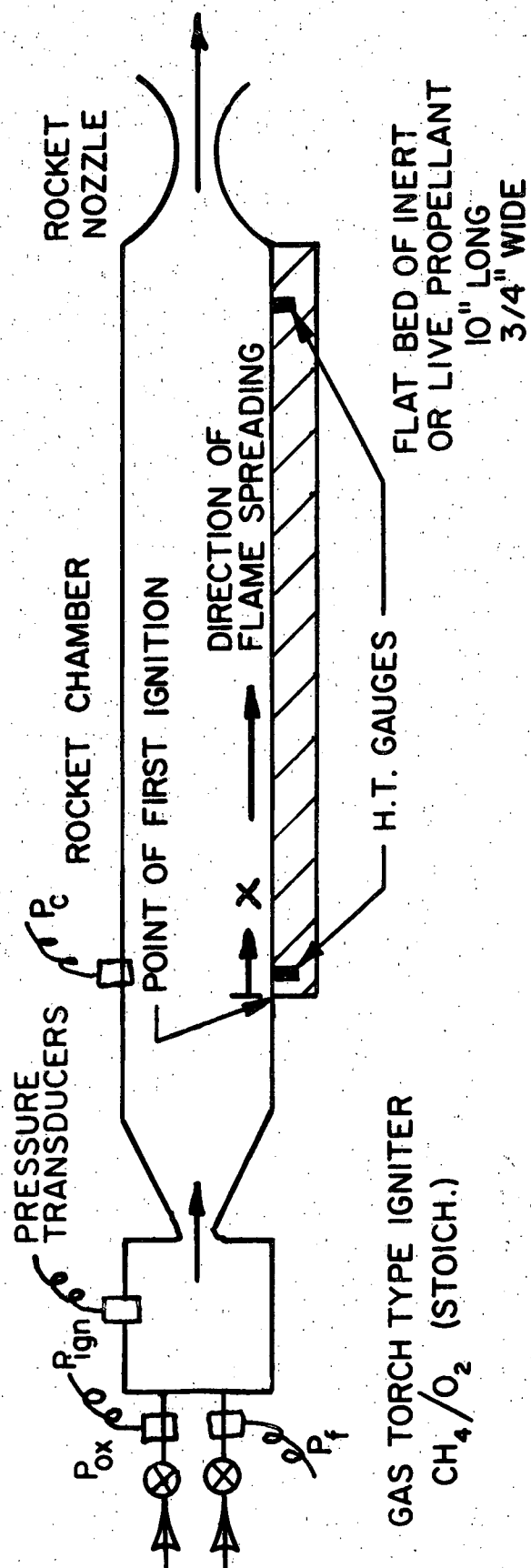
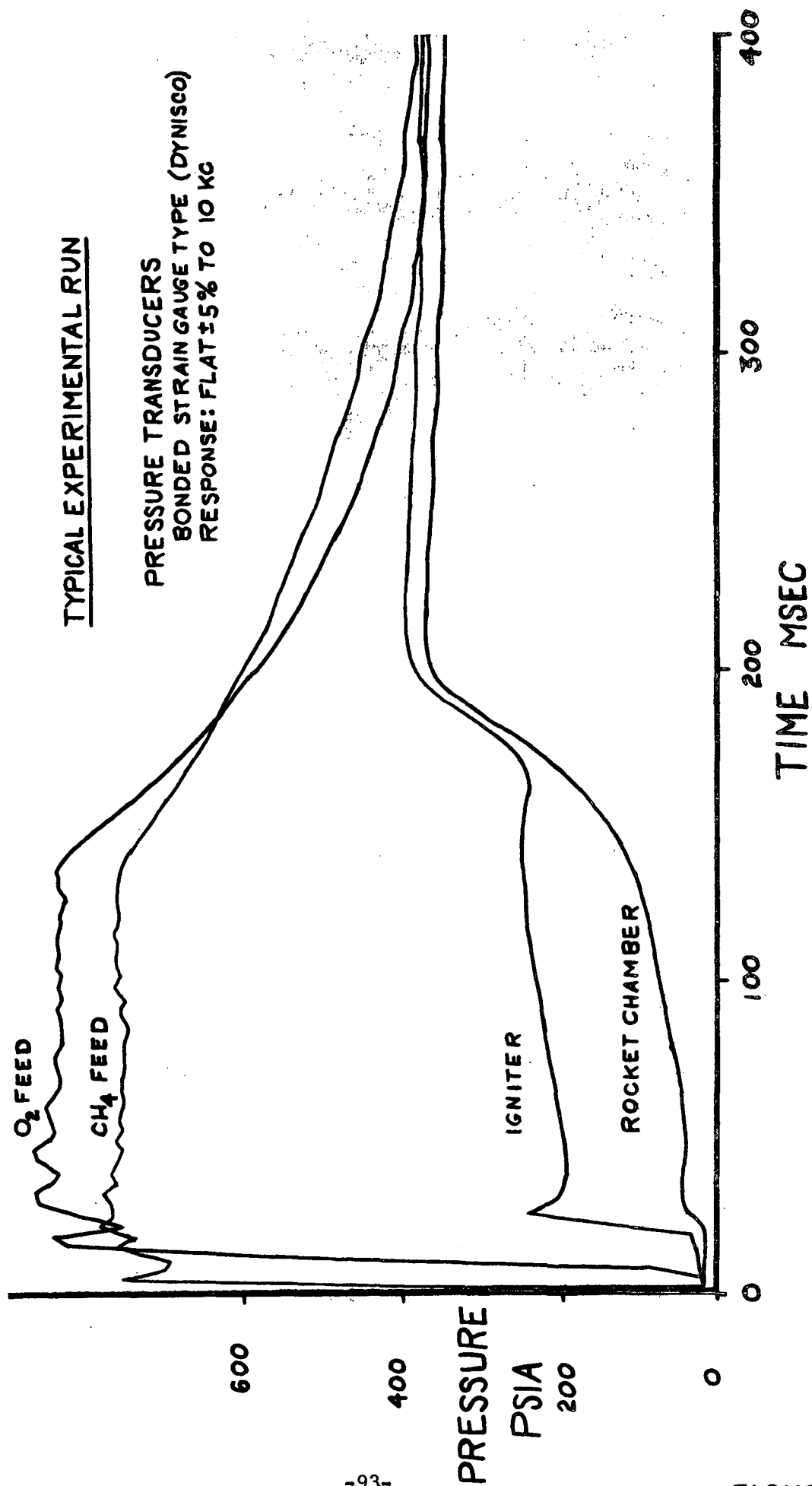
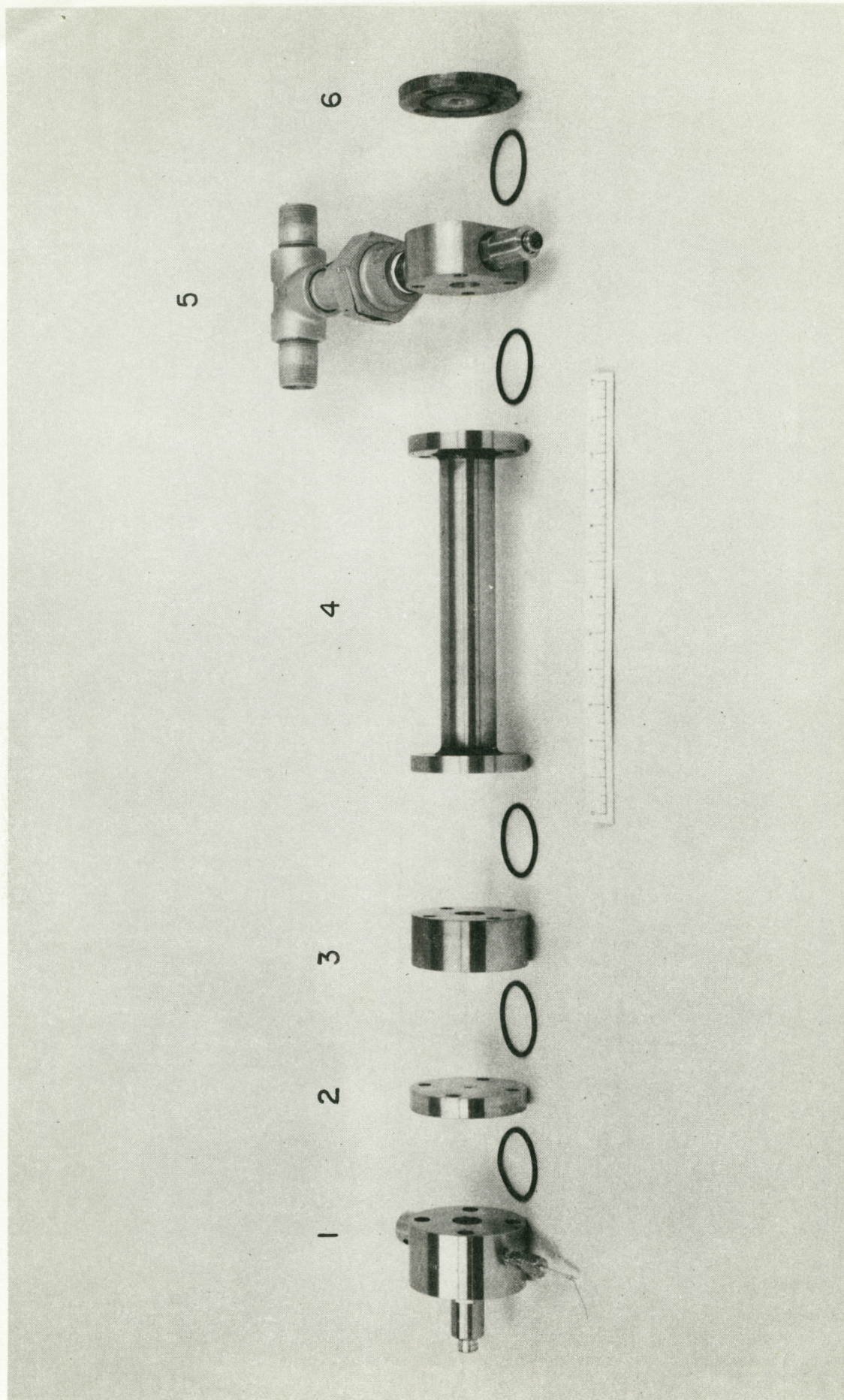


FIGURE 17





EXPLODED VIEW OF EXPERIMENTAL ROCKET MOTOR

1. IGNITER ASSEMBLY

3. IGNITER ADAPTER SECTION

5. AFT SECTION ASSEMBLY

2. IGNITER NOZZLE

4. MOTOR HOUSING

6. MOTOR NOZZLE

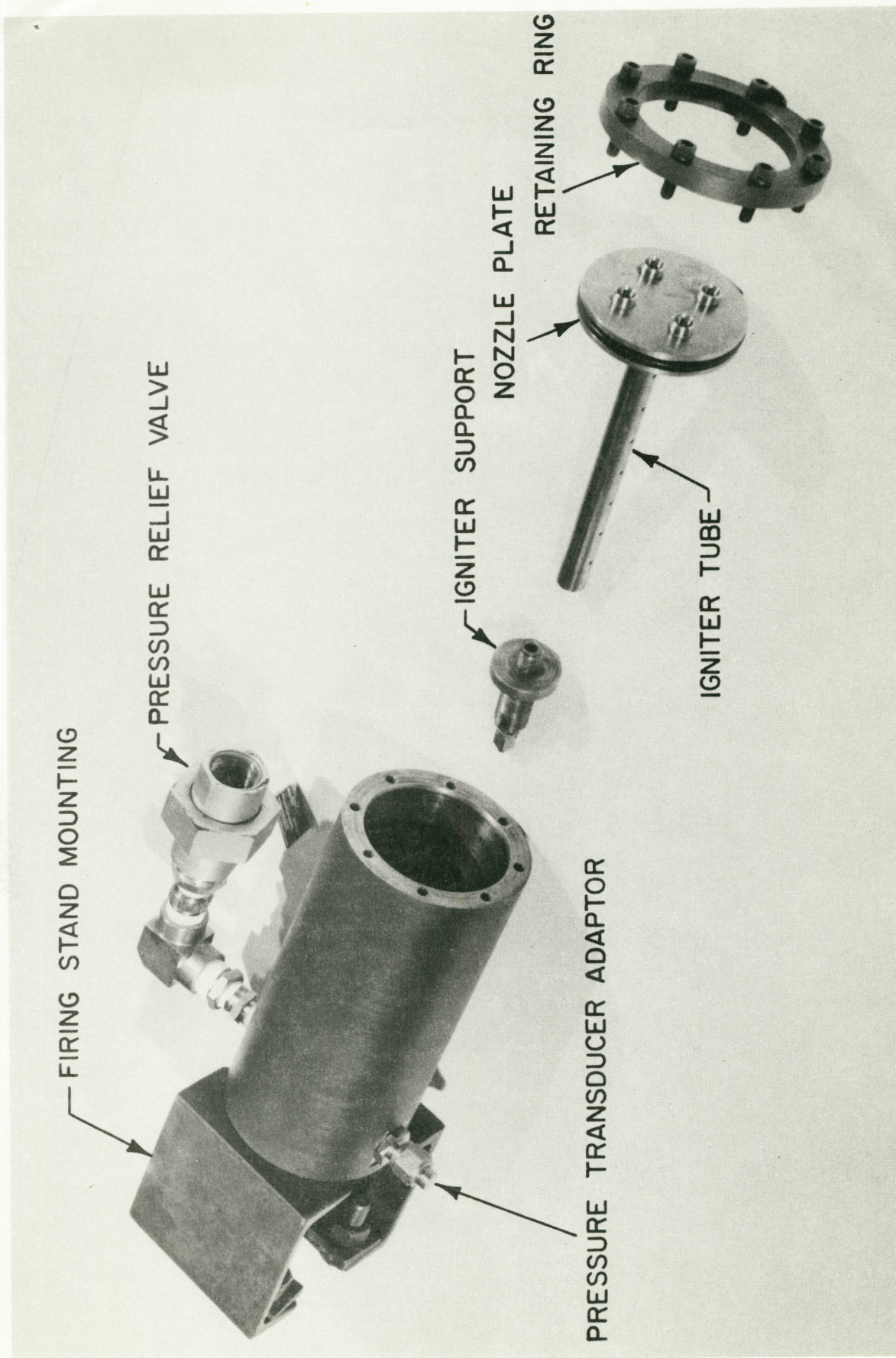


FIG.12 EXPLODED VIEW OF FRANKFORD ARSENAL COMBUSTOR

BURNING RATE CURVE FOR FRANKFORD ARSENAL PROPELLANT

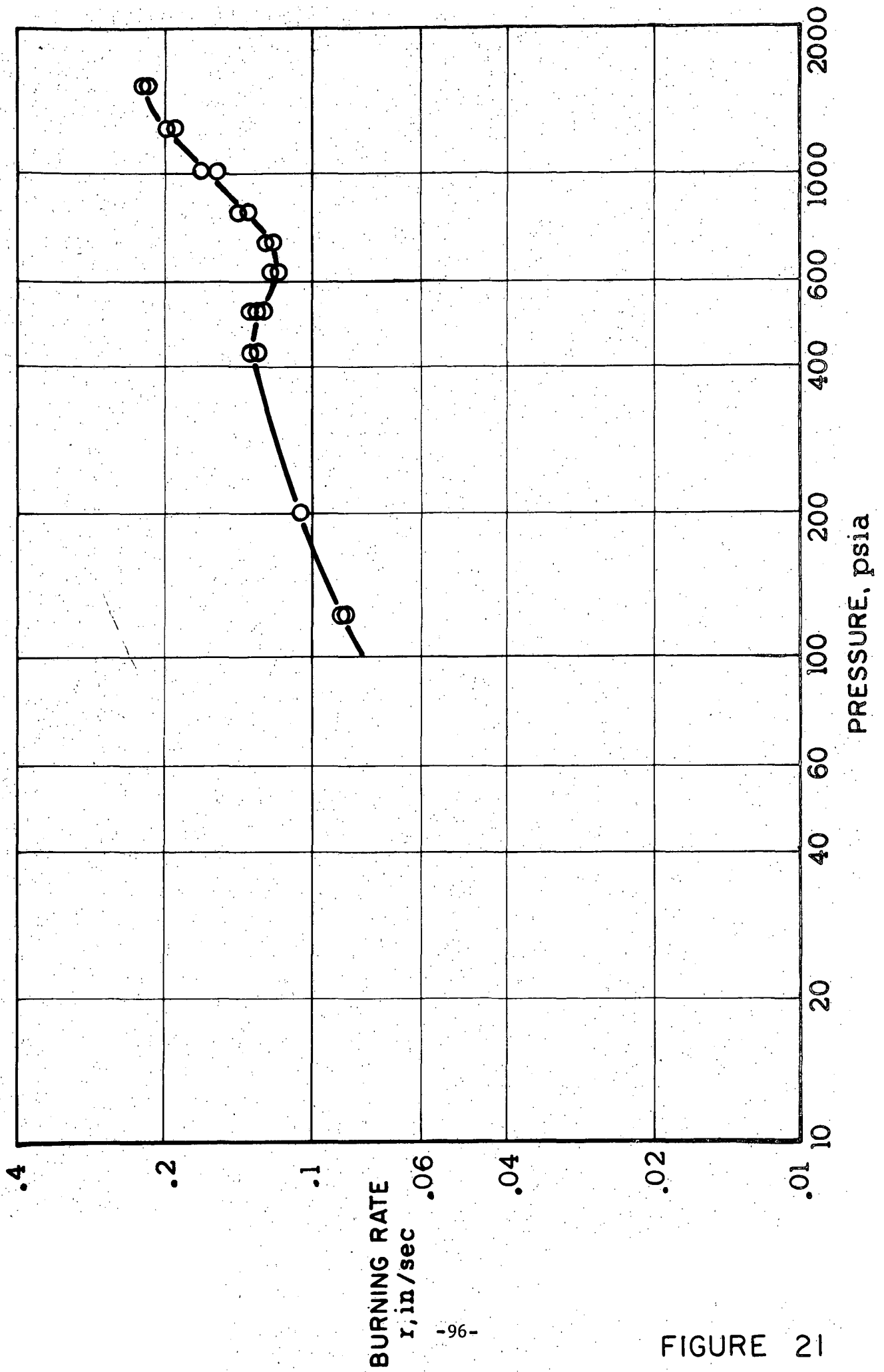
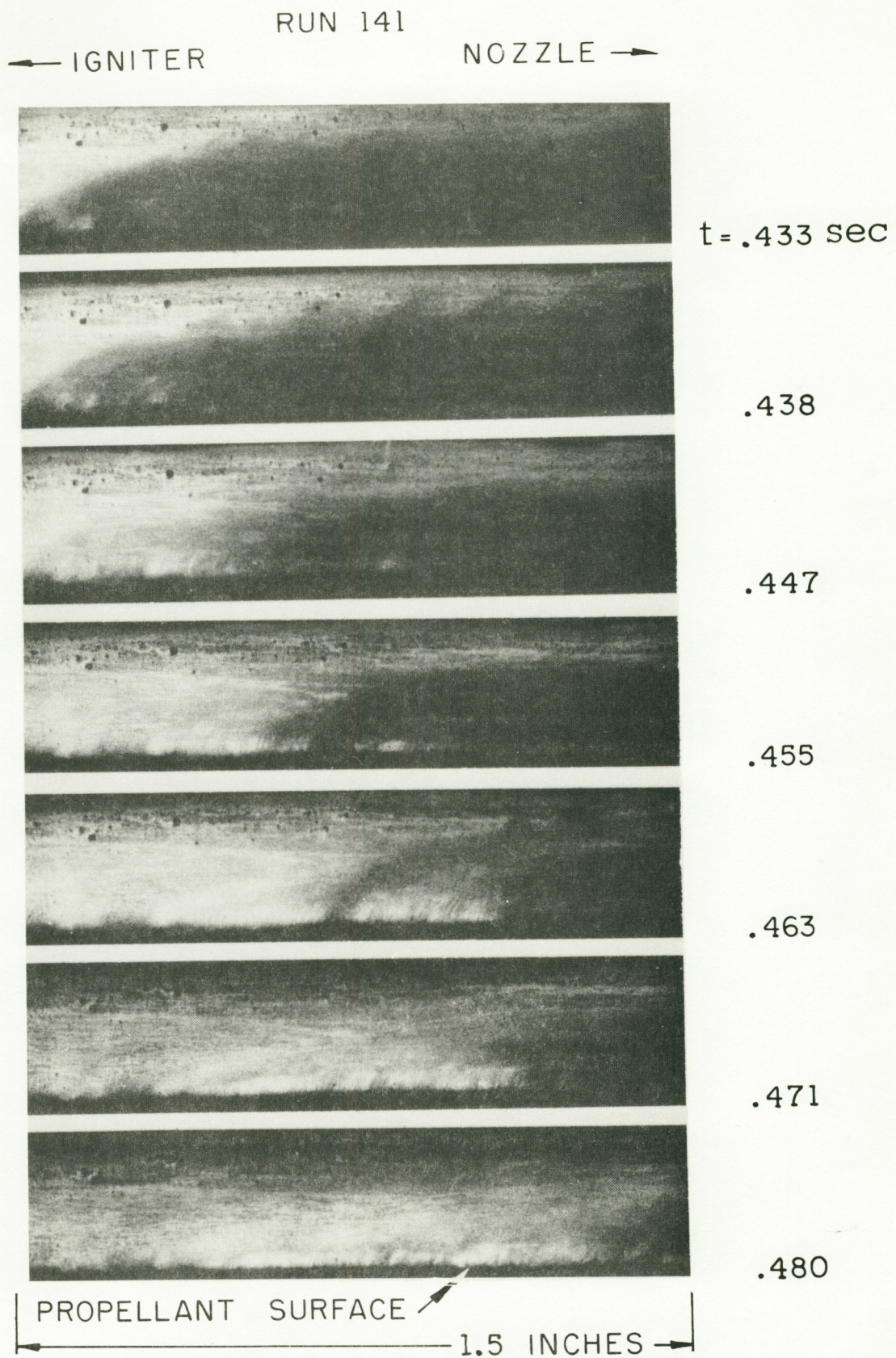


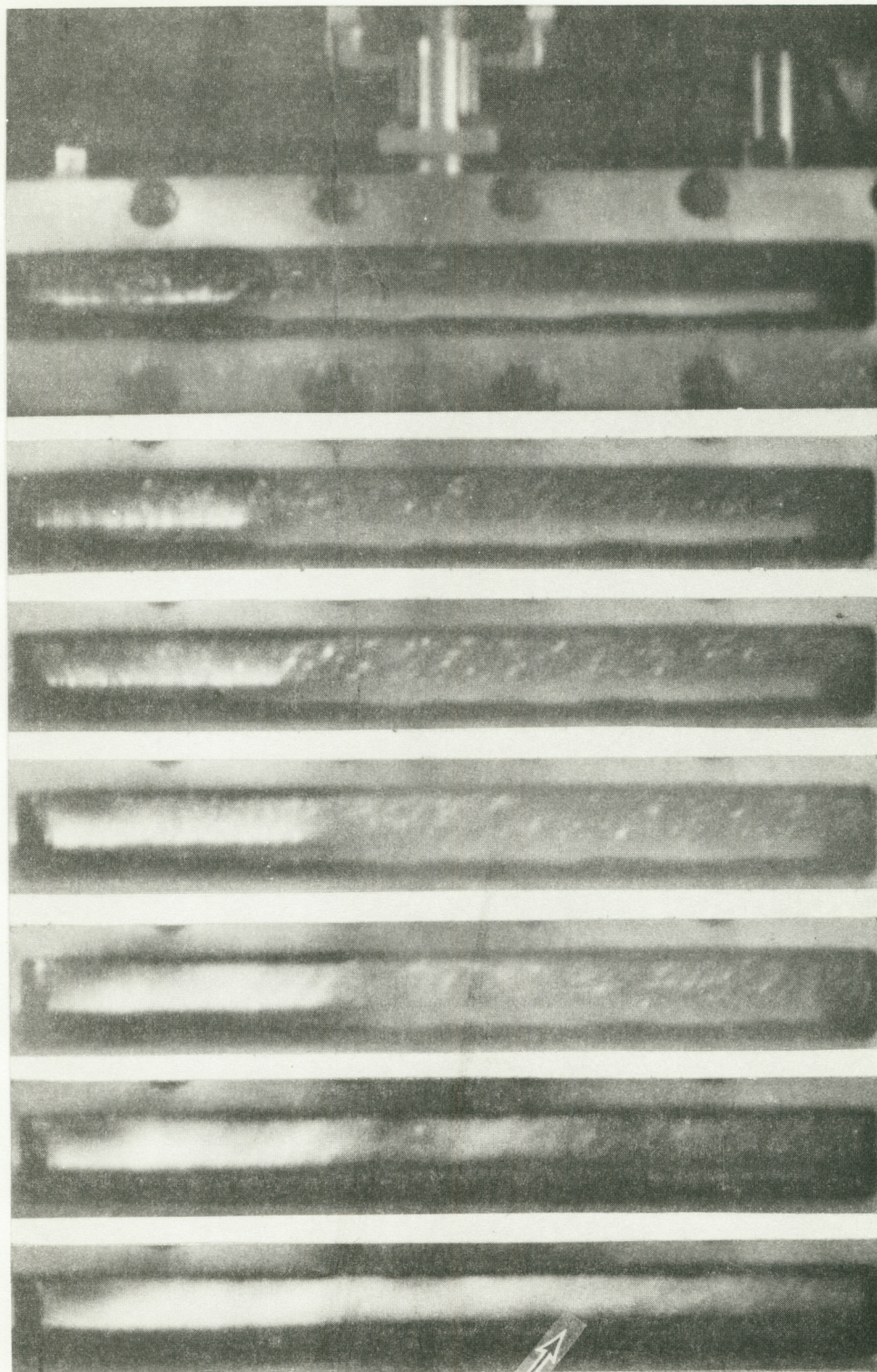
FIGURE 21



PHOTOGRAPHIC RECORD OF FLAME SPREADING

← IGNITER

NOZZLE →



$t = 170 \text{ msec}$

200

230

260

290

320

335

PROPELLANT SURFACE

9.5 INCHES

PHOTOGRAPHIC RECORD OF FLAME SPREADING OVER
ALUMINIZED PROPELLANT

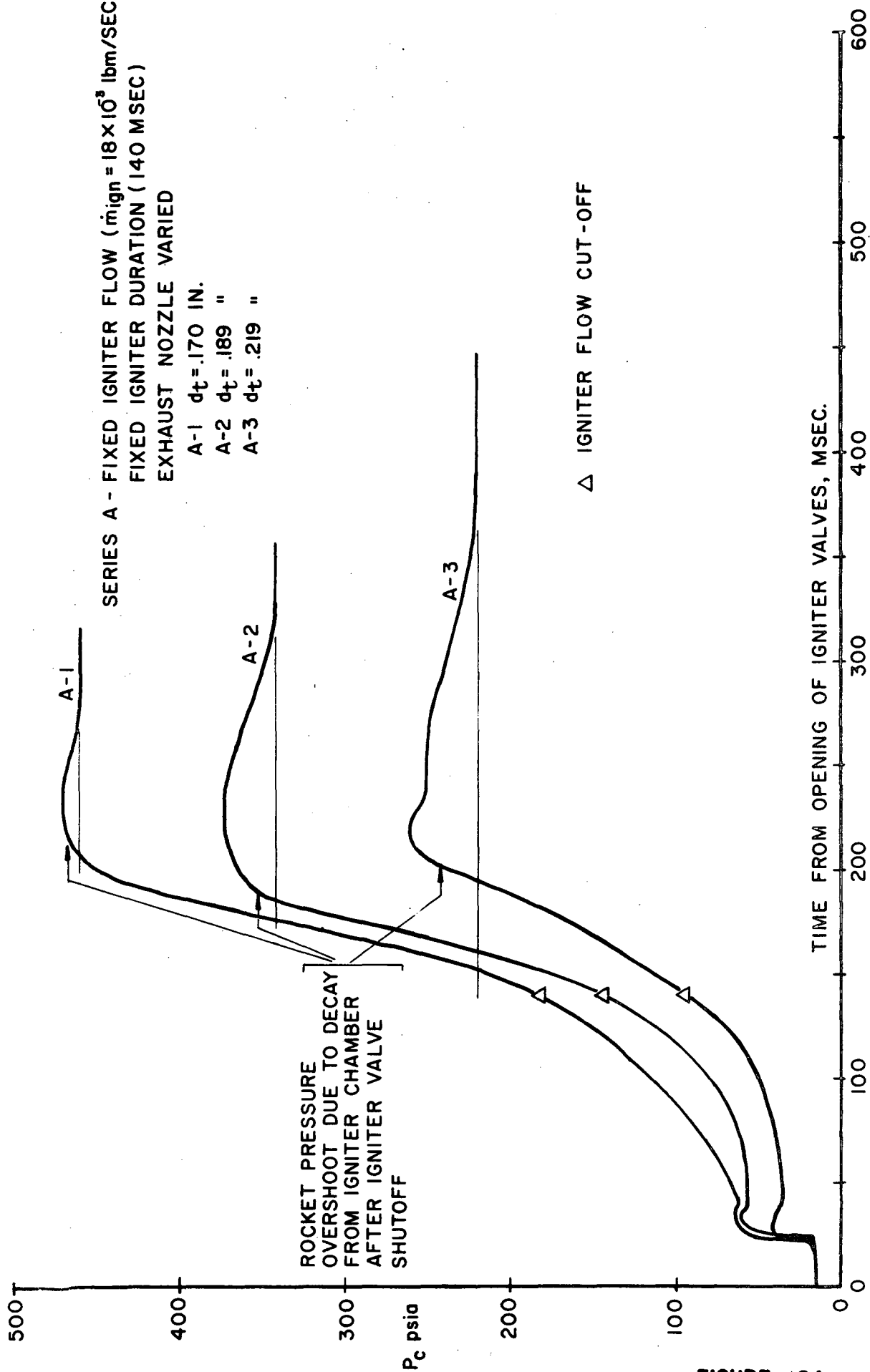


FIGURE 24

FIRING A-2

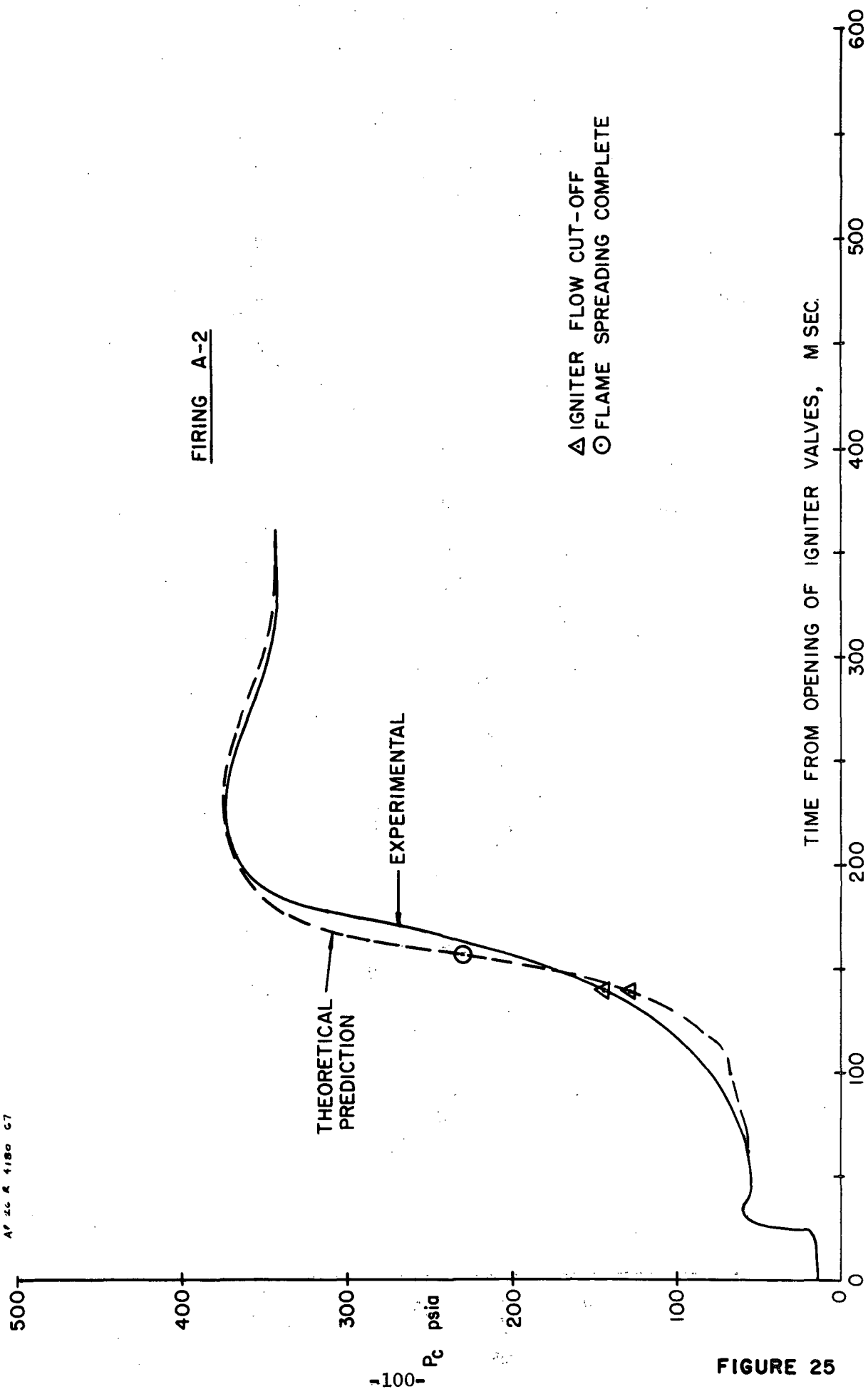


FIGURE 25

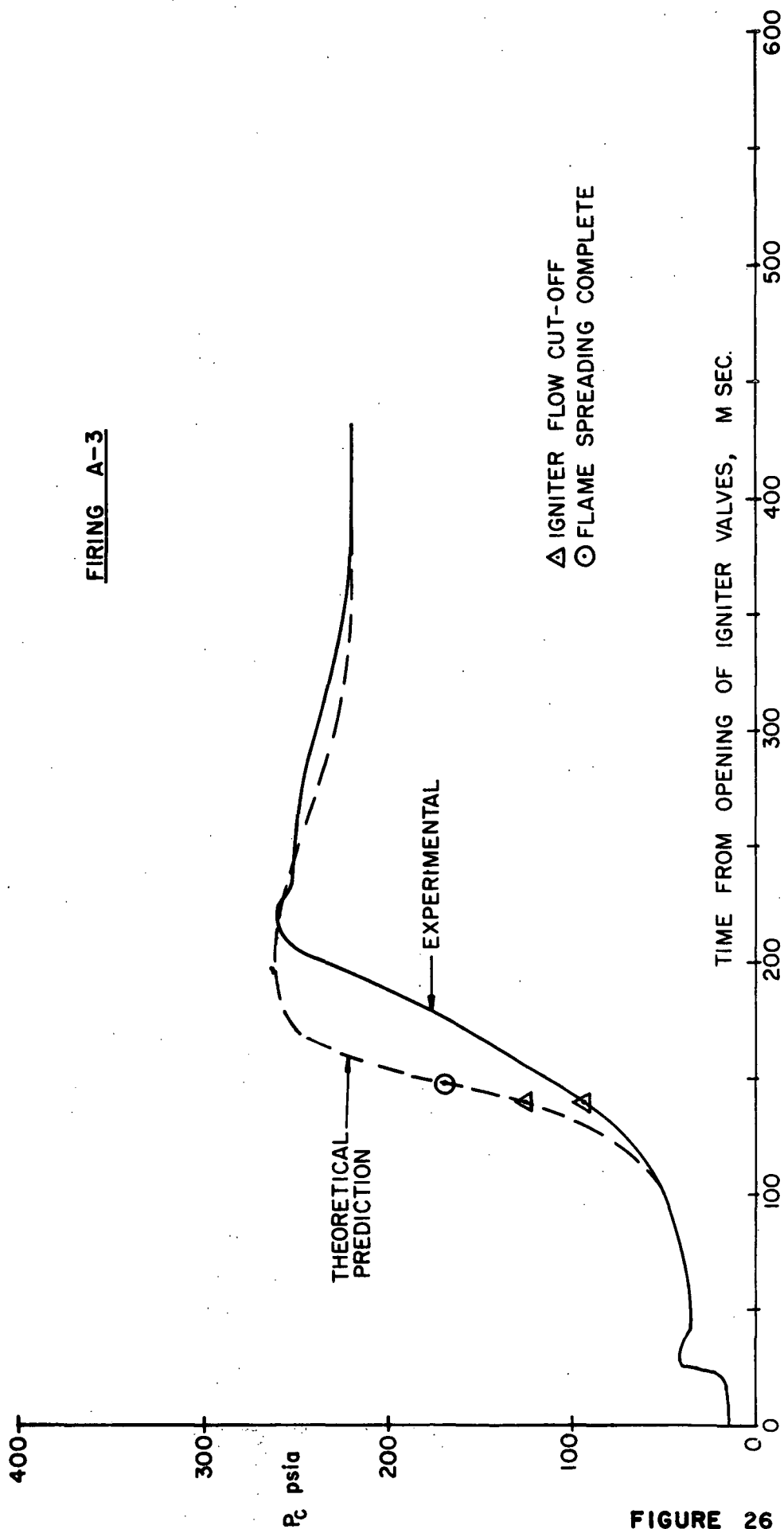
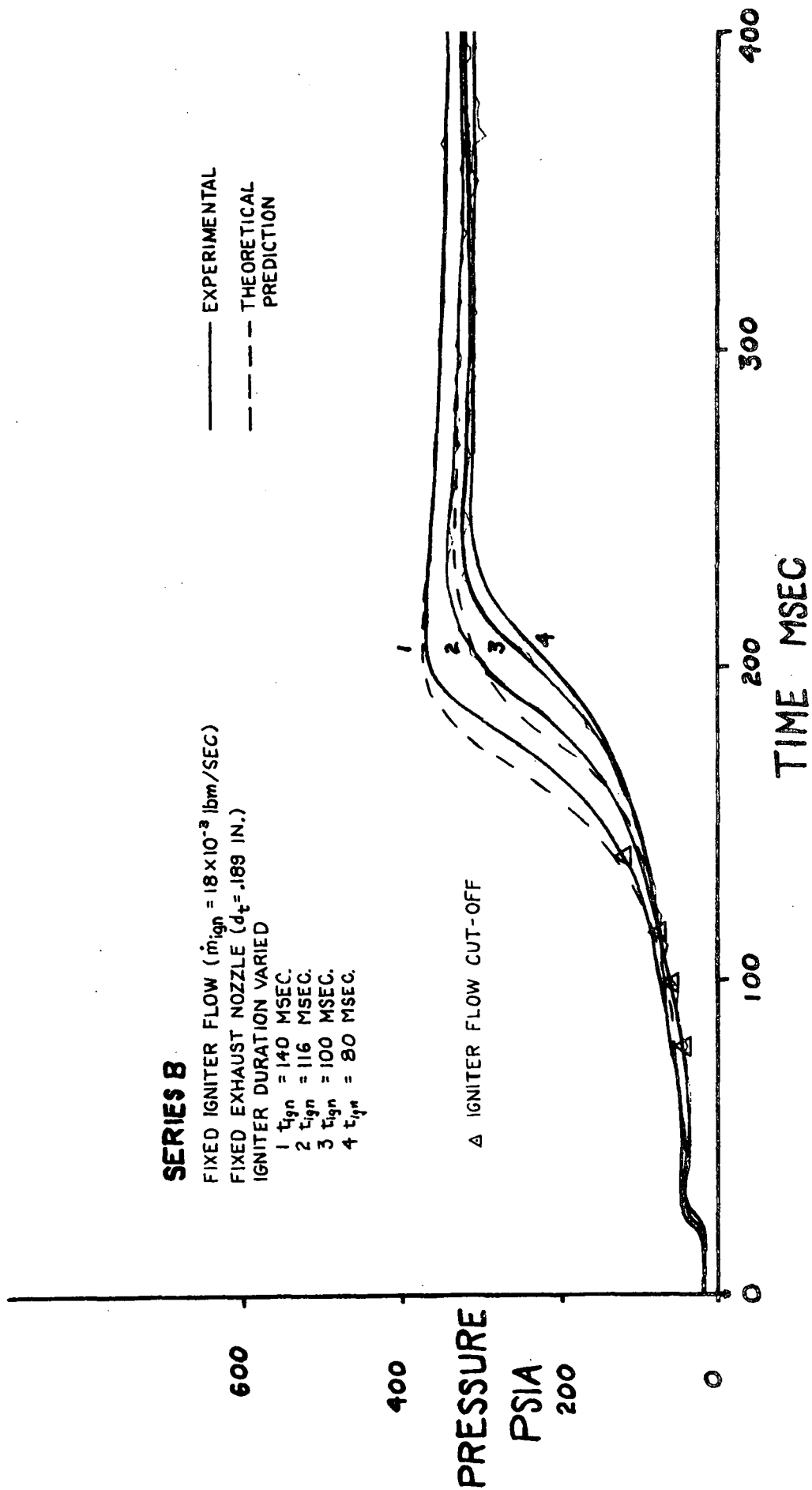
FIRING A-3

FIGURE 26



SERIES C -- FIXED EXHAUST NOZZLE ($d_t = .189$ in.)
 FIXED TOTAL IGNITER/MASS $[(m_{ign})_{Tot} = 1.44 \times 10^{-3} \text{ lbm}]$
 IGNITER FLOW VARIED

C-1	$m_{ign} = 18 \times 10^{-3} \text{ lbm/sec.}$
C-2	$= 13.41 \times 10^{-3} "$
C-3	$= 9.15 \times 10^{-3} "$
C-4	$= 4.89 \times 10^{-3} "$

OVERSHOOT DUE TO PREHEATING OF
 PROPELLANT BED IN DEPTH

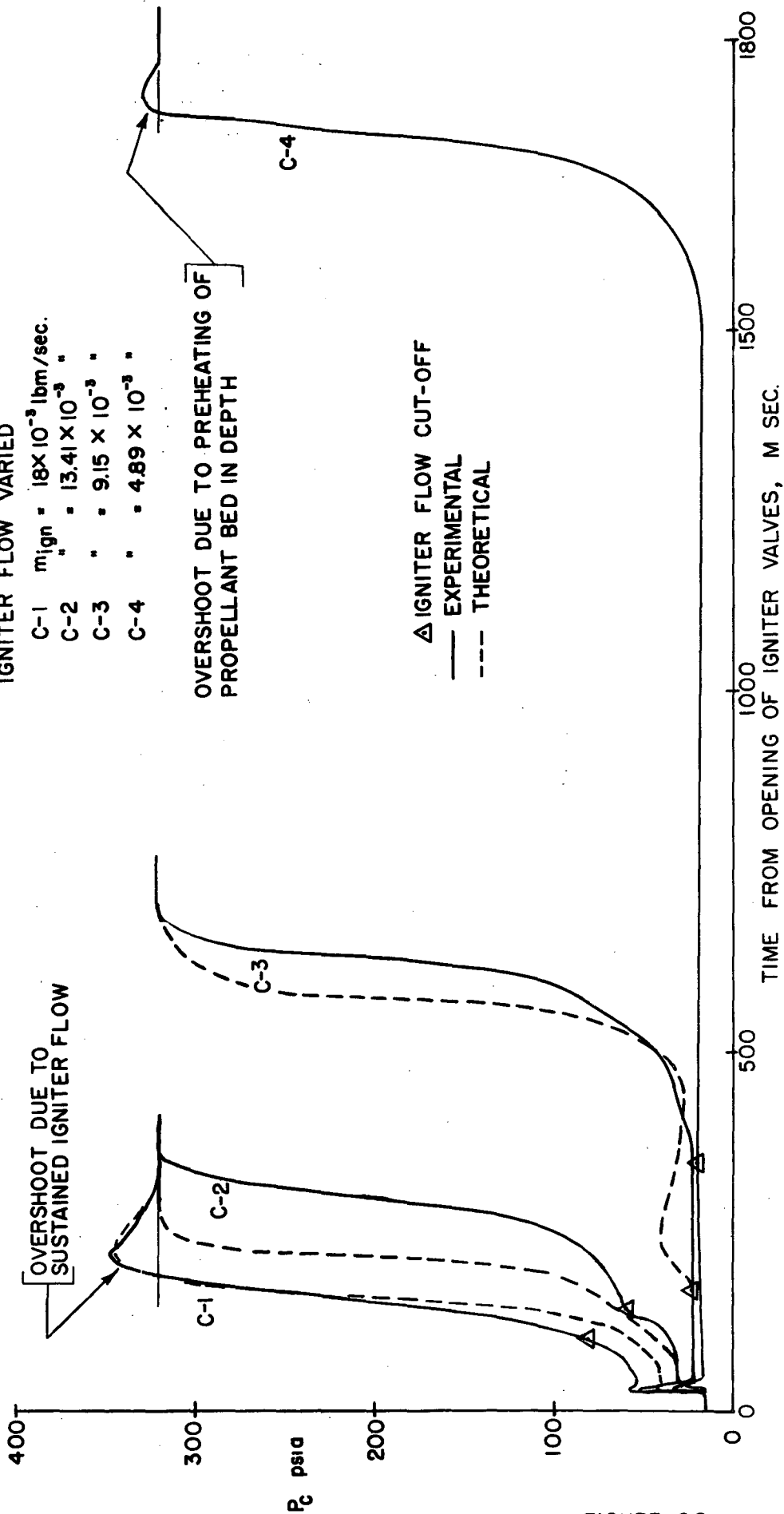
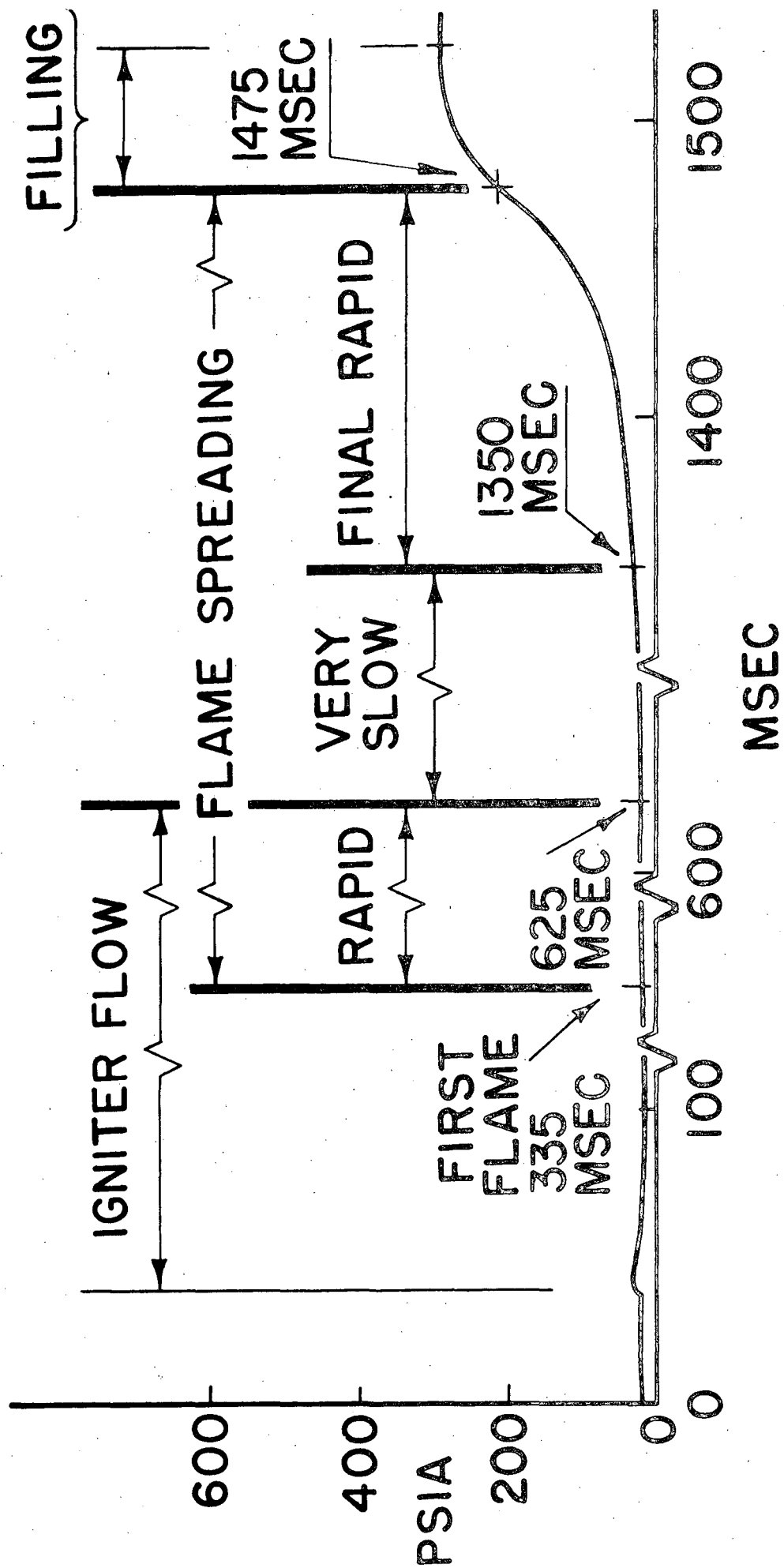


FIGURE 28

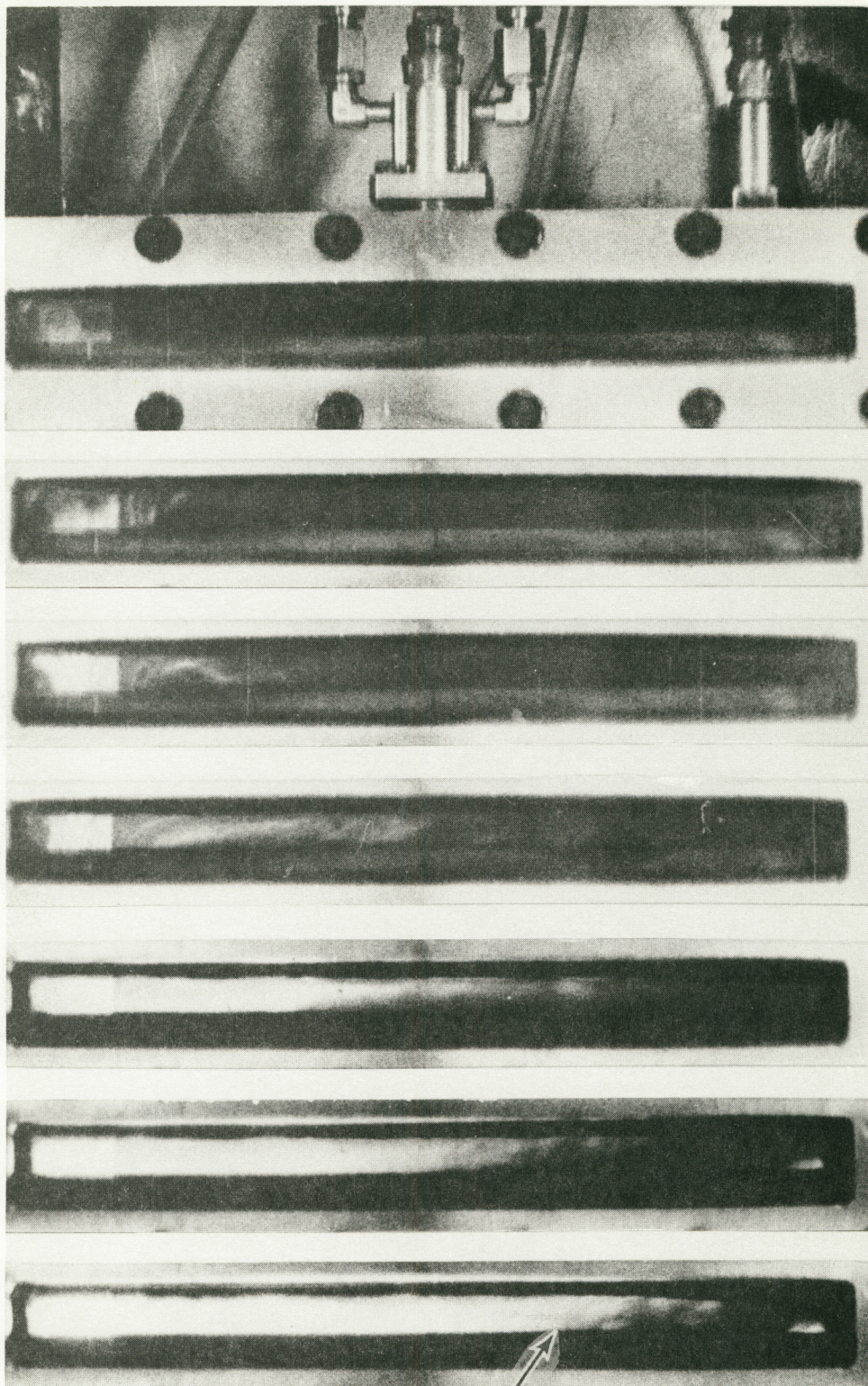
DETAILS OF A LONG DELAY FIRING

(See also Figure 34)



← IGNITER

NOZZLE →



$t = 360 \text{ msec}$

500

625

950

1350

1425

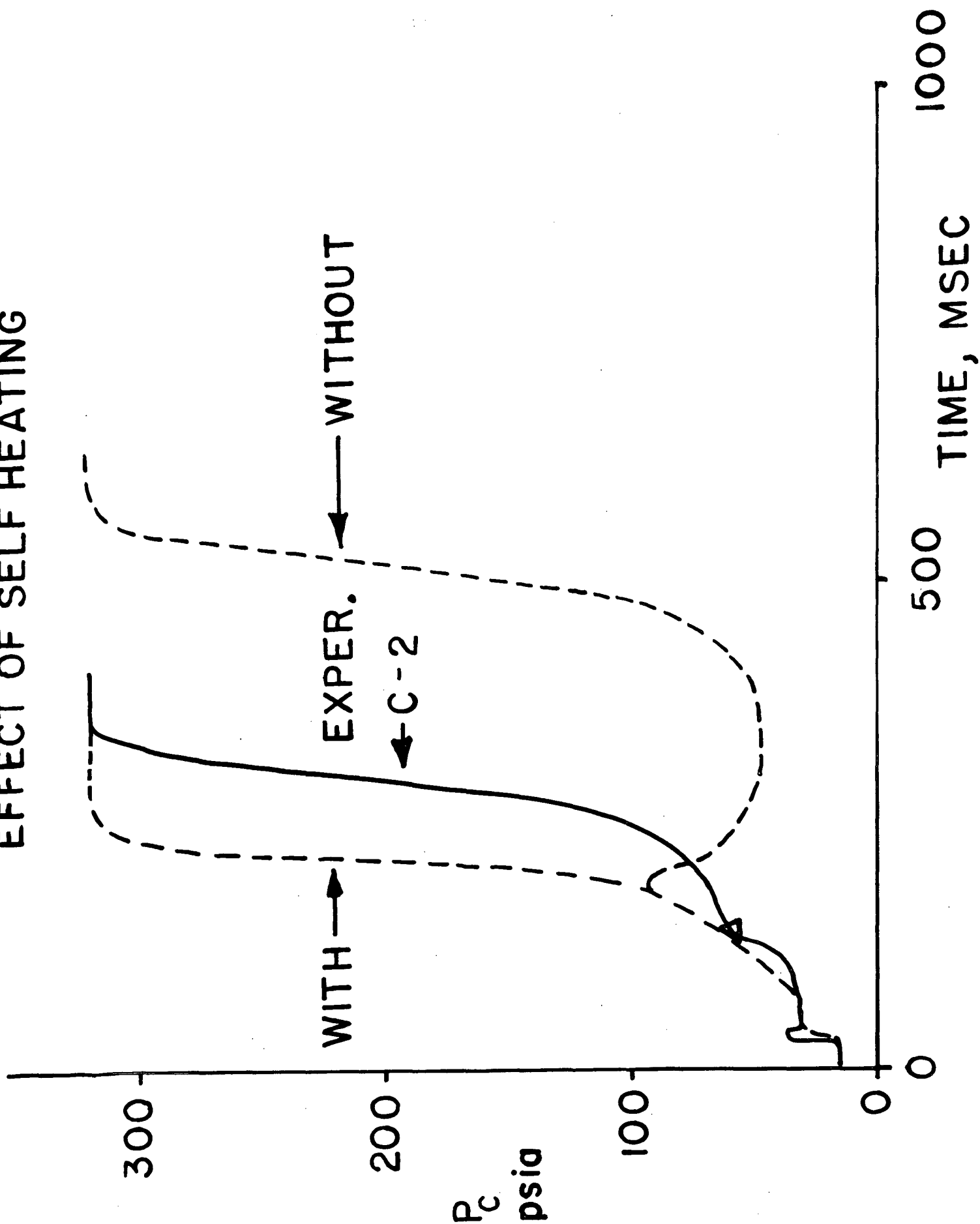
1450

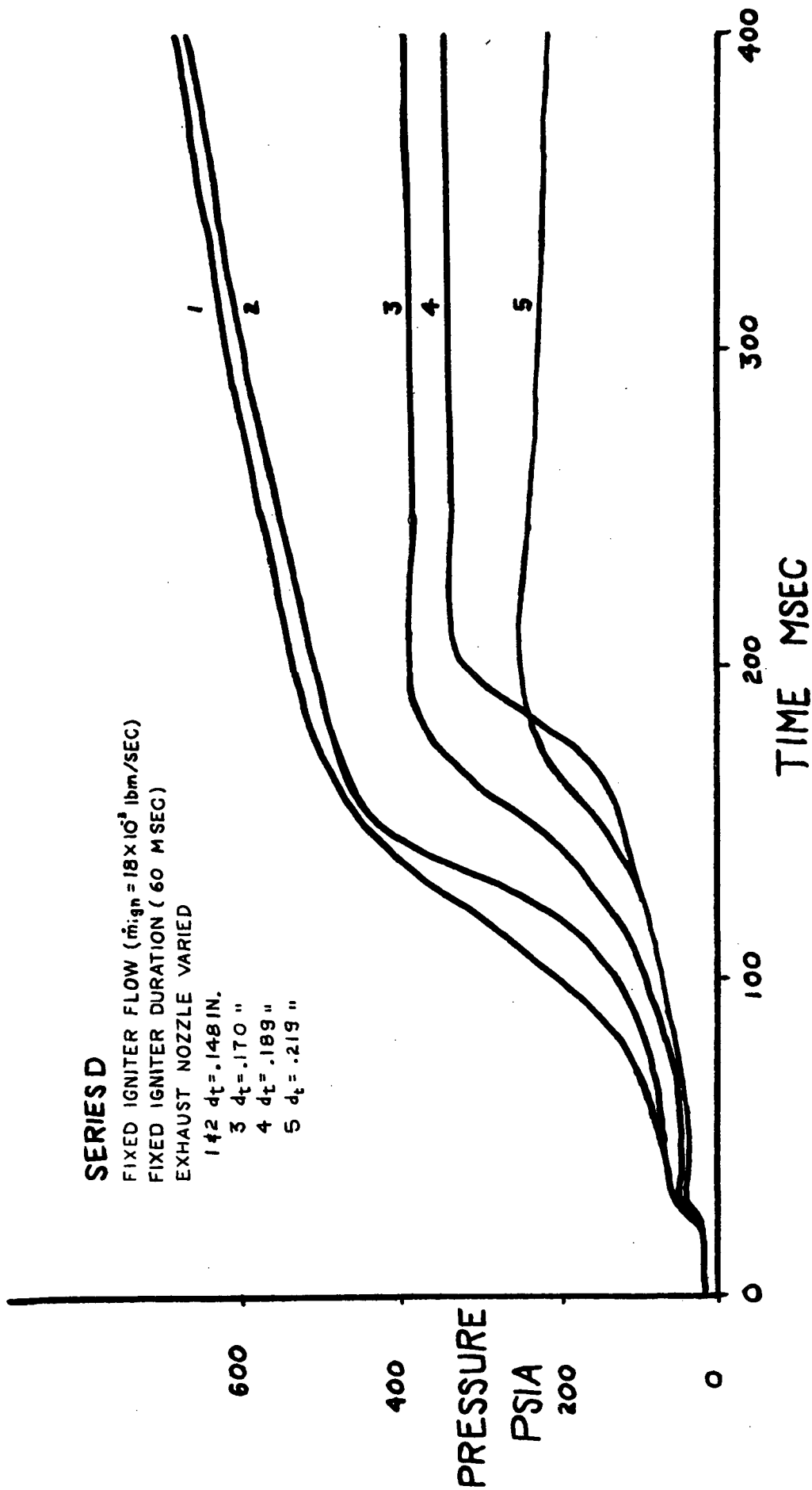
PROPELLANT SURFACE

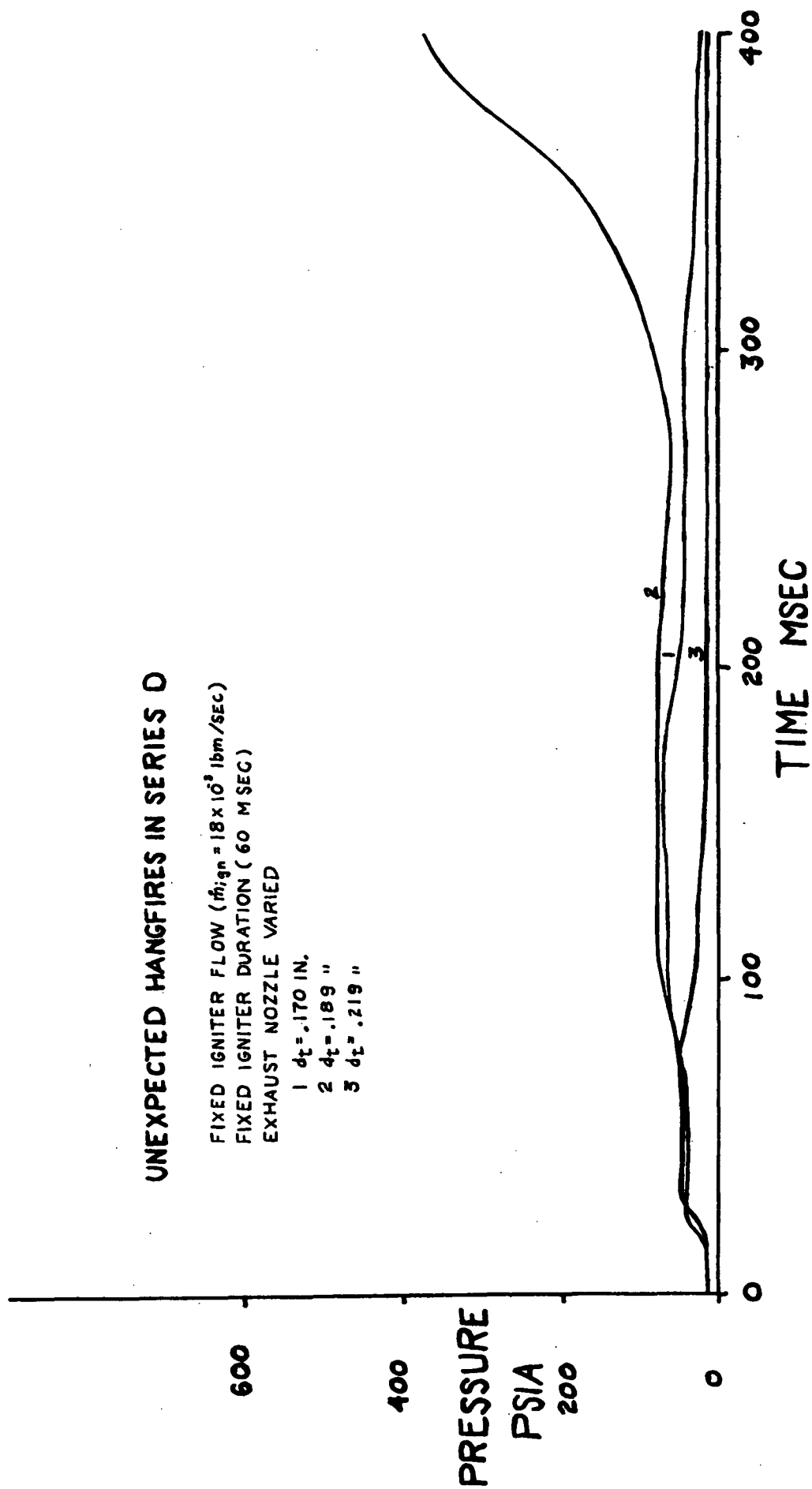
9.5 INCHES

PHOTOGRAPHIC RECORD OF FLAME SPREADING
DURING A LONG DELAY FIRING

EFFECT OF SELF HEATING







AP 26 R 4134 68

FIRING D-4

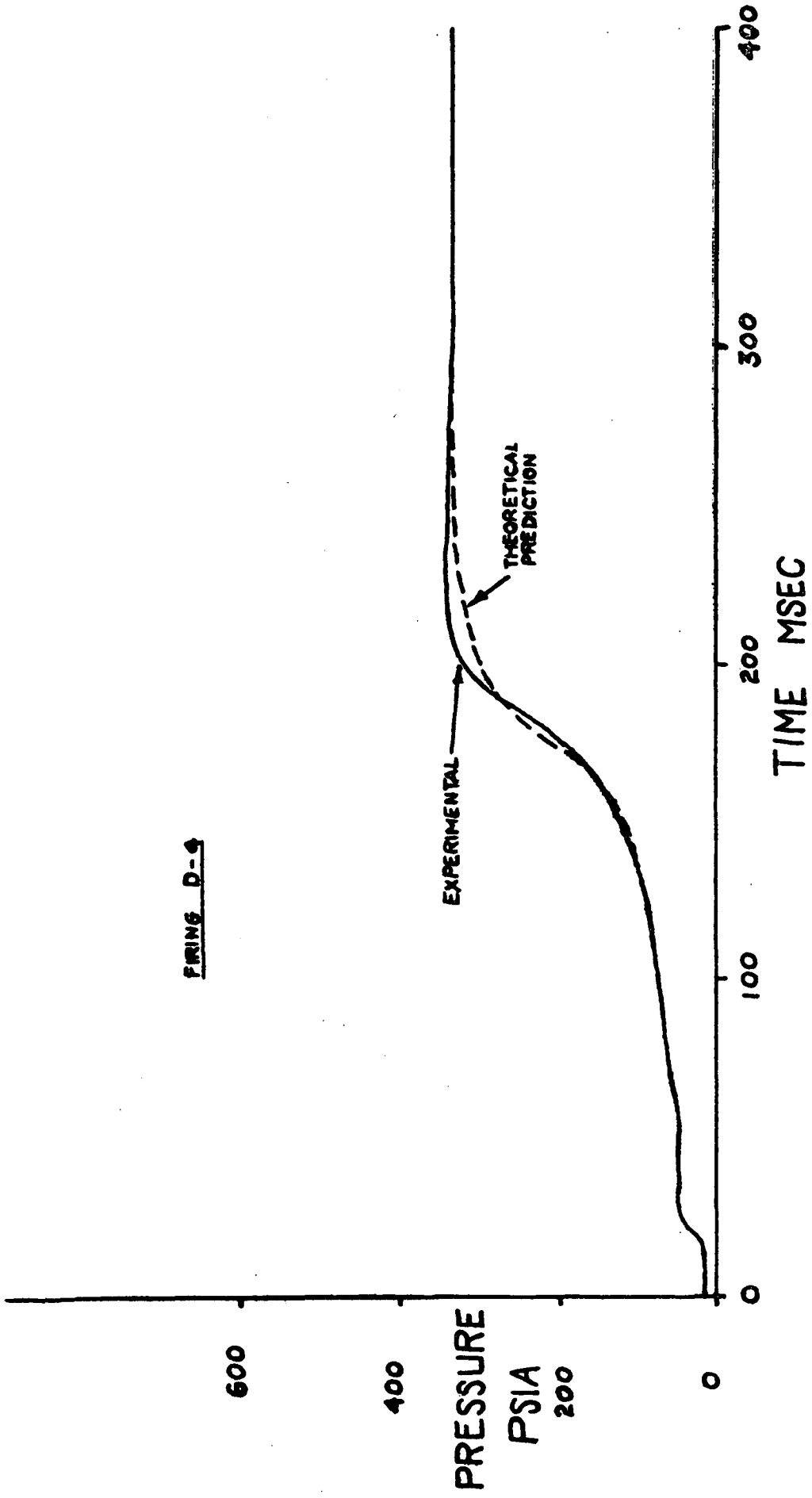
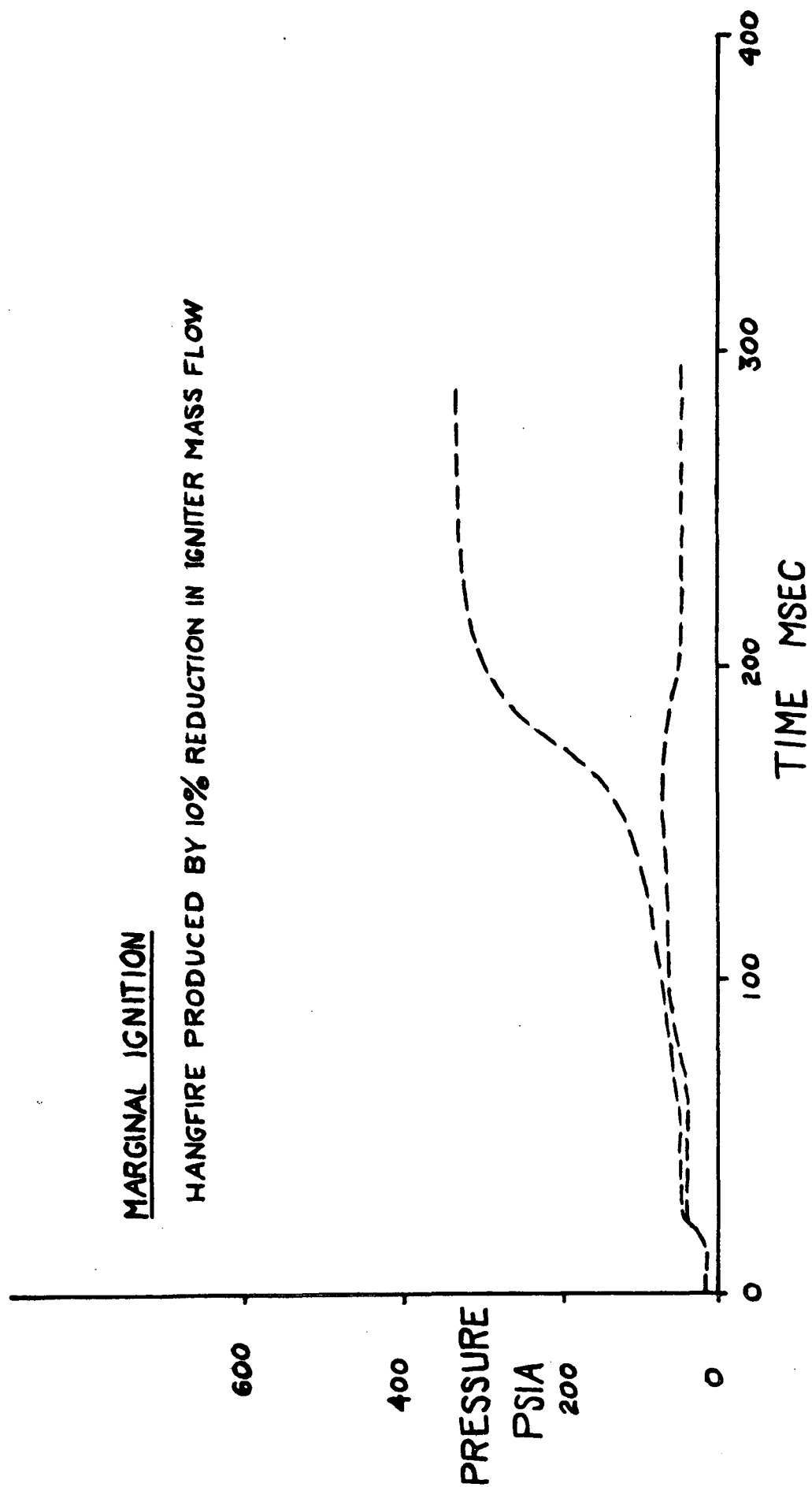
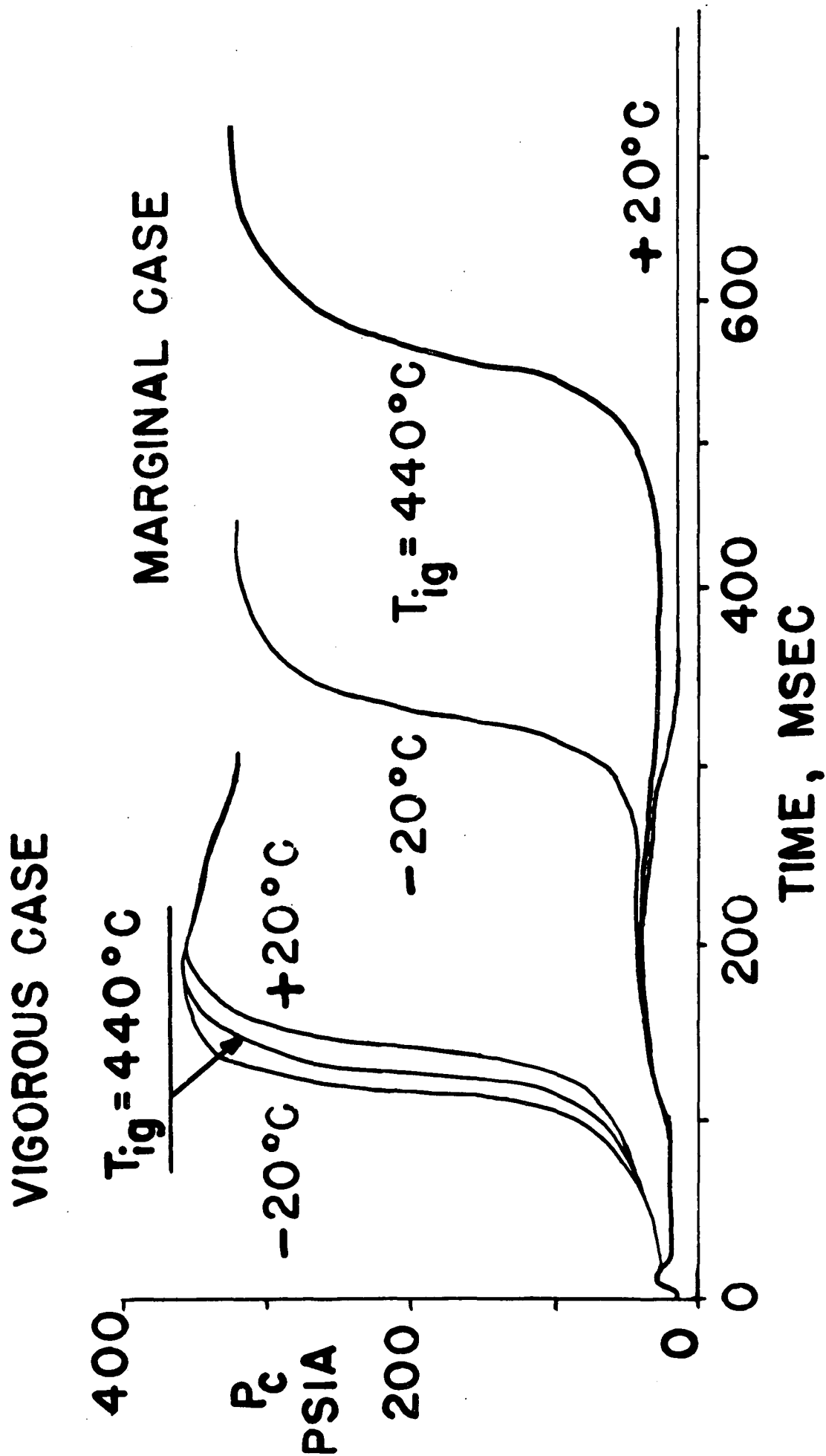


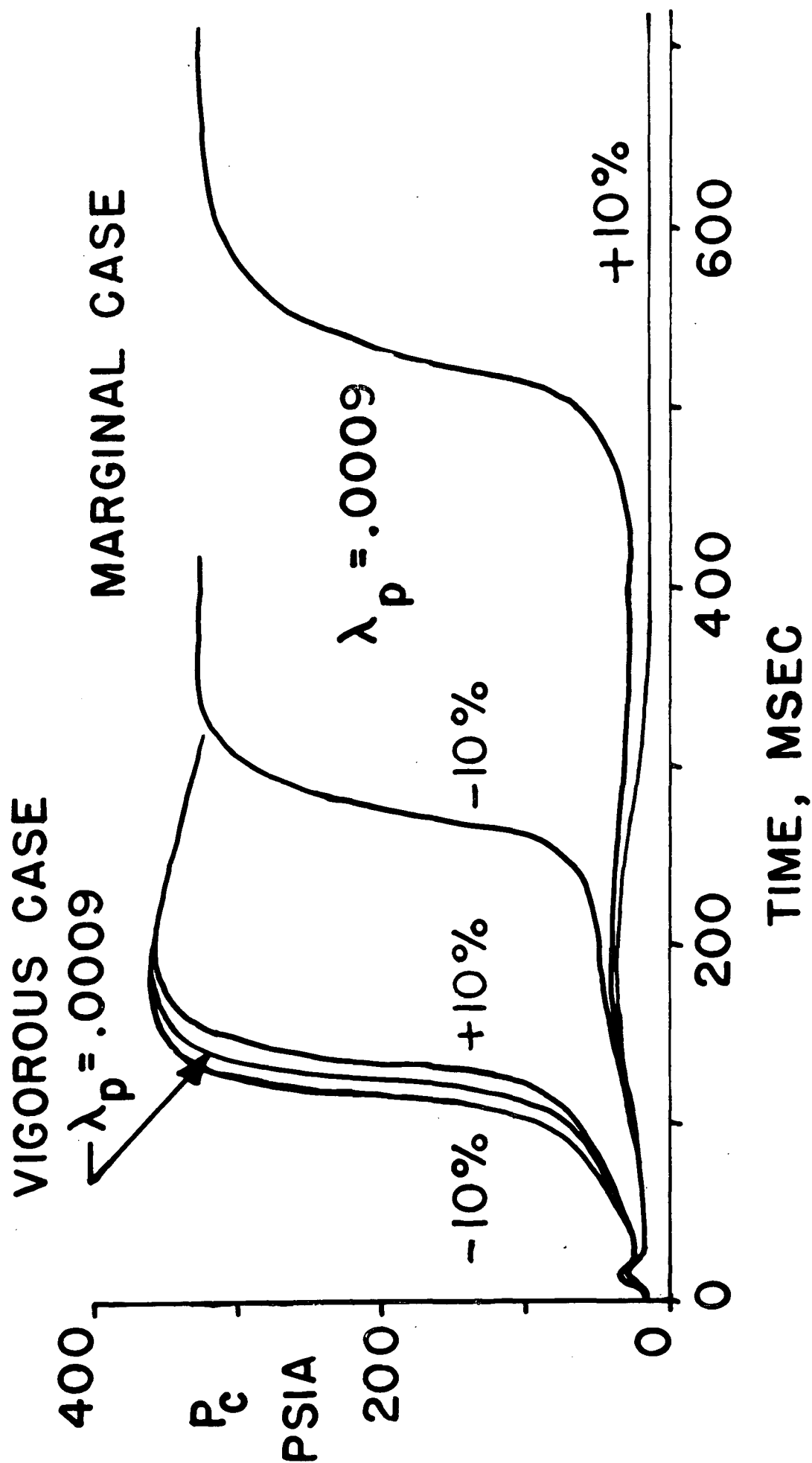
Figure 34



EFFECT OF UNCERTAINTY IN IGNITION TEMPERATURE



EFFECT OF UNCERTAINTY IN PROPELLANT THERMAL CONDUCTIVITY



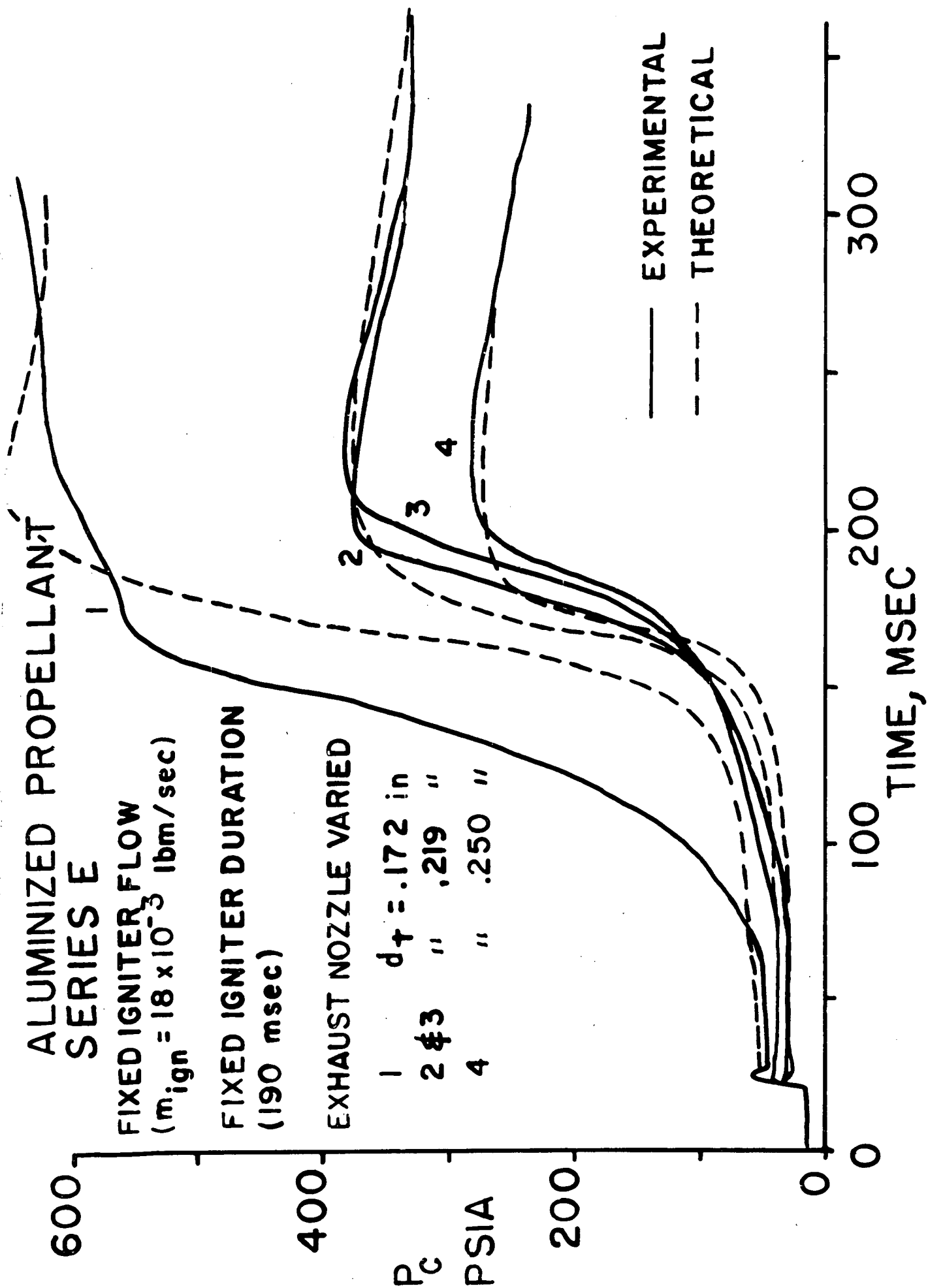
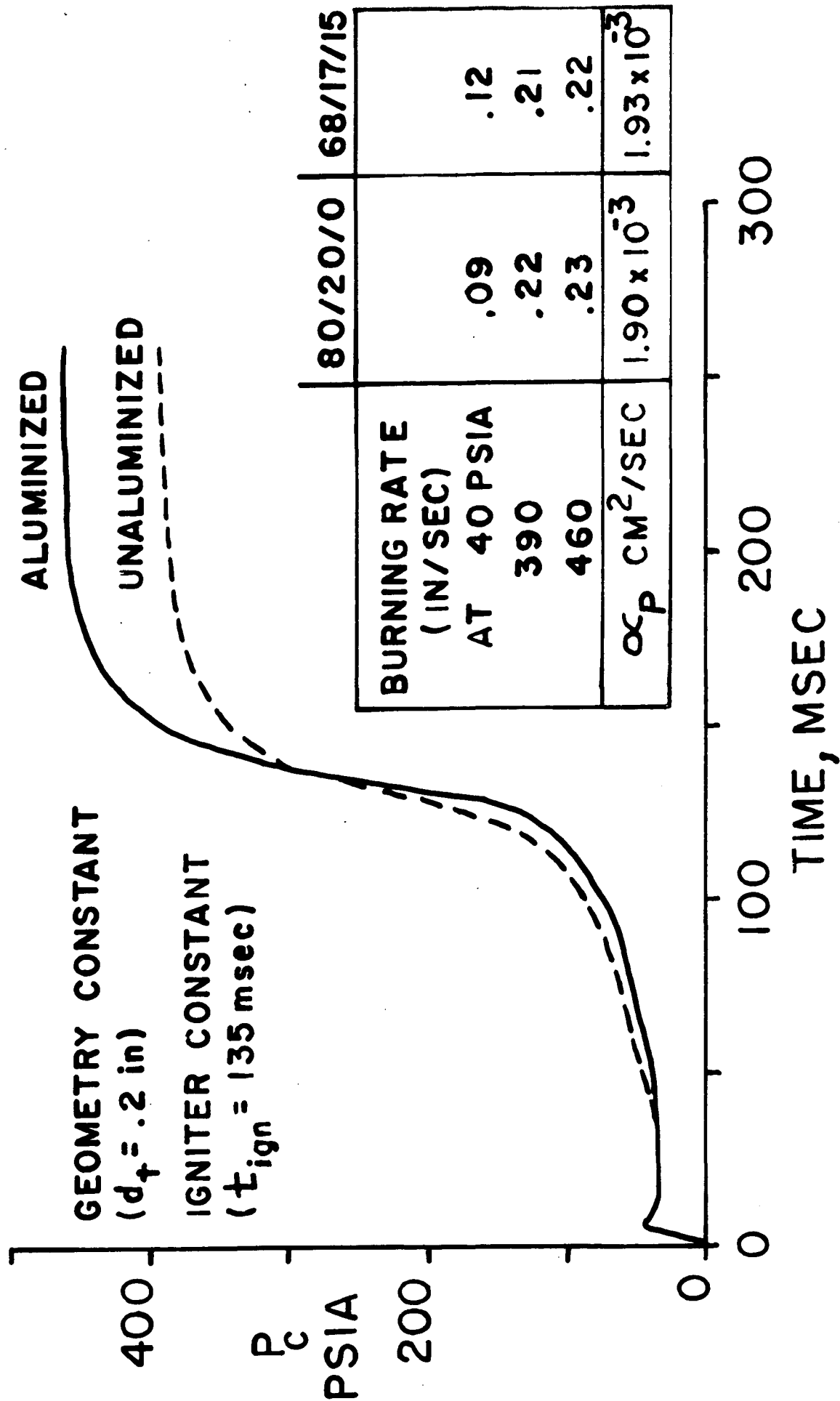
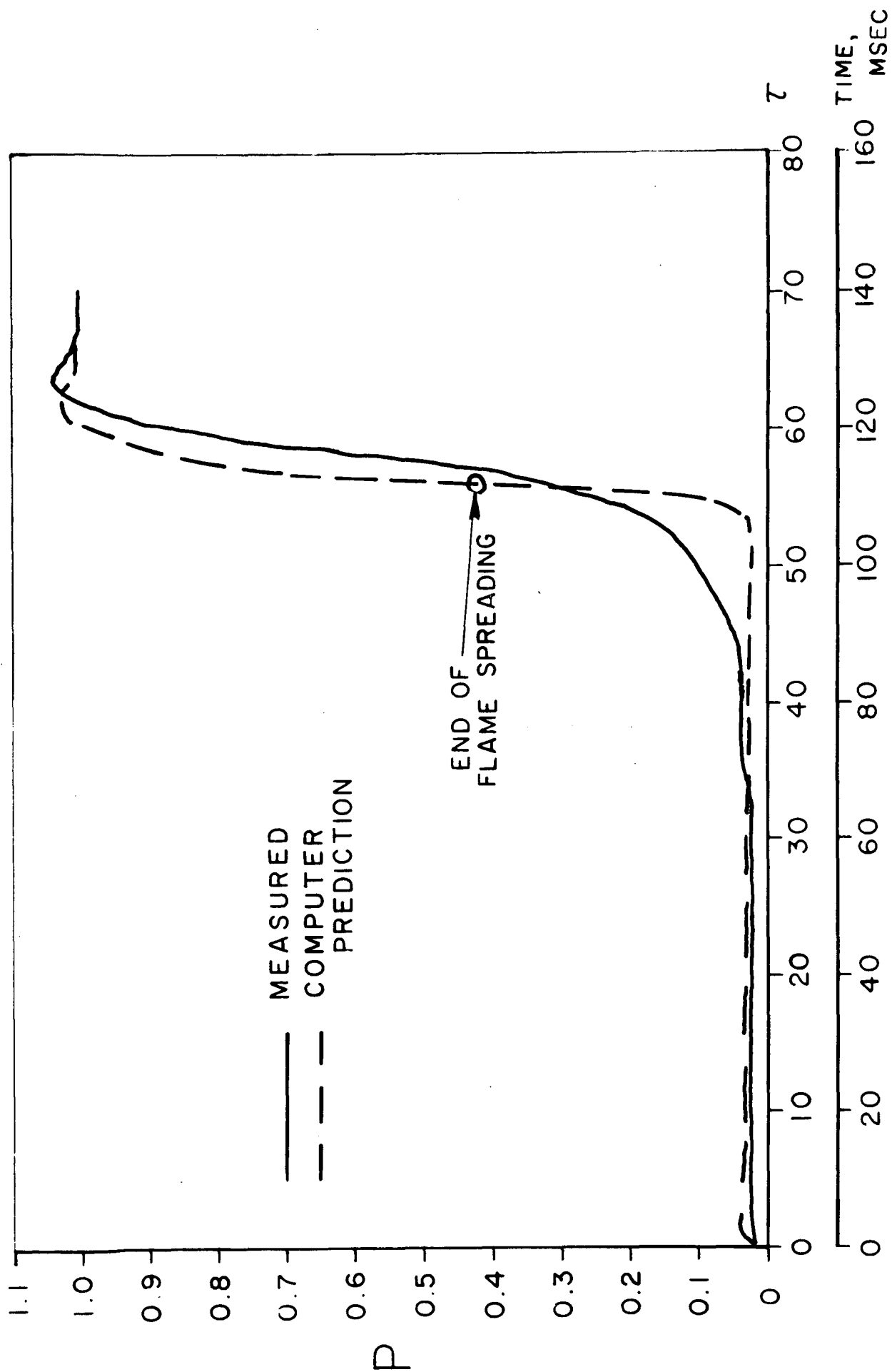


Figure 38

THEORETICAL PREDICTIONS FOR ALUMINIZED AND UNALUMINIZED PROPELLANT





COMPARISON OF COMPUTER PREDICTION AND MEASURED PRESSURE
TRACE FOR A TYPICAL STAR SHAPE GRAIN ROCKET MOTOR, RUN NO. 84

STUDY OF MOTOR WITH HOT PARTICLE IGNITER

